# USING MAIZE HEAT SHOCK FACTOR BINDING PROTEIN PARALOGUES TO STUDY HEAT SHOCK RESPONSE, DEVELOPMENT AND PROTEIN-PROTEIN INTERACTION SPECIFICITY DETERMINATION

by

SUNENG FU

(Under the Direction of Michael J. Scanlon)

## ABSTRACT

*Mutator* (*Mu*) transposon insertion induced mutants are a great genetic resource to clone genes and study molecular mechanisms of cellular and developmental processes. The research described in this dissertation exemplifies the significance of this approach.

The first part of this dissertation describes the characterization of a *Mu* induced, recessive, embryo lethal maize mutant, empty pericarp 2 (emp2) and the cloning of the *emp2* locus. It was found that emp2 mutant phenotypes co-segregated with a *Mu* transposon insertion in the first intron of the *emp2* locus. The transposon insertion was correlated with 5'-end truncation of the *emp2* transcripts and loss of EMP2 protein accumulation. EMP2 protein was found to be homologous to human HEAT SHOCK TRANSCRIPTION FACTOR BINDING PROTEIN 1 (HSBP1), a negative regulator of heat shock response (HSR). The un-attenuated HSR in emp2 loss of function mutant embryos indicates EMP2 is a functional homologue of HSBP1 in maize, and EMP2 represents the first protein found in plants to be essential for HSR attenuation.

*Emp2* gene was found to be constitutively expressed throughout maize development, which prompted me to study post-embryonic functions of EMP2. In order to overcome the embryo lethality of emp2 mutants, clonal mosaics of emp2 null mutant tissues were induced by X-ray

irradiation. As reported in the second part of this dissertation, emp2 null mosaics were associated with diverse developmental defects, and the mutant phenotypes are not affected by heat stress treatment. Therefore, the clonal mosaic analyses with emp2 mutant tissues elegantly demonstrated the separation of EMP2 functions in regulating HSR and normal development.

*Hsbp* genes were found to be duplicated in all monocot grass species. Consequently, the paralogue of *emp2*, *hsbp2* was cloned from maize. The maize *hsbp* paralogues exhibit differential expression patterns in response to heat stress and during normal development. In addition, yeast two-hybrid studies revealed that EMP2 and HSBP2 interact with different proteins through their coiled-coil domain. Comprehensive mutagenesis analyses identified that many residues within the coiled-coil domain of HSBP2 contributed to the hetero-oligomerization of HSBP2 and the maize HEAT SHOCK FACTOR, HSFA4b. More importantly, it was found that the specificity of HSBP2 and HSFA4b interaction is determined by non-coiled-coil peptide sequences that flank the coiled-coil domain of HSBP2. Thus, comparative study of the different protein-protein interaction selectivities of the maize paralogues not only provided novel insights about molecular determinants of protein interaction specificity, but also revealed important evolutionary mechanisms that lead to functional divergence of paralogous proteins.

INDEX WORDS: heat shock response, HEAT SHOCK FACTOR BINDING PROTEIN, EMP2, HSBP2, embryo lethal mutant, clonal mosaic analysis, coiled-coil, paralogue, protein-protein interaction specificity

# USING MAIZE HEAT SHOCK FACTOR BINDING PROTEIN PARALOGUES TO STUDY HEAT SHOCK RESPONSE, DEVELOPMENT AND PROTEIN-PROTEIN INTERACTION SPECIFICITY DETERMINATION

by

SUNENG FU

B.S., Fudan University, P.R.China, 1998

A Dissertation Submitted to the Graduate Faculty of The University of Georgia in Partial Fulfillment of the Requirement for the Degree

DOCTOR OF PHILOSOPHY

ATHENS, GEORGIA

2004

# USING MAIZE HEAT SHOCK FACTOR BINDING PROTEIN PARALOGUES TO STUDY HEAT SHOCK RESPONSE, DEVELOPMENT AND PROTEIN-PROTEIN INTERACTION SPECIFICITY DETERMINATION

by

SUNENG FU

Major Professor: Michael J. Scanlon

Committee: Kelly Dawe
Richard Meagher
Lee Pratt
Zhen-Hua Ye

Electronic Version Approved:

Maureen Grasso
Dean of the Graduate School
The University of Georgia
August, 2004

# DEDICATION

To all my family members: dad, mom, sister, brother, wife and son for their love and support

# ACKNOWLEDGEMENTS

For the last five years, I would like to thank my major professor, Dr. Scanlon, for all his guidance and support. From him I learned how to do science, how to treat students and how to manage a lab. I also want to thank my fantastic committee: Kelly Dawe, Richard Meagher, Lee Pratt and Zhen-Hua Ye for their enthusiasm about my projects and their broad expertise. I also learned a very important philosophy from them "Get to know what I have done sometimes is more important than to get more done". I am also very grateful to Dr. Sue Wessler for her insightful comments throughout my research. She also taught me another philosophy "One hypothesis (or interpretation) is not enough". I would also like to thank all current and past members of the Zea group, especially Evelyn Hiatt, Ning Jiang, Mark Osterlund, Hong-Guo Yu and Xiaoyu Zhang. Hong-Guo gave me lots of instructional advice during my first year of study here, and I will always remember one of his words "The smartest thing to do is to design experiments smartly". I would also like to thank all department members, especially the greenhouse staff. They set up a wonderful environment here that allows everybody to work here happily. Also, I want to thank many of my friends here, especially Weicheng Zhang, Xiaorong Lin and Ji Liu, for sharing their joys and experiences with me.

For the last ten years, I would like to thank all my teachers and colleagues, especially Professors Long Yu and Zhu Chen, in Fudan Univeristy and the Chinese National Human Genome Center at Shanghai. During this period, my enthusiasm and knowledge about science surged. I would also like to thank Chunlin Jiang, Min Zhang, Jun Xing, because they essentially trained my bench skills. I also want to say thanks to all my college friends, especially Jun Cai,

Lin Lu, Fangyi Wang and Cong Yu for all the wonderful time in Fudan. For the last twenty eight years, I want to thank my dad, mom, sister and brother. We were a poor family. Financially speaking, life was bitter throughout our childhood. However, we stood strong and worked hard, and we finally hung through. Thank you, dad and mom, sister and brother! I am truly grateful for being a member of such a sweet and strong family, and for all the support and teachings. I love so much about my life now, and that is all because of my family. I also want to thank all my teachers since elementary school. I really have enjoyed school, and learn a lot from school. I am also grateful for all my pals since my childhood. Life is so much more fun with them, and from time to time, I learned something from them.

For the past, present and future, I want to thank my wife Anjie and my son, Yiming. Anjie came into my life when I was in my low. It is her beautiful mind and her love that recharged me. It is her understanding and support that allowed me to explore the freedom of science. Since his birth, Yiming has been the greatest source of happiness in my life. To be honest, I also learned a lot about science by watching him growing up. I am truly grateful to them for the wonderful life I am enjoying and continue to enjoy.

TABLE OF CONTENTS

Page

# LIST OF TABLES

Page

## LIST OF FIGURES

Page

# CHAPTER 1

# INTRODUCTION AND LITERATURE REVIEW

## Overview

Temperature is a principle environmental factor that is important for every organism on earth; it affects not only the thermodynamics of basic metabolism like respiration and photosynthesis, but also more complex processes like cell cycle control, flowering, seed dormancy, sex determination and animal behavior (Precht et al., 1973). However, little is known about the molecular mechanisms by which organisms measure and respond to environmental temperature change.

The heat shock response describes the biological phenomenon by which organisms respond to abruptly elevated temperatures (Figure 1.1). A central event of the HSR is the rapid and specific induction of *heat shock protein* genes (*hsp*s), which are molecular chaperones that assist protein folding, translocation, activation and degradation. Since the first discovery of heat induced expression of *hsp*s in *Drosophila* (Ritossa, 1962), similar phenomena have been observed in both prokaryotes and eukaryotes from fungi to plants and animals (reviewed by Lindquist, 1986 and references therein). Therefore, the thermo-inducible *hsp* expression provides a great system to study the molecular machinery by which organisms measure the environmental temperature shift and re-adjust cellular and developmental programs. In addition, expression of *hsp*s can also be induced by other stress conditions and developmental cues (reviewed by Lindquist, 1986 and references therein). The expression of *hsp*s beyond the HSR suggests additional roles of *hsp*s in coping with other stresses and during development.

The HEAT SHOCK TRANSCRIPTION FACTOR (HSF) is a key player that activates the expression of heat shock proteins at the transcriptional level in response to heat stress (reviewed by Wu, 1995 and references therein). Heat shock induces multiple levels of HSF regulation such as transcription, phosphorylation, protein-protein interaction and sub-cellular localization

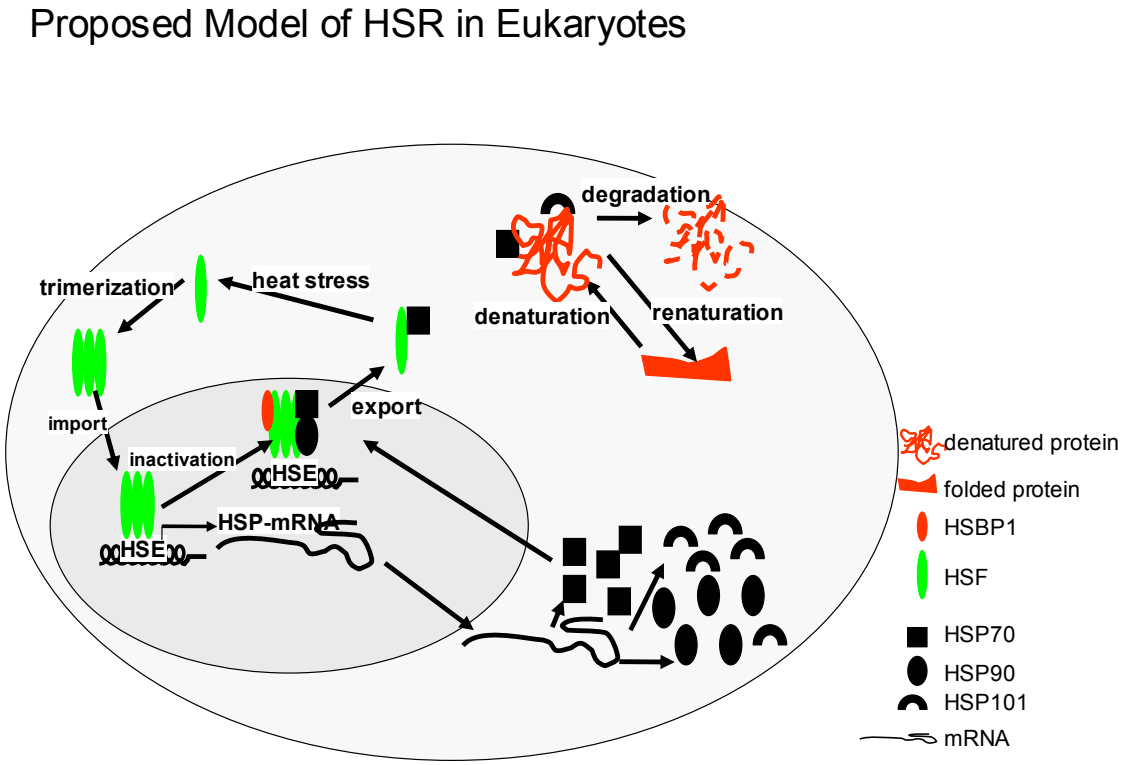


**Figure 1.1** The proposed model of the heat shock response (HSR) in eukaryotes (adapted from Morimoto et al., 1998). Under non-stress conditions, the HSF is in inactive complexes with HSPs (especially HSP70 and HSP40). Heat stress (HS) causes protein denaturation and aggregation. The abnormal protein aggregates sequester the HSPs and lower the cytoplasmic concentration of HSPs. Consequently, HSFs are disassociated from the complexes and activated. The active HSFs form trimers and are transported into the nucleus, bind to the heat shock element (HSE) and promote expression of *hsp* genes. The newly synthesized HSPs can either disassemble the abnormal protein aggregates and refold the denatured proteins, or take the unfolded proteins for degradation (see text for more details, also reviewed by Morimoto, 1998).

(reviewed by Nover et al., 2001; Wu 1995 and references therein). Several distinct protein-protein interactions among heat shock factors or between HSFs and other proteins are mediated by central α-helixes of HSFs (Rabindran et al., 1993; Satyal et al., 1998; Sorger and Nelson, 1989). The α-helixes wrap around each other and form a coiled coil structure, which is a versatile protein-protein interaction domain present in many protein structures (reviewed by Burkhard et al., 2001 and references therein). The coiled coils not only can form stable and specific protein-protein interactions, but can also adjust the specificity and strength of the interaction in response to pH change and temperature shift. Therefore, coiled coils can function as molecular switches at the interface between the macroscopic physiology (e.g. pH, temperature) and microscopic biology (e.g. signal transduction, gene transcription). Understanding the specificity and regulation of the coiled-coil will facilitate our study about how organisms monitor and adapt to their environment, and allow broad applications in drug design and bio-mechanic engineering (reviewed by Yu, 2002 and references therein).

## Heat Shock Response and Heat Shock Proteins

### Heat induced expression of *hsp* genes

Man has long sought to study the effects of heat stress on themselves and other organisms. The first cytological consequence of heat stress was observed by Dr. Ritossa in the fruit fly, *Drosophila busckii*, as the appearance of a new set of chromosome puffs and disappearance of previously present puffs (Ritossa, 1962). The puffs were later demonstrated to correspond with actively transcribing *hsp* gene loci (Livak et al., 1978; Spradling et al., 1977). The rapid (within minutes), specific induction of *hsp* genes is a universal phenomenon of the HSR (Altschuler et al., 1981; Key et al., 1981; Schuman, 2003; Spradling et al., 1977; Trinklein et al., 2004), and

has been observed in all species studied as well as in cell cultures and explanted organs (reviewed by Lindquist, 1986 and references therein). The induction of *hsp* genes is accompanied by genome-wide suppressed expression of other actively transcribed genes (Ritossa, 1962; Spradling et al., 1977; Trinklein et al., 2004; also see review by Lindquist, 1986 and references therein). The transcriptional activation of *hsp* genes is further augmented by selective translation (Lindquist and Peterson, 1990; reviewed by Sierra and Zapata, 1994 and references therein). Consequently, the majority of newly synthesized proteins in heat stressed cells are HEAT SHOCK PROTEINs (HSPs, reviewed by Rosen and Ron, 2002 and references therein).

**Roles of HSPs during heat shock response**

HSPs are classified according to their size and homology: HSP100, HSP90, HSP70, HSP60, DnaJ, small HSPs and UBIQUITIN (reviewed by Lindquist and Craig, 1988 and references therein). The overall purpose of the HSPs is to minimize protein aggregation and to promote protein folding and translocation. The HSP100 family members are specialized for the disassembly of higher order denatured protein aggregates (Saibil, 2000 and references therein), whereas HSP70 holds unfolded substrates in an intermediate state to prevent aggregation and catalyzes the refolding of denatured substrate in a co-chaperone and energy dependent manner (Bukau and Horwich, 1998 and references therein). HSPs often function with their cohort proteins in chaperone machineries: HSP70 (DnaK) with DnaJ and GrpE; HSP60 (GrpEL) with HSP10 (GrpES) (reviewed by Georgopoulos 1992 and references therein). Despite their general chaperone activities, HSPs like HSP90 and HSP70 can have rather specific substrates (Table 1.1). HSPs play regulatory roles during the maturation and activation of receptors and kinases in response to stresses and other types of external stimuli. In addition, there are some other HSPs involved in the degradation of denatured or aggregated proteins under heat stress. For example,

the *E.coli* HSP100 (ClpA, B and X) and Lon are ATP-dependent proteases that are capable of degrading unfolded polypeptides (reviewed by Gottesman and Maurizi 1992 and references therein). In eukaryotes, the ubiquitin proteasome instead is responsible for the bulk of protein degradation, and many components of this machinery (e.g. ubiquitin, ubiquitin conjugating enzymes) are heat inducible (reviewed by Jentsch 1992 and references therein).

The biochemical properties of HSPs are well suited for heat stressed cells to temporarily halt cell cycle and devote most of the energy to prevent the formation of, or dissolve, massive aggregates of newly synthesized peptides or pre-existing folded proteins. Indeed, expression of *hsp* genes is correlated with the tolerance of extreme temperatures in a wide variety of cells and tissues, either in a heat induced or developmentally regulated manner (reviewed by Parsell and Lindquist, 1993 and references therein). Conversely, tissues and organisms often are highly thermosensitive if they are unable to express *hsp*s (Bowder et al., 1989; Dura, 1981; Heikkila et al., 1985; Muller et al., 1985). Mutant analyses also revealed the essential requirement for individual *hsp*s during heat shock response, and different *hsp*s may function under distinct temperature ranges. For example, *hsp70* in *Saccharomyces cerevisiae* is required for growth at temperatures near the upper end of normal growth range, whereas *ubiquitin* is required for long term survivability in moderately high temperatures and *hsp104* plays a role in tolerance to extreme temperatures (Craig and Jackbosen, 1984; Finley et al., 1987; Sanchez and Lindquist, 1990). In contrast, the same temperature range may require different *hsp*s in different species. Although *hsp104* is required to cope with extreme temperatures in yeast and *Arabidopsis*, *Drosophila* depends on *hsp70*, whereas mammals depend upon *hsp70*, *hsp27* and *hsp101* for severe heat stress (Hong and Vierling, 2000; Landry et al., 1989; Lee and Schoffl, 1996; Li and Laszlo, 1985; Queitsch et al., 2000; Soloman et al., 1991).

**Functions of HSPs beyond heat shock response**

Although the *hsp*s were originally characterized as genes specifically induced upon heat stress, expression of *hsp*s is also upregulated in response to other types of stress treatments and developmental cues (reviewed by Lindquist, 1986 and references therein). Chemical stress by induced by ethanol or sodium arsenite, and physiological stress induced by cold, drought and pathogen infection can promote *hsp* gene expression in a broad range of species including yeast, plants, *Drosophila* and mammals. Induced expression of *hsp*s by one type of stress treatment is correlated with cross protection of other type of stresses (Li, 1983; Nagao et al., 1985; Plesset et al., 1982; Velazquez and Lindquist, 1984). Loss of function mutations and over expression analyses also revealed functions of individual *hsp*s in coping with other type of stresses. For example, deletion of one *hsp70* (*hsp70.1*) is correlated with increased sensitivity to radiation in mice, and over expression of a 17 kDa small HSP in *Arabidopsis* (AtHSP17.6A) enhances osmotolerance (Hunt et al, 2004; Sun et al, 2001).

Many of the *hsp* genes are expressed also under non-stressed conditions, and loss of function mutants exhibit distinct developmental defects (Table 1.1 and references therein). The mechanisms of HSP functions under non-stressed conditions are multi-fold. First, they are required in multiple steps of protein biogenesis such as folding and translocation (Hartl, 1996). Loss of HSP function results in accumulation of unfolded proteins and consequently leads to cell death and developmental abnormalities (Elfant and Palter, 1999). Also, some HSPs (e.g. HSP90, BAG-1) are required for the maturation or activation of specific receptors, kinases and transcription factors, which are important for developmentally important signal transduction pathways (reviewed by Nollen and Morimoto, 2002; Pratt, 1997; also see Table 1.2 and references therein). Lastly, some other HSPs like α-crystallin are themselves integral

**Table 1.1** Examples of HSP Functions beyond HSR

| gene | organism | proposed function and loss of function phenotype | references |
|---|---|---|---|
| *hsp83* | fruit fly | ensure proper centrosome function, required for phl kinase activation during eye development, affect spermatocyte and recessive lethal | Dickson et al, 1996; van der Straten et al, 1997; Lange et al, 2000 |
| | worm | moderate growth defect on NaCl, chemosensory defect | www.wormbase.org |
| | Arabidopsis | chlorate resistant, photomorphogenesis defect | Cao et al, 2003 |
| *hsp70* | fruit fly | supress neurodegeneration | Warrick et al, 1999 |
| *hsp70-2* | mouse | present Cdc2 to form heterodimer with cyclin B1, essential for G2-M transition during spermatocyte meiosis, male infertility | Dix et al, 1996; Eddy 1998 |
| | human | polymorphism of hsp70-2 is associated with multiple diseases: Alzheimer's disease, obesity, Crohn's diease, renal tumor and others | Clarimon et al, 2003 |
| *hsc70* | fruit fly | required for protein folding in the ER, expression of dominant negative form of hsc70 leads to lethality and multiple developmental abnormalities | Elfant and Palter, 1999 |
| *hsp60* | human | spastic paraplegias | Hansen et al, 2002 |
| | fruit fly | essential for early embryogenesis | Perezgasga et al, 1999 |
| *hsp60B* | fruit fly | essential for spermatid individualization, male infertility | Timakov et al, 2001 |
| *CyP40* | Arabidopsis | cochaperone of hsp90, promotes the expression of juvenile phase of vegetative development. | Beradini et al, 2001 |
| *Tid1 (DnaJ)* | mouse | co-chaperone of hsp70, essential for early embryo development and cell survival. | Lo et al, 2004 |
| | human | co-chaperone of hsp70, modulator of apoptosis, lethal imaginal disc tumor | Syken et al, 1999 |
| | yeast | co-chaperone of hsp70, promotes colocalization of rad51 and dmc1 during meiotic recombination | Shinohara et al, 2000 |
| | fruit fly | co-chaperone of hsp70, lethal imaginal disc tumor | Kurzik-Dumke, 1992 |
| *α-A-crystalin* | human | maintains lens transparency, congenital progressive cataract | Brady et al, 1997; Litt et al, 1998 |
| *α-B-crystalin* | human | inhibits caspase-3 auto-proteolytic activation, promotes myogenic differentiation into multinucleated myotubes, myopathy, congenital cataract | Kamradt et al, 2002 Vicart et al, 1998 |
| *γ-E-crystalin* | human | important for embryonic development of the anterior segment of the eye, cataract and microphtalmia | Cartier et al, 1992; Fu and Liang, 2003 |
| *hsp27* | human | decrease ROS in cells expressing mutant huntingtin, supress polyQ mediated cell death and neurodegeneration | Wyttenbach et al, 2002 |
| *hsp26* | worm | mutant with increased longevity | Seong et al, 2001 |
| *hsp25* | human | differentiation of PAM212 keratinocytes | Duverger et al, 2003 |

**Table 1.2** Examples of HSP Interaction Partners

| chaperone | cellular function | co-chaperone | interaction partner(s) | references |
|---|---|---|---|---|
| Hsp90 | Ras/Raf signal transduction | Cdc37 | Raf-1, Akt, Ksr-1, Src, | Cutforth and Rubin, 1994 |
| | hormone complex assembly/hormone response | p23/ immunophilin CyP40/PP5/ FKBP52 | progesteron/glucocorticoid aporeceptor | Davies et al., 2002 |
| | cell death | unknown | Apaf-1 | Pandey et al., 2000 |
| | stress response | unknown | HSF-1 | Zou et al., 1998 |
| | disease resistance | Sgt1 | Rpm1, Rar1, | Takahashi er al., 2003; Hubert et al., 2003 |
| | growth | FKBP42 | calmodulin | Kampausen et al., 2002 |
| hsp70 | hormone complex assembly/hormone response | hsp40/Hip/Hop | progesteron/glucocorticoid aporeceptor | Gebauer et al., 1998 |
| | DNA synthesis arrest | Bag1 | Raf-1 | Wang et al., 1996 |
| | apoptosis | Bag1 | Bcl-2 | Takayama et al., 1996 |
| | apoptosis | Bag1 | HGF receptor | Bardelli et al., 1996 |
| | apoptosis | Bag1 | activated glucocorticoid receptor | Kullman et al., 1998 |
| | apoptosis | unknown | Apaf-1 | Beere et al., 2000 |
| | stress response | unknown | HSF-1 | Abravaya et al., 1992 |
| | redox response | AtTDX (hip) | | Vignols et al., 2003 |
| hTid-1 (DnaJ) | Hormone response (kinase) | hsp70/hsc70 | IFNgammaR2 and Jak2 | Sarka et al., 2001 |
| Grp94 (SHD) | meristem size | | | Ishiguro et al., 2002 |

components of biological structures (e.g. lens), and mutations in α-crystallin cause blindness (Brady et al., 1997).

The chaperone activities of HSPs can also act as buffer reagent during molecular evolution as well as during the progression of disease. For example, suppression of HSP90 functions in both fruit fly and *Arabidopsis* exposed numerous morphological novelties that resulted from previous cryptic genetic variants (Queitsch, 2002; Rutherford and Lindquist, 1998). On the other hand, expression of HSP70 (HSPAL) in *Drosophila* suppresses polyglutamine-induced neurodegenerative disease by binding to the mutant proteins and reduceing their neurotoxity (Warrick, 1999).

**Consequences and applications of constitutive *hsp* gene expression**

The broad functions of HSPs in stress response, human pathogenesis as well as normal development offer promise for their use in medical and agricultural applications. Indeed, constitutive expression of HSP70, HSP40 and TPR2 can successfully suppress the progress of Huntington's disease in *Drosophila* model (Chan et al., 2000; Kazemi-Esfarjani and Benzer, 2000; Warrick et al., 1999; Wyttenbach et al., 2000). Transgenic *Arabidopsis* and rice plants expressing *hsp101* show remarkably increased thermotolerance (Katiyar-Agarwal et al., 2003; Queitsch, 2000). However, adverse effect of *hsp* over expression has also been noted in other cases. Over expression of the heat inducible *hsp70* in *Drosophila* suppresses growth at normal temperatures (Feder et al., 1992). In both *E.coli* and yeast strains carrying null mutations of *hsp70* genes, increased over expression of other *hsp* genes also resulted in growth inhibition under non-stressed temperatures (Bukau et al., 1989, 1990; Craig and Jacobsen, 1984; Halladay and Craig, 1995).

## Functions and Regulations of the HSF

### Structures and functions of HSFs

In eukaryotes, the expression of *hsp* genes in response to stress is activated by the *cis*-acting heat shock elements (HSE) (variations of an inverted repeat nGAAn) and the *trans*-acting protein HSF (reviewed by Gurley and Key, 1991; Wu, 1995). The first HSF was cloned from *Saccharomyces cerevisiae*, and subsequently from *Drosophila*, tomato, *Kluyveromyces lactis*, human, *Schizosaccharomyces pombe*, chicken, *Arabidopsis*, *Xenopus* and almost any other organisms studied (Clos et al., 1990; ; Gallo et al., 1993; Hubel and Schoffl, 1994; Jakobsen and Pelham, 1991; Nakai and Morimoto, 1993; Rabindran et al., 1991; Scharf et al., 1990; Sorger and Pelham, 1988; Stump et al., 1995; Wiederrecht et al., 1988). Except in *Saccharomyces cerevisiae* and *Drosophila melanogaster*, both of which harbor a single HSF, multiple members of HSF have been identified from tomato, human, chicken and *Arabidopsis* (Hubel and Schoffl, 1994; Nakai and Morimoto, 1993; Scharf et al., 1990; Schuetz et al, 1991). Generally, vertebrates have three HSFs (mammal: HSF1,2,4; avian: HSF1,2,3), while plants often have more than twenty HSFs (reviewed by Nover et al., 2001; Pirkkala et al., 2001; Wu, 1995 and references therein). Despite their variations in protein sizes (244 residues of AtHSFB3 vs 833 residues of ScHSF), HSFs from all species share a conserved modular structure (Fig.1.2). Located on the N-terminal of the proteins are a conserved DNA binding domain (DBD) followed by a trimerization domain (HR-A/B). The spacing between DBD, HR-A and HR-B is highly variable and used for classification of plant HSFs into A, B and C three classes (Nover et al., 2001). The domain required for transactivation of *hsp* genes is localized on the far C-terminal of the HSF. The activation domain (AD) is not widely conserved and may be present at multiple

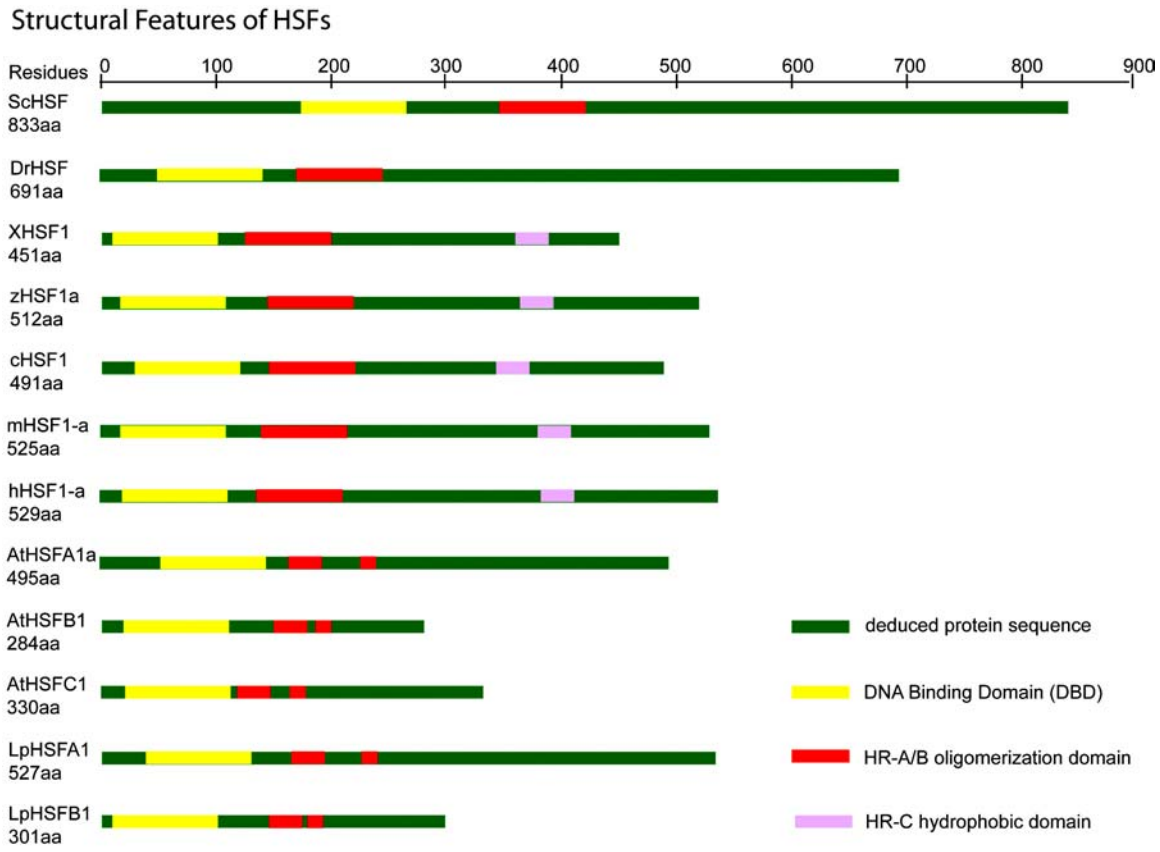


**Figure 1.2** Conserved structural features of HSFs. All HSFs contain a highly conserved DNA binding domain (DBD). The oligomerization domain (HR-A/B) is also present in all HSF members, but HR-A and HR-B are not continuous in plant HSFs. The animal HSF has an additional hydrophobic heptad repeat (HR-C) that is not present in plant and fungi HSFs. Yeast and *Drosophila* each have a single HSF, ScHSF and DrHSF, respectively. Animals often have three HSFs, but only the HSF1 orthologues are shown above. Alternative splicing isoforms (α and β) of HSF1 are present in human, mouse and zebrafish (hHSF1- α, mHSF1-α, and zHSF1α), but no splicing isoform of HSF1 has been isolated from Xenopus yet (XHSF1). The plant HSF families are comprised of more than twenty members categorized into A, B and C classes. Representative HSFs isolated from *Arabidopsis* and tomato are termed as AtHSFA1, AtHSFB1, AtHSFC1, LpHSFA1 and LpHSFB1 (see Pirkkala et al., 2001; Nover et al., 2001).

copies or absent in some HSF members (Nover et al., 2001). There are two additional elements located between the trimerization domain and the activation domain: the nucleus localization signal (NLS) and the hydrophobic trimerization suppressor domain (HR-C) (Nover et al., 2001; Wu, 1995 and references therein).

HSFs bind to the HSE in the promoter region of *hsp* genes to activate the latter's expression in response to heat stress (see Figure 1.1; also Gurley et al., 1986; Shuey and Parker, 1986; reviewed by Gurley and Key, 1991; Wu, 1995). Three HSEs are required for high affinity binding (Perisic et al., 1989; Sorger and Nelson, 1989). Although multiple copies of hsf genes are present in mammalian genome, only one of them, namely HSF1, is involved in heat shock response and thermotolerance (McMillan et al., 1998; McMillan et al., 2002; Sarge et al., 1993). Among the twenty plus HSFs in Arabidopsis, there is accumulating evidence to suggest that the HSFA1a and HSFA1b play redundant roles in regulating heat induced expression of *hsp* genes and *hsf* genes (Lee et al., 1995; Lohmann et al., 2004; Prandl et al., 1998; Wunderlich et al., 2003). In addition to a role in heat shock regulation, HSF1 is also involved in other types of stress induced, as well as developmentally regulated, expression of *hsp* genes (Christians et al., 1997; Fiorenza et al., 2004; Hahn and Thiele, 2004; Zou et al., 2003). HSF1 also mediates other cellular processes such as polyadenylation and ubiquitin-proteasome degradation (Pirkkala et al., 2000; Xing et al., 2004). The broad functions of HSF1 are consistent with the genetic analysis of *hsf1* loss of function mutants. The vertebrate *hsf1* homologue in yeast is required for viability during non-stress conditions (Sorger and Pelham, 1988). The *hsf* gene in fruit fly is required for oogenesis and early larval development in an *hsp*-independent fashion (Jedlicka et al., 1997). *Hsf1* deficient mice display severe defects in the chorioallantoic placenta and increased lethality

(Xiao et al., 1999). Female *hsf1* knockout mice are infertile, whereas constitutive expression of an active form of *hsf1* leads to abortion of spermatogenesis (Naikai et al., 2000).

In contrast to the prominent roles of *hsf1* in regulating stress responses, HSF2 has been proposed as a development regulator (Alastalo et al., 1998; Mezger et al., 1994; Pirkklal et al., 1999; Rallu et al., 1997; Sistonen et al., 1992). The avian HSF3 seems to have dual functions in both heat shock response and cell cycle control (Kanei-Ishii et al., 1997; Tanikawa et al., 2000). HSF3 is required for the trimerization of HSF1 after heat shock, and it is the principle HSF activated by severe heat stress (Kawazoe et al., 1999; Tanabe et al., 1997; Tanabe et al., 1998). Relatively little is known about plant HSFs (Nover et al., 2001). The synthesis of the A2 class of *Arabidopsis* HSFs is heat inducible, and they can form hetero-oligomers with HSFA1 (Bharti et al., 2001; Scharf et al., 1998). However, the significance of the hetero-oligomerization is unknown. AtHSFB1 is among a group of HSFs that lack the transcription activation domain but can function synergistically with HSFA1 in reporter gene activation (Nover et al., 2001).

**Regulation of HSF in stress response**

Based on previous studies carried out in yeast, *Drosohpila*, vertebrates and plants, HSFs can be present in cells in five different states (Figure 1.3). The yeast and *Xenopus* HSF proteins are always in the nucleus and bind to DNA (Status#4), although they are still unable to promote *hsp* gene expression in the absence of heat stress (Bharadwaj et al., 1998; Sorger and Pelham, 1988). In contrast, both the vertebrate HSF1 and plant HSFA1 are present as inert monomers either in the nucleus or cytoplasm, and require heat shock induction in order to be translocated to heat shock granules and bind to HSE (Hubel and Schoffl, 1994; Jolly et al., 1999; Jolly et al., 2002; Mercier et al., 1999; Zhang et al., 2003).

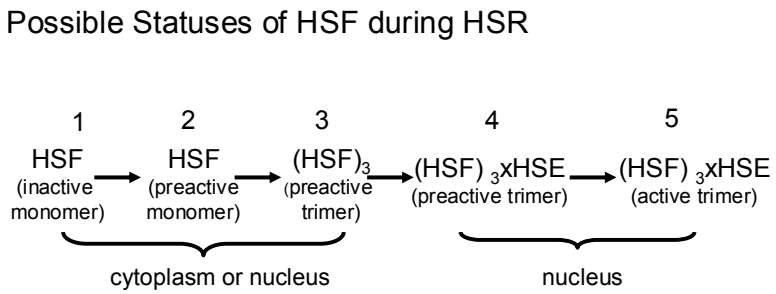


**Figure 1.3** Heat stress activation of HSFs may involve multiple steps. Except in yeast and Xenopus oocytes, HSFs from other organisms are not bound to HSE under non-stress conditions. Heat stress activates the repressed monomeric HSF (status #1), which could be bound to HSPs, and the formation of HSF trimers (status #3). The preactivated HSF trimers then will be translocated into the nucleus and bind to the HSE (status #4) to promote expression of *hsp* genes (status #5). Mammalian HSF1 is mostly localized to the nucleus even before HS (status #1), whereas HSFs from plants show various patterns of cellular localizations.

A simplified model of autoregulation has been proposed to explain the mechanisms of HSF protein activation and inactivation (Craig and Gross, 1991). The autoregulation model proposed that HSFs are repressed by cytoplasmic HSPs under non-stress conditions (Figure 1.1). The repression is released when the HSPs are sequestered by denatured proteins during heat stress, which consequently activates the expression of *hsp* genes. After sufficient amounts of HSP proteins are produced, they feedback inhibit HSFs. Both HSP70 and HSP90 are involved in the feedback regulation of HSFs. The interactions between HSF1 and HSP70 as well as HSP90 has been observed in yeast, *Drosohpila*, human and *Arabidopsis* (Abravaya et al., 1992; Ali et al., 1998; Bharadwaj et al, 1999; Bonner et al., 2000; Kim and Schoffl, 2002; Marchler and Wu, 2001; Rabindran et al., 1994; Shi et al., 1998). Over-expression of HSP70 results in premature termination of the heat shock response in *Drosohpila,* rat and human, whereas depletion of cellular HSP90 by HSP90 antibody injection delayed the attenuation process in *Xenopus* (Ali et al., 1998; Mosser et al., 1993; Rabindran et al., 1994). The roles of HSP70 in regulating HSF1 activity are further supported by mutation and transgenic analyses. Double deletion mutant of yeast *hsp70*s (*SSA1* and *SSA2*) leads to constitutive expression of heat inducible *hsp* genes, which can be suppressed by additional mutations in *hsf* (Craig and Jacobsen, 1984; Halladay and Craig, 1995). *Arabidopsis* plants transformed with antisense *hsp70* also exhibit constitutive expression of *hsp* genes (Lee and Schoffl, 1996).

Although accumulated evidence supports a necessary role of HSPs in repressing the transcriptional activity of HSFs under non-stress conditions as well as during attenuation of the heat shock response, other factors are also involved in the complex regulation of HSFs. First of all, there are intrinsic features of HSF that regulate their own activation. One of them is the HR-C domain, which can form an intramolecular coiled coil structure with the HR-A/B domain and

prevents the HR-A/B mediated oligomerization of HSFs (Zuo et al., 1994). Two cysteine residues in the DBD of HSF1 can also directly sense heat or oxidative stress and result in HSF1 homotrimerization (Ahn and Thiele, 2003). Intermolecular interactions between HSF and other non-HSP proteins have also been documented (Lin and Lis, 1999). Most remarkable is the detection of a small HSF-BINDING PROTEIN (HSBP1) in nematodes, mammals and plants (Satyal et al., 1998 and herein). Over-expression of *hsbp1* in nematodes results in decreased strength and duration of the heat shock response, while loss of function of *hsbp1* mutations in maize lead to over-expression of *hsp* genes even under non-stress conditions (Satyal et al., 1998; Fu et al., 2002). Lastly, activation and inactivation of HSFs is also correlated with phosphorylation on multiple serine and threonine residues in yeast and animals (Figure 1.5; Hoj and Jakobsen, 1994; Larson et al., 1988; Sorger et al., 1987; Sorger 1990; Sorger and Pelham, 1988). However, phosphorylation of plant HSFs has never been demonstrated.

## Coiled Coils Mediated Protein-Protein Interactions in Biology and Engineering

### The structure of coiled-coil domain

The α-helical coiled-coil is a principle protein oligomerization domain (see Fig.1.6 for an example; reviewed by Burkhard, 2001 and references therein). Coiled coils consist of two or more α-helices that wrap around each other in a knobs-into-holes fashion with a slight superhelical twist (Crick, 1953). It has been predicted that 2~3 percent of protein residues as well as about 5 percent of eukaryotic proteins form coiled coils (Newman et al., 2000; Wolf et al., 1995). The regular structure of coiled coils results from the amino acid heptad repeat denoted $(\mathbf{abcdefg})_n$(Fig1.6). In typical double-or triple-stranded coiled coils, the amino acids at **a** and **d** positions are predominantly hydrophobic, and they make up the core of the coiled-coil interface

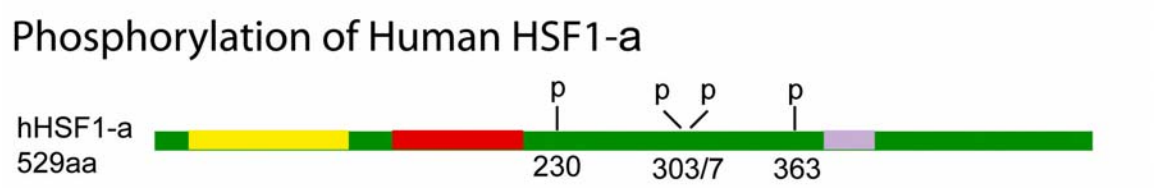


**Figure 1.4** Multiple phosphorylation events are correlated with the activity of human HSF1. Under non-stress temperatures, Ser303, Ser307 and Ser363 are all phosphorylated either by the glycogen synthase kinase (GSK-3β), or the c-Jun N-terminal kinase (JNK). In response to HS, an additional residue, the Ser270 is phosphorylated, probably by the calcium/calmodulin dependent protein kinase II (CaMKII). The phosphorylation of Ser270 is not required for the immediate activation of HSF1, but rather for the latter's sustained activity under extended HS (modified from Pirkkala et a., 2001).

(Fig1.6B&C). The interhelical hydrophobic interactions between **a** residues and **d** residues are the main driving force of coiled coil formation (Crick, 1953; Thompson et al., 1993). In contrast, the **e** and **g** residues are typically polar or charged (McLachlan and Stewart, 1975). The electrostatic interactions between **e** and **g'** and/or between **g** and **e'** can either strengthen or destabilize the coiled-coil structure (Krylov et al., 1998; Moll et al., 2000; Spek et al., 1998). The ionic interactions depend on the charge, orientation and distance between paired residues. Therefore, ionic interactions are important for the alignment, orientation and selectivity of coiled coils (Kohn et al, 1995; Krylov et al., 1994; Lavigne et al., 1995; O'Shea et al., 1992; Vinson et al., 1993). In a four-stranded coiled-coil structure, the **b** and **c** residues instead are responsible for the specificity of coiled-coil formation (Vu et al., 2001). Nonetheless, it is common that one α-helix strand can pair with several different α-helixes to form coiled coils. HSF1 is one such example. The HRA/B domain of HSF1 can form either homotypic coiled coils with itself, or heterotypic coiled coils with the HR-C domain as well as the HSBP1 protein (reviewed by Morimoto, 1998 and references therein). In a more extensive survey, 10 out of 74 coiled coil domains from yeast proteins have more than one interaction partner (Newman et al., 2000).

**Regulations of coiled coils formation**

Besides the primary structure of the heptad repeats, physiological factors also regulate the formation of coiled coils. The first level of regulation is executed on the α-helix formation level. Interactions between osmolytes and the peptide backbone are energetically unfavorable (Liu and Bolen, 1995). Consequently, osmolytes are preferentially excluded from the immediate contact area around protein molecules, and this phenomenon is termed the osmophobic effect (Timasheff, 1993). Therefore, addition of osmolytes induces the formation of α-helix and stabilizes coiled coils (Celinski and Scholtz, 2002). In contrast, increase in temperature diminishes the

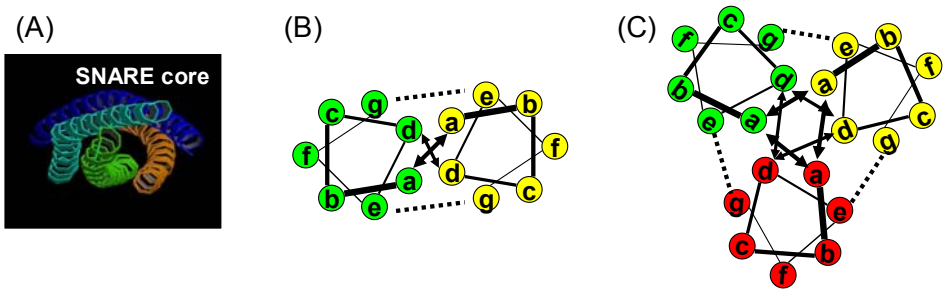


**Figure 1.5** Structures of the coiled-coil domain. (**A**) The crystal structure of the four-stranded coiled-coil of the SNARE core complex formed by syntaxin, synaptobrevin and SNAP-25 (Sutton et al., 1998). (**B**) Helical wheel representation of a parallel two-stranded coiled coil. (**C**) Helical wheel representation of a parallel three-stranded coiled-coil. Letters '**a**' through '**g**' denotes the seven residues in a heptad repeat.

intrahelical hydrogen bonding and subverts the α-helix formation. The second level of regulation is targeted at the interhelical electrostatic interactions (Krylov et al., 1998; Vu et al., 2001). The charge of amino acids depends on pKa and pH. Therefore, changes in pH directly affect the charge of residues at **e** and **g** positions. Discharging of residues involved in ionic interactions can effectively destabilize the coiled coils mediated assembly of intermediate filament (Wu et al., 2000). In addition, salt can also effectively shield off electrostatic interactions between adjacent residues, because salt itself can partner with charged residues in electrostatic interactions. Lastly, formation of coiled coils can also be regulated by extra-helical regions, the conformation of which can be affected by microenvironments. For example, when Cysteine residues are placed nearby α-helixes, the formation of disulfide bridges can bring two α-helixes together and facilitate the formation of coiled coils. The regulation of the disulfide bridge formation by the redox status consequently enables the latter to indirectly affect the process of coiled coils formation (Wagschal et al., 1999). The formation of three-stranded coiled coils among HSF trimers after heat and redox stress also requires the formation of disulfide bridge on the N-terminal of HRA/B α-helixes region (Ahn and Thiele, 2003). Another extra-helical modification event that affects coiled coil formation is phosphorylation. Phosphorylation of threonine residues between two helical regions of myosin heavy chain introduces a bend in the myosin heavy chain, which results in the formation of an intra-molecular antiparallel two stranded coiled coil and prohibits myosin assembly (Liang et al., 1999). Heat induced phosphorylations of HSFs also results in a shift from the intramolecular two-stranded coiled-coil between HR-A/B and HR-C to an intermolecular three-stranded coiled-coil among HR-A/Bs (Rabindran et al., 1993; Sorger and Nelson, 1989).

**Biological functions of coiled coils and their applications in engineering**

The abundance and the amenability of regulation allow coiled-coil domains to mediate almost every aspect of cell biology (examples shown in Table 1.3 and references therein). By modulating the interfaces, coiled coils can have either high rigidity, which is important for cytoskeletons to provide mechanical support for cells, or relative lability, which is essential for the dynamic assembly and disassembly of cytoskeletons during movement (Herrmann et al., 1999; Herrmann et al., 2002). The specificity and multiplicity of coiled-coil interactions enables them to mediate signal transductions, transcription regulation, as well as vesicle trafficking events. Coiled-coil domains are also extensively utilized in stress responses and developmental regulations because the stability and specificity of their interactions is susceptible to post-translational and physiological regulation.

## Purpose of the Study

Heat stress is one of the major environmental challenges to both animals and plants. A better understanding of how organisms respond to heat stress will enable us to improve both health care and agricultural productivity. In the last two decades, we have seen an exponential growth of our knowledge regarding the mechanism of heat shock response as well as the roles of each molecular component in this system. The maize embryo lethal mutant empty pericarp 2 (emp2) shows defective regulation of heat shock response. The *emp2* gene is predicted to be a coiled-coil protein that is homologous to human heat shock transcription factor binging protein. The purpose of this dissertation is to address several very important questions regarding heat shock response and its regulation in maize using the emp2 mutant and the EMP2 protein.

**Table 1.3** Examples of Coiled-coil Proteins

| protein | cellular function | site of regulation | references |
|---|---|---|---|
| vimentin | cytoskeleton (intermediate filament) | salt bridge | Herrman et al., 2000 |
| myosin | motor protein | $Ca^{2+}$ dependent interaction of coiled coil domain with regulatory domain | Malnasi-Csizmadia et al., 1998 |
| kinesin | motor protein | the kinesin neck region beyond the coiled coil domain | Kozielski et al., 1997; Romeberg et al., 1998 |
| dynein | motor protein | binding of ATP to the head region adjacent to the coiled-coil stalks | Johnson, 1985; Burgess, 1995 |
| macrophage scavenger receptor | macrophage associated cell adhesion and low density lipoprotein uptake by endocytosis | low pH leads to protonation of His260 at core positions of coiled coil, unfolding of the coiled-coil domain and release of ligand | Doi et al., 1994 |
| SNARE proteins | protein trafficking. syntaxin, synaptobrevin and SNAP-25 forms a core complex by forming a tetra-stranded coiled-coil structure. Glutamine residue at **d** positions of heptad repeat in syntaxin and SNAP-25 interact with the arginine residues also at **d** positions of synaptobrevin. | N-terminal coiled coil domain forms intra-molecular with the C-terminal heptad repeat and inhibits coiled coils formation between syntaxin and other SNARE proteins. | Munson et al., 2000; Nicholson et al., 1998 |
| *c-fos* and *c-jun* | b/ZIP class transcription factor. heterodimerize to promote gene transcription in response to mitogenic stimuli | homodimerization disables transcriptional activity | O'Shea et al., 1992 |
| c-Myc and Max | b/HLH/ZIP class transcription factor | heterodimerization is pH dependent (pH4.6 is the optimum) | Lavigne et al., 1998 |

1) What are the consequences of unattenuated heat shock response? Although over expression of active HSF or loss of function of HSP70 results in the over expression of *hsp* genes, there is still no system that specifically blocks the attenuation of HSR;

2) What are the additional biological functions of a coiled-coil domain? It is obvious that coiled-coil domains are involved in every aspect of cellular processes. However, most of the proteins containing coiled-coil domains have not yet been studied;

3) How do ionic interactions contribute to the protein-protein interaction specificities of coiled-coil proteins? It is known that inter-helical ionic interactions are important for the pairing specificities of α-helixes. However, it is still impossible to predict coiled coil specificity based on primary structures.

This thesis is organized as follows. Chapter 1 is the introduction and literature review. Chapter 2 is entitled "empty pericarp2 encodes a negative regulator of the heat shock response and is required for maize embryogenesis", which has been published in Plant Cell. Chapter 3 is entitiled "Clonal mosaic analysis of empty pericarp2 reveals non-redundant functions of the duplicated HEAT SHOCK FACTOR BINDING PROTEINs during maize shoot development". It will be published in the July issue (2004) of Genetics. Chapter 4 is entitled "Maize Coiled-coil Protein Paralogues, EMP2 and HSBP2, Have Distinct Protein-Protein Interaction Specificities", which will be submitted to Plant Cell upon completion.

## References

Abravaya, K., Myers, M. P., Murphy, S. P. and Morimoto, R. I. (1992). The human heat shock protein hsp70 interacts with HSF, the transcription factor that regulates heat shock gene expression. Genes Dev 6, 1153-64.

Ahn, S. G. and Thiele, D. J. (2003). Redox regulation of mammalian heat shock factor 1 is essential for Hsp gene activation and protection from stress. Genes Dev 17, 516-28.

Alastalo, T. P., Hellesuo, M., Sandqvist, A., Hietakangas, V., Kallio, M. and Sistonen, L. (2003). Formation of nuclear stress granules involves HSF2 and coincides with the nucleolar localization of Hsp70. J Cell Sci 116, 3557-70.

Ali, A., Bharadwaj, S., O'Carroll, R. and Ovsenek, N. (1998). HSP90 interacts with and regulates the activity of heat shock factor 1 in Xenopus oocytes. Mol Cell Biol 18, 4949-60.

Altshculer, M., and Mascarenhas, J.P. (1981). Synthesis of heat shock proteins in soybean seedlings. Plant Physiol 67S, 91.

Bardelli, A., Longati, P., Albero, D., Goruppi, S., Schneider, C., Ponzetto, C. and Comoglio, P. M. (1996). HGF receptor associates with the anti-apoptotic protein BAG-1 and prevents cell death. Embo J 15, 6205-12.

Beere, H. M., Wolf, B. B., Cain, K., Mosser, D. D., Mahboubi, A., Kuwana, T., Tailor, P., Morimoto, R. I., Cohen, G. M. and Green, D. R. (2000). Heat-shock protein 70 inhibits apoptosis by preventing recruitment of procaspase-9 to the Apaf-1 apoptosome. Nat Cell Biol 2, 469-75.

Berardini, T. Z., Bollman, K., Sun, H. and Poethig, R. S. (2001). Regulation of vegetative phase change in Arabidopsis thaliana by cyclophilin 40. Science 291, 2405-7.

Bharadwaj, S., Ali, A. and Ovsenek, N. (1999). Multiple components of the HSP90 chaperone complex function in regulation of heat shock factor 1 In vivo. Mol Cell Biol 19, 8033-41.

Bharadwaj, S., Hnatov, A., Ali, A. and Ovsenek, N. (1998). Induction of the DNA-binding and transcriptional activities of heat shock factor 1 is uncoupled in Xenopus oocytes. Biochim Biophys Acta 1402, 79-85.

Bharti, K., Schmidt, E., Lyck, R., Heerklotz, D., Bublak, D. and Scharf, K. D. (2000). Isolation and characterization of HsfA3, a new heat stress transcription factor of Lycopersicon peruvianum. Plant J 22, 355-65.

Bonner, J. J., Carlson, T., Fackenthal, D. L., Paddock, D., Storey, K. and Lea, K. (2000). Complex regulation of the yeast heat shock transcription factor. Mol Biol Cell 11, 1739-51.

Brady, J. P., Garland, D., Duglas-Tabor, Y., Robison, W. G., Jr., Groome, A. and Wawrousek, E. F. (1997). Targeted disruption of the mouse alpha A-crystallin gene induces cataract and cytoplasmic inclusion bodies containing the small heat shock protein alpha B-crystallin. Proc Natl Acad Sci U S A 94, 884-9.

Browder, L. W., Pollock, M., Nickells, R. W., Heikkila, J. J. and Winning, R. S. (1989). Developmental regulation of the heat-shock response. Dev Biol (N Y 1985) 6, 97-147.

Bukau, B. and Horwich, A. L. (1998). The Hsp70 and Hsp60 chaperone machines. Cell 92, 351-66.

Bukau, B. and Walker, G. C. (1989). Cellular defects caused by deletion of the Escherichia coli dnaK gene indicate roles for heat shock protein in normal metabolism. J Bacteriol 171, 2337-46.

Bukau, B. and Walker, G. C. (1990). Mutations altering heat shock specific subunit of RNA polymerase suppress major cellular defects of E. coli mutants lacking the DnaK chaperone. Embo J 9, 4027-36.

Burgess, S. A. (1995). Rigor and relaxed outer dynein arms in replicas of cryofixed motile flagella. J Mol Biol 250, 52-63.

Burkhard, P., Stetefeld, J. and Strelkov, S. V. (2001). Coiled coils: a highly versatile protein folding motif. Trends Cell Biol 11, 82-8.

Cao, D., Froehlich, J. E., Zhang, H. and Cheng, C. L. (2003). The chlorate-resistant and photomorphogenesis-defective mutant cr88 encodes a chloroplast-targeted HSP90. Plant J 33, 107-18.

Cartier, M., Breitman, M. L. and Tsui, L. C. (1992). A frameshift mutation in the gamma E-crystallin gene of the Elo mouse. Nat Genet 2, 42-5.

Celinski, S. A. and Scholtz, J. M. (2002). Osmolyte effects on helix formation in peptides and the stability of coiled-coils. Protein Sci 11, 2048-51.

Chan, H. Y., Warrick, J. M., Andriola, I., Merry, D. and Bonini, N. M. (2002). Genetic modulation of polyglutamine toxicity by protein conjugation pathways in Drosophila. Hum Mol Genet 11, 2895-904.

Chao, H., Bautista, D. L., Litowski, J., Irvin, R. T. and Hodges, R. S. (1998). Use of a heterodimeric coiled-coil system for biosensor application and affinity purification. J Chromatogr B Biomed Sci Appl 715, 307-29.

Christians, E., Michel, E., Adenot, P., Mezger, V., Rallu, M., Morange, M. and Renard, J. P. (1997). Evidence for the involvement of mouse heat shock factor 1 in the atypical expression of the HSP70.1 heat shock gene during mouse zygotic genome activation. Mol Cell Biol 17, 778-88.

Clarimon, J., Bertranpetit, J., Boada, M., Tarraga, L. and Comas, D. (2003). HSP70-2 (HSPA1B) is associated with noncognitive symptoms in late-onset Alzheimer's disease. J Geriatr Psychiatry Neurol 16, 146-50.

Clos, J., Westwood, J. T., Becker, P. B., Wilson, S., Lambert, K. and Wu, C. (1990). Molecular cloning and expression of a hexameric Drosophila heat shock factor subject to negative regulation. Cell 63, 1085-97.

Craig, E. A. and Gross, C. A. (1991). Is hsp70 the cellular thermometer? Trends Biochem Sci 16, 135-40.

Craig, E. A. and Jacobsen, K. (1984). Mutations of the heat inducible 70 kilodalton genes of yeast confer temperature sensitive growth. Cell 38, 841-9.

Crick, F. C. H. (1953). The packing of a-helices:simple coiled coils. Acta Crystallographica 6, 689-697.

Cutforth, T. and Rubin, G. M. (1994). Mutations in Hsp83 and cdc37 impair signaling by the sevenless receptor tyrosine kinase in Drosophila. Cell 77, 1027-36.

Davies, T. H., Ning, Y. M. and Sanchez, E. R. (2002). A new first step in activation of steroid receptors: hormone-induced switching of FKBP51 and FKBP52 immunophilins. J Biol Chem 277, 4597-600.

Dickson, B. J., van der Straten, A., Dominguez, M. and Hafen, E. (1996). Mutations Modulating Raf signaling in Drosophila eye development. Genetics 142, 163-71.

Dix, D. J., Allen, J. W., Collins, B. W., Mori, C., Nakamura, N., Poorman-Allen, P., Goulding, E. H. and Eddy, E. M. (1996). Targeted gene disruption of Hsp70-2 results in failed meiosis, germ cell apoptosis, and male infertility. Proc Natl Acad Sci U S A 93, 3264-8.

Doi, T., Kurasawa, M., Higashino, K., Imanishi, T., Mori, T., Naito, M., Takahashi, K., Kawabe, Y., Wada, Y., Matsumoto, A. et al. (1994). The histidine interruption of an alpha-helical coiled coil allosterically mediates a pH-dependent ligand dissociation from macrophage scavenger receptors. J Biol Chem 269, 25598-604.

Dura, J. M. (1981). Stage dependent synthesis of heat shock induced proteins in early embryos of Drosophila melanogaster. Mol Gen Genet 184, 381-5.

Duverger, O., Paslaru, L. and Morange, M. (2003). HSP25 is involved in two steps of the differentiation of PAM212 keratinocytes. J Biol Chem.

Eddy, E. M. (1998). HSP70-2 heat-shock protein of mouse spermatogenic cells. J Exp Zool 282, 261-71.

Elefant, F. and Palter, K. B. (1999). Tissue-specific expression of dominant negative mutant Drosophila HSC70 causes developmental defects and lethality. Mol Biol Cell 10, 2101-17.

Feder, J. H., Rossi, J. M., Solomon, J., Solomon, N. and Lindquist, S. (1992). The consequences of expressing hsp70 in Drosophila cells at normal temperatures. Genes Dev 6, 1402-13.

Finley, D., Ozkaynak, E. and Varshavsky, A. (1987). The yeast polyubiquitin gene is essential for resistance to high temperatures, starvation, and other stresses. Cell 48, 1035-46.

Fiorenza, M. T., Bevilacqua, A., Canterini, S., Torcia, S., Pontecorvi, M. and Mangia, F. (2004). Early Transcriptional Activation of the Hsp70.1 Gene by Osmotic Stress in One-Cell Embryos of the Mouse. Biol Reprod.

Fu, L. and Liang, J. J. (2003). Alteration of protein-protein interactions of congenital cataract crystallin mutants. Invest Ophthalmol Vis Sci 44, 1155-9.

Fu, S., Meeley, R. and Scanlon, M. J. (2002). Empty pericarp2 encodes a negative regulator of the heat shock response and is required for maize embryogenesis. Plant Cell 14, 3119-32.

Gallo, G. J., Prentice, H. and Kingston, R. E. (1993). Heat shock factor is required for growth at normal temperatures in the fission yeast Schizosaccharomyces pombe. Mol Cell Biol 13, 749-61.

Gebauer, M., Zeiner, M. and Gehring, U. (1998). Interference between proteins Hap46 and Hop/p60, which bind to different domains of the molecular chaperone hsp70/hsc70. Mol Cell Biol 18, 6238-44.

Georgopoulos, C. (1992). The emergence of the chaperone machines. Trends Biochem Sci 17, 295-9.

Gottesman, S. and Maurizi, M. R. (1992). Regulation by proteolysis: energy-dependent proteases and their targets. Microbiol Rev 56, 592-621.

Gurley, W. B., Czarnecka, E., Nagao, R. T. and Key, J. L. (1986). Upstream sequences required for efficient expression of a soybean heat shock gene. Mol Cell Biol 6, 559-65.

Gurley, W. B. and Key, J. L. (1991). Transcriptional regulation of the heat-shock response: a plant perspective. Biochemistry 30, 1-12.

Hahn, J. S. and Thiele, D. J. (2004). Activation of the Saccharomyces cerevisiae heat shock transcription factor under glucose starvation conditions by Snf1 protein kinase. J Biol Chem 279, 5169-76.

Halladay, J. T. and Craig, E. A. (1995). A heat shock transcription factor with reduced activity suppresses a yeast HSP70 mutant. Mol Cell Biol 15, 4890-7.

Hansen, J. J., Durr, A., Cournu-Rebeix, I., Georgopoulos, C., Ang, D., Nielsen, M. N., Davoine, C. S., Brice, A., Fontaine, B., Gregersen, N. et al. (2002). Hereditary spastic paraplegia SPG13 is associated with a mutation in the gene encoding the mitochondrial chaperonin Hsp60. Am J Hum Genet 70, 1328-32.

Hartl, F. U. (1996). Molecular chaperones in cellular protein folding. Nature 381, 571-9.

Heikkila, J. J., Kloc, M., Bury, J., Schultz, G. A. and Browder, L. W. (1985). Acquisition of the heat-shock response and thermotolerance during early development of Xenopus laevis. Dev Biol 107, 483-9.

Herrmann, H. and Aebi, U. (2000). Intermediate filaments and their associates: multi-talented structural elements specifying cytoarchitecture and cytodynamics. Curr Opin Cell Biol 12, 79-90.

Herrmann, H., Haner, M., Brettel, M., Ku, N. O. and Aebi, U. (1999). Characterization of distinct early assembly units of different intermediate filament proteins. J Mol Biol 286, 1403-20.

Herrmann, H., Wedig, T., Porter, R. M., Lane, E. B. and Aebi, U. (2002). Characterization of early assembly intermediates of recombinant human keratins. J Struct Biol 137, 82-96.

Hoj, A. and Jakobsen, B. K. (1994). A short element required for turning off heat shock transcription factor: evidence that phosphorylation enhances deactivation. Embo J 13, 2617-24.

Hong, S. W. and Vierling, E. (2001). Hsp101 is necessary for heat tolerance but dispensable for development and germination in the absence of stress. Plant J 27, 25-35.

Hubel, A. and Schoffl, F. (1994). Arabidopsis heat shock factor: isolation and characterization of the gene and the recombinant protein. Plant Mol Biol 26, 353-62.

Hubert, D. A., Tornero, P., Belkhadir, Y., Krishna, P., Takahashi, A., Shirasu, K. and Dangl, J. L. (2003). Cytosolic HSP90 associates with and modulates the Arabidopsis RPM1 disease resistance protein. Embo J 22, 5679-89.

Hunt, C. R., Dix, D. J., Sharma, G. G., Pandita, R. K., Gupta, A., Funk, M. and Pandita, T. K. (2004). Genomic instability and enhanced radiosensitivity in Hsp70.1- and Hsp70.3-deficient mice. Mol Cell Biol 24, 899-911.

Ishiguro, S., Watanabe, Y., Ito, N., Nonaka, H., Takeda, N., Sakai, T., Kanaya, H. and Okada, K. (2002). SHEPHERD is the Arabidopsis GRP94 responsible for the formation of functional CLAVATA proteins. Embo J 21, 898-908.

Jakobsen, B. K. and Pelham, H. R. (1991). A conserved heptapeptide restrains the activity of the yeast heat shock transcription factor. Embo J 10, 369-75.

Jedlicka, P., Mortin, M. A. and Wu, C. (1997). Multiple functions of Drosophila heat shock transcription factor in vivo. Embo J 16, 2452-62.

Jentsch, S. (1992). The ubiquitin-conjugation system. Annu Rev Genet 26, 179-207.

Johnson, K. A. (1985). Pathway of the microtubule-dynein ATPase and the structure of dynein: a comparison with actomyosin. Annu Rev Biophys Biophys Chem 14, 161-88.

Jolly, C., Konecny, L., Grady, D. L., Kutskova, Y. A., Cotto, J. J., Morimoto, R. I. and Vourc'h, C. (2002). In vivo binding of active heat shock transcription factor 1 to human chromosome 9 heterochromatin during stress. J Cell Biol 156, 775-81.

Jolly, C., Usson, Y. and Morimoto, R. I. (1999). Rapid and reversible relocalization of heat shock factor 1 within seconds to nuclear stress granules. Proc Natl Acad Sci U S A 96, 6769-74.

Kamphausen, T., Fanghanel, J., Neumann, D., Schulz, B. and Rahfeld, J. U. (2002). Characterization of Arabidopsis thaliana AtFKBP42 that is membrane-bound and interacts with Hsp90. Plant J 32, 263-76.

Kamradt, M. C., Chen, F., Sam, S. and Cryns, V. L. (2002). The small heat shock protein alpha B-crystallin negatively regulates apoptosis during myogenic differentiation by inhibiting caspase-3 activation. J Biol Chem 277, 38731-6.

Kanei-Ishii, C., Tanikawa, J., Nakai, A., Morimoto, R. I. and Ishii, S. (1997). Activation of heat shock transcription factor 3 by c-Myb in the absence of cellular stress. Science 277, 246-8.

Katiyar-Agarwal, S., Agarwal, M. and Grover, A. (2003). Heat-tolerant basmati rice engineered by over-expression of hsp101. Plant Mol Biol 51, 677-86.

Kawazoe, Y., Tanabe, M., Sasai, N., Nagata, K. and Nakai, A. (1999). HSF3 is a major heat shock responsive factor duringchicken embryonic development. Eur J Biochem 265, 688-97.

Kazemi-Esfarjani, P. and Benzer, S. (2000). Genetic suppression of polyglutamine toxicity in Drosophila. Science 287, 1837-40.

Key, J., Lin, CY and Chen, YM. (1981). Heat shock proteins of higher plants. Proc Natl Acad Sci U S A 78, 3526-3530.

Kim, B. H. and Schoffl, F. (2002). Interaction between Arabidopsis heat shock transcription factor 1 and 70 kDa heat shock proteins. J Exp Bot 53, 371-5.

Kosano, H., Stensgard, B., Charlesworth, M. C., McMahon, N. and Toft, D. (1998). The assembly of progesterone receptor-hsp90 complexes using purified proteins. J Biol Chem 273, 32973-9.

Kozielski, F., Sack, S., Marx, A., Thormahlen, M., Schonbrunn, E., Biou, V., Thompson, A., Mandelkow, E. M. and Mandelkow, E. (1997). The crystal structure of dimeric kinesin and implications for microtubule-dependent motility. Cell 91, 985-94.

Krylov, D., Barchi, J. and Vinson, C. (1998). Inter-helical interactions in the leucine zipper coiled coil dimer: pH and salt dependence of coupling energy between charged amino acids. J Mol Biol 279, 959-72.

Kullmann, M., Schneikert, J., Moll, J., Heck, S., Zeiner, M., Gehring, U. and Cato, A. C. (1998). RAP46 is a negative regulator of glucocorticoid receptor action and hormone-induced apoptosis. J Biol Chem 273, 14620-5.

Kurzik-Dumke, U., Phannavong, B., Gundacker, D. and Gateff, E. (1992). Genetic, cytogenetic and developmental analysis of the Drosophila melanogaster tumor suppressor gene lethal(2)tumorous imaginal discs (1(2)tid). Differentiation 51, 91-104.

Landry, J., Chretien, P., Lambert, H., Hickey, E. and Weber, L. A. (1989). Heat shock resistance conferred by expression of the human HSP27 gene in rodent cells. J Cell Biol 109, 7-15.

Lange, B. M., Bachi, A., Wilm, M. and Gonzalez, C. (2000). Hsp90 is a core centrosomal component and is required at different stages of the centrosome cycle in Drosophila and vertebrates. Embo J 19, 1252-62.

Larson, J. S., Schuetz, T. J. and Kingston, R. E. (1988). Activation in vitro of sequence-specific DNA binding by a human regulatory factor. Nature 335, 372-5.

Lavigne, P., Crump, M. P., Gagne, S. M., Hodges, R. S., Kay, C. M. and Sykes, B. D. (1998). Insights into the mechanism of heterodimerization from the 1H-NMR solution structure of the c-Myc-Max heterodimeric leucine zipper. J Mol Biol 281, 165-81.

Lee, J. H., Hubel, A. and Schoffl, F. (1995). Derepression of the activity of genetically engineered heat shock factor causes constitutive synthesis of heat shock proteins and increased thermotolerance in transgenic Arabidopsis. Plant J 8, 603-12.

Lee, J. H. and Schoffl, F. (1996). An Hsp70 antisense gene affects the expression of HSP70/HSC70, the regulation of HSF, and the acquisition of thermotolerance in transgenic Arabidopsis thaliana. Mol Gen Genet 252, 11-9.

Li, G. C. (1983). Induction of thermotolerance and enhanced heat shock protein synthesis in Chinese hamster fibroblasts by sodium arsenite and by ethanol. J Cell Physiol 115, 116-22.

Li, G. C. and Laszlo, A. (1985). Amino acid analogs while inducing heat shock proteins sensitize CHO cells to thermal damage. J Cell Physiol 122, 91-7.

Liang, W., Warrick, H. M. and Spudich, J. A. (1999). A structural model for phosphorylation control of Dictyostelium myosin II thick filament assembly. J Cell Biol 147, 1039-48.

Lin, J. T. and Lis, J. T. (1999). Glycogen synthase phosphatase interacts with heat shock factor to activate CUP1 gene transcription in Saccharomyces cerevisiae. Mol Cell Biol 19, 3237-45.

Lindquist, S. (1986). The heat-shock response. Annu Rev Biochem 55, 1151-91.

Lindquist, S. and Craig, E. A. (1988). The heat-shock proteins. Annu Rev Genet 22, 631-77.

Lindquist, S. and Petersen, R. (1990). Selective translation and degradation of heat-shock messenger RNAs in Drosophila. Enzyme 44, 147-66.

Litowski, J. R. and Hodges, R. S. (2001). Designing heterodimeric two-stranded alpha-helical coiled-coils: the effect of chain length on protein folding, stability and specificity. J Pept Res 58, 477-92.

Litt, M., Kramer, P., LaMorticella, D. M., Murphey, W., Lovrien, E. W. and Weleber, R. G. (1998). Autosomal dominant congenital cataract associated with a missense mutation in the human alpha crystallin gene CRYAA. Hum Mol Genet 7, 471-4.

Liu, Y. and Bolen, D. W. (1995). The peptide backbone plays a dominant role in protein stabilization by naturally occurring osmolytes. Biochemistry 34, 12884-91.

Livak, K. J., Freund, R., Schweber, M., Wensink, P. C. and Meselson, M. (1978). Sequence organization and transcription at two heat shock loci in Drosophila. Proc Natl Acad Sci U S A 75, 5613-7.

Lo, J. F., Hayashi, M., Woo-Kim, S., Tian, B., Huang, J. F., Fearns, C., Takayama, S., Zapata, J. M., Yang, Y. and Lee, J. D. (2004). Tid1, a Cochaperone of the Heat Shock 70 Protein and the Mammalian Counterpart of the Drosophila Tumor Suppressor l(2)tid, Is Critical for Early Embryonic Development and Cell Survival. Mol Cell Biol 24, 2226-2236.

Lohmann, C., Eggers-Schumacher, G., Wunderlich, M. and Schoffl, F. (2004). Two different heat shock transcription factors regulate immediate early expression of stress genes in Arabidopsis. Mol Genet Genomics 271, 11-21.

Malnasi-Csizmadia, A., Shimony, E., Hegyi, G., Szent-Gyorgyi, A. G. and Nyitray, L. (1998). Dimerization of the head-rod junction of scallop myosin. Biochem Biophys Res Commun 252, 595-601.

Marchler, G. and Wu, C. (2001). Modulation of Drosophila heat shock transcription factor activity by the molecular chaperone DROJ1. Embo J 20, 499-509.

McLachlan, A. D. and Stewart, M. (1975). Tropomyosin coiled-coil interactions: evidence for an unstaggered structure. J Mol Biol 98, 293-304.

McMillan, D. R., Christians, E., Forster, M., Xiao, X., Connell, P., Plumier, J. C., Zuo, X., Richardson, J., Morgan, S. and Benjamin, I. J. (2002). Heat shock transcription factor 2 is not essential for embryonic development, fertility, or adult cognitive and psychomotor function in mice. Mol Cell Biol 22, 8005-14.

McMillan, D. R., Xiao, X., Shao, L., Graves, K. and Benjamin, I. J. (1998). Targeted disruption of heat shock transcription factor 1 abolishes thermotolerance and protection against heat-inducible apoptosis. J Biol Chem 273, 7523-8.

Mercier, P. A., Winegarden, N. A. and Westwood, J. T. (1999). Human heat shock factor 1 is predominantly a nuclear protein before and after heat stress. J Cell Sci 112 ( Pt 16), 2765-74.

Mezger, V., Rallu, M., Morimoto, R. I., Morange, M. and Renard, J. P. (1994). Heat shock factor 2-like activity in mouse blastocysts. Dev Biol 166, 819-22.

Moll, J. R., Olive, M. and Vinson, C. (2000). Attractive interhelical electrostatic interactions in the proline- and acidic-rich region (PAR) leucine zipper subfamily preclude heterodimerization with other basic leucine zipper subfamilies. J Biol Chem 275, 34826-32.

Morimoto, R. I. (1998). Regulation of the heat shock transcriptional response: cross talk between a family of heat shock factors, molecular chaperones, and negative regulators. Genes Dev 12, 3788-96.

Mosser, D. D., Caron, A. W., Bourget, L., Denis-Larose, C. and Massie, B. (1997). Role of the human heat shock protein hsp70 in protection against stress-induced apoptosis. Mol Cell Biol 17, 5317-27.

Muller, W. U., Li, G. C. and Goldstein, L. S. (1985). Heat does not induce synthesis of heat shock proteins or thermotolerance in the earliest stage of mouse embryo development. Int J Hyperthermia 1, 97-102.

Munson, M., Chen, X., Cocina, A. E., Schultz, S. M. and Hughson, F. M. (2000). Interactions within the yeast t-SNARE Sso1p that control SNARE complex assembly. Nat Struct Biol 7, 894-902.

Nagao, R. T., Czarnecka, E., Gurley, W. B., Schoffl, F. and Key, J. L. (1985). Genes for low-molecular-weight heat shock proteins of soybeans: sequence analysis of a multigene family. Mol Cell Biol 5, 3417-28.

Nakai, A. and Morimoto, R. I. (1993). Characterization of a novel chicken heat shock transcription factor, heat shock factor 3, suggests a new regulatory pathway. Mol Cell Biol 13, 1983-97.

Nakai, A., Suzuki, M. and Tanabe, M. (2000). Arrest of spermatogenesis in mice expressing an active heat shock transcription factor 1. Embo J 19, 1545-54.

Newman, J. R., Wolf, E. and Kim, P. S. (2000). A computationally directed screen identifying interacting coiled coils from Saccharomyces cerevisiae. Proc Natl Acad Sci U S A 97, 13203-8.

Nicholson, K. L., Munson, M., Miller, R. B., Filip, T. J., Fairman, R. and Hughson, F. M. (1998). Regulation of SNARE complex assembly by an N-terminal domain of the t-SNARE Sso1p. Nat Struct Biol 5, 793-802.

Nollen, E. A. and Morimoto, R. I. (2002). Chaperoning signaling pathways: molecular chaperones as stress-sensing 'heat shock' proteins. J Cell Sci 115, 2809-16.

Nover, L., Bharti, K., Doring, P., Mishra, S. K., Ganguli, A. and Scharf, K. D. (2001). Arabidopsis and the heat stress transcription factor world: how many heat stress transcription factors do we need? Cell Stress Chaperones 6, 177-89.

Omelyanenko, V., Kopeckova, P., Gentry, C., Shiah, J. G. and Kopecek, J. (1996). HPMA copolymer-anticancer drug-OV-TL16 antibody conjugates. 1. influence of the method of synthesis on the binding affinity to OVCAR-3 ovarian carcinoma cells in vitro. J Drug Target 3, 357-73.

O'Shea, E. K., Rutkowski, R. and Kim, P. S. (1992). Mechanism of specificity in the Fos-Jun oncoprotein heterodimer. Cell 68, 699-708.

Pandey, P., Saleh, A., Nakazawa, A., Kumar, S., Srinivasula, S. M., Kumar, V., Weichselbaum, R., Nalin, C., Alnemri, E. S., Kufe, D. et al. (2000). Negative regulation of cytochrome c-mediated oligomerization of Apaf-1 and activation of procaspase-9 by heat shock protein 90. Embo J 19, 4310-22.

Parsell, D. A. and Lindquist, S. (1993). The function of heat-shock proteins in stress tolerance: degradation and reactivation of damaged proteins. Annu Rev Genet 27, 437-96.

Perezgasga, L., Segovia, L. and Zurita, M. (1999). Molecular characterization of the 5' control region and of two lethal alleles affecting the hsp60 gene in Drosophila melanogaster. FEBS Lett 456, 269-73.

Perisic, O., Xiao, H. and Lis, J. T. (1989). Stable binding of Drosophila heat shock factor to head-to-head and tail-to-tail repeats of a conserved 5 bp recognition unit. Cell 59, 797-806.

Pirkkala, L., Alastalo, T. P., Nykanen, P., Seppa, L. and Sistonen, L. (1999). Differentiation lineage-specific expression of human heat shock transcription factor 2. Faseb J 13, 1089-98.

Pirkkala, L., Alastalo, T. P., Zuo, X., Benjamin, I. J. and Sistonen, L. (2000). Disruption of heat shock factor 1 reveals an essential role in the ubiquitin proteolytic pathway. Mol Cell Biol 20, 2670-5.

Pirkkala, L., Nykanen, P. and Sistonen, L. (2001). Roles of the heat shock transcription factors in regulation of the heat shock response and beyond. Faseb J 15, 1118-31.

Plesset, J., Palm, C. and McLaughlin, C. S. (1982). Induction of heat shock proteins and thermotolerance by ethanol in Saccharomyces cerevisiae. Biochem Biophys Res Commun 108, 1340-5.

Prandl, R., Hinderhofer, K., Eggers-Schumacher, G. and Schoffl, F. (1998). HSF3, a new heat shock factor from Arabidopsis thaliana, derepresses the heat shock response and confers thermotolerance when overexpressed in transgenic plants. Mol Gen Genet 258, 269-78.

Pratt, W. B. (1997). The role of the hsp90-based chaperone system in signal transduction by nuclear receptors and receptors signaling via MAP kinase. Annu Rev Pharmacol Toxicol 37, 297-326.

Precht, H., Christophersen, J., Hensel, H. and Larcher, W. (1973). Temperature and Life. Springer-Verlag.

Queitsch, C., Hong, S. W., Vierling, E. and Lindquist, S. (2000). Heat shock protein 101 plays a crucial role in thermotolerance in Arabidopsis. Plant Cell 12, 479-92.

Queitsch, C., Sangster, T. A. and Lindquist, S. (2002). Hsp90 as a capacitor of phenotypic variation. Nature 417, 618-24.

Rabindran, S. K., Haroun, R. I., Clos, J., Wisniewski, J. and Wu, C. (1993). Regulation of heat shock factor trimer formation: role of a conserved leucine zipper. Science 259, 230-4.

Rabindran, S. K., Wisniewski, J., Li, L., Li, G. C. and Wu, C. (1994). Interaction between heat shock factor and hsp70 is insufficient to suppress induction of DNA-binding activity in vivo. Mol Cell Biol 14, 6552-60.

Rallu, M., Loones, M., Lallemand, Y., Morimoto, R., Morange, M. and Mezger, V. (1997). Function and regulation of heat shock factor 2 during mouse embryogenesis. Proc Natl Acad Sci U S A 94, 2392-7.

Ritossa, F. (1962). A new puffing pattern induced by heat shock and DNP in Drosophila. Experientia 18, 571-573.

Romberg, L., Pierce, D. W. and Vale, R. D. (1998). Role of the kinesin neck region in processive microtubule-based motility. J Cell Biol 140, 1407-16.

Rosen, R. and Ron, E. Z. (2002). Proteome analysis in the study of the bacterial heat-shock response. Mass Spectrom Rev 21, 244-65.

Rutherford, S. L. and Lindquist, S. (1998). Hsp90 as a capacitor for morphological evolution. Nature 396, 336-42.

Saibil, H. (2000). Molecular chaperones: containers and surfaces for folding, stabilising or unfolding proteins. Curr Opin Struct Biol 10, 251-8.

Sanchez, Y. and Lindquist, S. L. (1990). HSP104 required for induced thermotolerance. Science 248, 1112-5.

Sarge, K. D., Murphy, S. P. and Morimoto, R. I. (1993). Activation of heat shock gene transcription by heat shock factor 1 involves oligomerization, acquisition of DNA-binding activity, and nuclear localization and can occur in the absence of stress. Mol Cell Biol 13, 1392-407.

Sarkar, S., Pollack, B. P., Lin, K. T., Kotenko, S. V., Cook, J. R., Lewis, A. and Pestka, S. (2001). hTid-1, a human DnaJ protein, modulates the interferon signaling pathway. J Biol Chem 276, 49034-42.

Satyal, S. H., Chen, D., Fox, S. G., Kramer, J. M. and Morimoto, R. I. (1998). Negative regulation of the heat shock transcriptional response by HSBP1. Genes Dev 12, 1962-74.

Scharf, K. D., Heider, H., Hohfeld, I., Lyck, R., Schmidt, E. and Nover, L. (1998). The tomato Hsf system: HsfA2 needs interaction with HsfA1 for efficient nuclear import and may be localized in cytoplasmic heat stress granules. Mol Cell Biol 18, 2240-51.

Scharf, K. D., Rose, S., Zott, W., Schoffl, F., Nover, L. and Schoff, F. (1990). Three tomato genes code for heat stress transcription factors with a region of remarkable homology to the DNA-binding domain of the yeast HSF. Embo J 9, 4495-501.

Schuetz, T. J., Gallo, G. J., Sheldon, L., Tempst, P. and Kingston, R. E. (1991). Isolation of a cDNA for HSF2: evidence for two heat shock factor genes in humans. Proc Natl Acad Sci U S A 88, 6911-5.

Schumann, W. (2003). The Bacillus subtilis heat shock stimulon. Cell Stress Chaperones 8, 207-17.

Seong, K. H., Ogashiwa, T., Matsuo, T., Fuyama, Y. and Aigaki, T. (2001). Application of the gene search system to screen for longevity genes in Drosophila. Biogerontology 2, 209-17.

Shi, Y., Mosser, D. D. and Morimoto, R. I. (1998). Molecular chaperones as HSF1-specific transcriptional repressors. Genes Dev 12, 654-66.

Shinohara, M., Gasior, S. L., Bishop, D. K. and Shinohara, A. (2000). Tid1/Rdh54 promotes colocalization of rad51 and dmc1 during meiotic recombination. Proc Natl Acad Sci U S A 97, 10814-9.

Shuey, D. J. and Parker, C. S. (1986). Binding of Drosophila heat-shock gene transcription factor to the hsp 70 promoter. Evidence for symmetric and dynamic interactions. J Biol Chem 261, 7934-40.

Sierra, J. M. and Zapata, J. M. (1994). Translational regulation of the heat shock response. Mol Biol Rep 19, 211-20.

Sistonen, L., Sarge, K. D., Phillips, B., Abravaya, K. and Morimoto, R. I. (1992). Activation of heat shock factor 2 during hemin-induced differentiation of human erythroleukemia cells. Mol Cell Biol 12, 4104-11.

Solomon, J. M., Rossi, J. M., Golic, K., McGarry, T. and Lindquist, S. (1991). Changes in hsp70 alter thermotolerance and heat-shock regulation in Drosophila. New Biol 3, 1106-20.

Sorger, P. K. (1990). Yeast heat shock factor contains separable transient and sustained response transcriptional activators. Cell 62, 793-805.

Sorger, P. K., Lewis, M. J. and Pelham, H. R. (1987). Heat shock factor is regulated differently in yeast and HeLa cells. Nature 329, 81-4.

Sorger, P. K. and Nelson, H. C. (1989). Trimerization of a yeast transcriptional activator via a coiled-coil motif. Cell 59, 807-13.

Sorger, P. K. and Pelham, H. R. (1988). Yeast heat shock factor is an essential DNA-binding protein that exhibits temperature-dependent phosphorylation. Cell 54, 855-64.

Spek, E. J., Bui, A. H., Lu, M. and Kallenbach, N. R. (1998). Surface salt bridges stabilize the GCN4 leucine zipper. Protein Sci 7, 2431-7.

Spradling, A., Pardue, M. L. and Penman, S. (1977). Messenger RNA in heat-shocked Drosophila cells. J Mol Biol 109, 559-87.

Stump, D. G., Landsberger, N. and Wolffe, A. P. (1995). The cDNA encoding Xenopus laevis heat-shock factor 1 (XHSF1): nucleotide and deduced amino-acid sequences, and properties of the encoded protein. Gene 160, 207-11.

Sun, W., Bernard, C., van de Cotte, B., Van Montagu, M. and Verbruggen, N. (2001). At-HSP17.6A, encoding a small heat-shock protein in Arabidopsis, can enhance osmotolerance upon overexpression. Plant J 27, 407-15.

Sutton, R. B., Fasshauer, D., Jahn, R. and Brunger, A. T. (1998). Crystal structure of a SNARE complex involved in synaptic exocytosis at 2.4 A resolution. Nature 395, 347-53.

Syken, J., De-Medina, T. and Munger, K. (1999). TID1, a human homolog of the Drosophila tumor suppressor l(2)tid, encodes two mitochondrial modulators of apoptosis with opposing functions. Proc Natl Acad Sci U S A 96, 8499-504.

Takahashi, A., Casais, C., Ichimura, K. and Shirasu, K. (2003). HSP90 interacts with RAR1 and SGT1 and is essential for RPS2-mediated disease resistance in Arabidopsis. Proc Natl Acad Sci U S A 100, 11777-82.

Takayama, K., Ogata, K., Nakanishi, Y., Yatsunami, J., Kawasaki, M. and Hara, N. (1996). Bcl-2 Expression as a Predictor of Chemosensitivities and Survival in Small Cell Lung Cancer. Cancer J Sci Am 2, 212.

Tanabe, M., Kawazoe, Y., Takeda, S., Morimoto, R. I., Nagata, K. and Nakai, A. (1998). Disruption of the HSF3 gene results in the severe reduction of heat shock gene expression and loss of thermotolerance. Embo J 17, 1750-8.

Tanabe, M., Nakai, A., Kawazoe, Y. and Nagata, K. (1997). Different thresholds in the responses of two heat shock transcription factors, HSF1 and HSF3. J Biol Chem 272, 15389-95.

Tang, A., Wang, C., Stewart, R. J. and Kopecek, J. (2001). The coiled coils in the design of protein-based constructs: hybrid hydrogels and epitope displays. J Control Release 72, 57-70.

Tanikawa, J., Ichikawa-Iwata, E., Kanei-Ishii, C., Nakai, A., Matsuzawa, S., Reed, J. C. and Ishii, S. (2000). p53 suppresses the c-Myb-induced activation of heat shock transcription factor 3. J Biol Chem 275, 15578-85.

Thompson, K. S., Vinson, C. R. and Freire, E. (1993). Thermodynamic characterization of the structural stability of the coiled-coil region of the bZIP transcription factor GCN4. Biochemistry 32, 5491-6.

Timakov, B. and Zhang, P. (2001). The hsp60B gene of Drosophila melanogaster is essential for the spermatid individualization process. Cell Stress Chaperones 6, 71-7.

Timasheff, S. N. (1993). The control of protein stability and association by weak interactions with water: how do solvents affect these processes? Annu Rev Biophys Biomol Struct 22, 67-97.

Trinklein, N. D., Murray, J. I., Hartman, S. J., Botstein, D. and Myers, R. M. (2004). The Role of Heat Shock Transcription Factor 1 in the Genome-wide Regulation of the Mammalian Heat Shock Response. Mol Biol Cell 15, 1254-61.

van der Straten, A., Rommel, C., Dickson, B. and Hafen, E. (1997). The heat shock protein 83 (Hsp83) is required for Raf-mediated signalling in Drosophila. Embo J 16, 1961-9.

Velazquez, J. M. and Lindquist, S. (1984). hsp70: nuclear concentration during environmental stress and cytoplasmic storage during recovery. Cell 36, 655-62.

Vicart, P., Caron, A., Guicheney, P., Li, Z., Prevost, M. C., Faure, A., Chateau, D., Chapon, F., Tome, F., Dupret, J. M. et al. (1998). A missense mutation in the alphaB-crystallin chaperone gene causes a desmin-related myopathy. Nat Genet 20, 92-5.

Vignols, F., Mouaheb, N., Thomas, D. and Meyer, Y. (2003). Redox control of Hsp70-Co-chaperone interaction revealed by expression of a thioredoxin-like Arabidopsis protein. J Biol Chem 278, 4516-23.

Vinson, C. R., Hai, T. and Boyd, S. M. (1993). Dimerization specificity of the leucine zipper-containing bZIP motif on DNA binding: prediction and rational design. Genes Dev 7, 1047-58.

Vu, C., Robblee, J., Werner, K. M. and Fairman, R. (2001). Effects of charged amino acids at b and c heptad positions on specificity and stability of four-chain coiled coils. Protein Sci 10, 631-7.

Wagschal, K., Tripet, B. and Hodges, R. S. (1999). De novo design of a model peptide sequence to examine the effects of single amino acid substitutions in the hydrophobic core on both stability and oligomerization state of coiled-coils. J Mol Biol 285, 785-803.

Wang, C., Stewart, R. J. and Kopecek, J. (1999). Hybrid hydrogels assembled from synthetic polymers and coiled-coil protein domains. Nature 397, 417-20.

Wang, H. G., Takayama, S., Rapp, U. R. and Reed, J. C. (1996). Bcl-2 interacting protein, BAG-1, binds to and activates the kinase Raf-1. Proc Natl Acad Sci U S A 93, 7063-8.

Warrick, J. M., Chan, H. Y., Gray-Board, G. L., Chai, Y., Paulson, H. L. and Bonini, N. M. (1999). Suppression of polyglutamine-mediated neurodegeneration in Drosophila by the molecular chaperone HSP70. Nat Genet 23, 425-8.

Wiederrecht, G., Seto, D. and Parker, C. S. (1988). Isolation of the gene encoding the S. cerevisiae heat shock transcription factor. Cell 54, 841-53.

Wolf, E., Kim, P. S. and Berger, B. (1997). MultiCoil: a program for predicting two- and three-stranded coiled coils. Protein Sci 6, 1179-89.

Wu, C. (1995). Heat shock transcription factors: structure and regulation. Annu Rev Cell Dev Biol 11, 441-69.

Wu, K. C., Bryan, J. T., Morasso, M. I., Jang, S. I., Lee, J. H., Yang, J. M., Marekov, L. N., Parry, D. A. and Steinert, P. M. (2000). Coiled-coil trigger motifs in the 1B and 2B rod domain segments are required for the stability of keratin intermediate filaments. Mol Biol Cell 11, 3539-58.

Wunderlich, M., Werr, W. and Schoffl, F. (2003). Generation of dominant-negative effects on the heat shock response in Arabidopsis thaliana by transgenic expression of a chimaeric HSF1 protein fusion construct. Plant J 35, 442-51.

Wyttenbach, A., Carmichael, J., Swartz, J., Furlong, R. A., Narain, Y., Rankin, J. and Rubinsztein, D. C. (2000). Effects of heat shock, heat shock protein 40 (HDJ-2), and proteasome inhibition on protein aggregation in cellular models of Huntington's disease. Proc Natl Acad Sci U S A 97, 2898-903.

Wyttenbach, A., Sauvageot, O., Carmichael, J., Diaz-Latoud, C., Arrigo, A. P. and Rubinsztein, D. C. (2002). Heat shock protein 27 prevents cellular polyglutamine toxicity and suppresses the increase of reactive oxygen species caused by huntingtin. Hum Mol Genet 11, 1137-51.

Xiao, X., Zuo, X., Davis, A. A., McMillan, D. R., Curry, B. B., Richardson, J. A. and Benjamin, I. J. (1999). HSF1 is required for extra-embryonic development, postnatal growth and protection during inflammatory responses in mice. Embo J 18, 5943-52.

Xing, H., Mayhew, C. N., Cullen, K. E., Park-Sarge, O. K. and Sarge, K. D. (2004). HSF1 modulation of hsp70 mRNA polyadenylation via interaction with symplekin. J Biol Chem.

Yu, Y. B. (2002). Coiled-coils: stability, specificity, and drug delivery potential. Adv Drug Deliv Rev 54, 1113-29.

Zhang, L., Lohmann, C., Prandl, R. and Schoffl, F. (2003). Heat stress-dependent DNA binding of Arabidopsis heat shock transcription factor HSF1 to heat shock gene promoters in Arabidopsis suspension culture cells in vivo. Biol Chem 384, 959-63.

Zou, J., Guo, Y., Guettouche, T., Smith, D. F. and Voellmy, R. (1998). Repression of heat shock transcription factor HSF1 activation by HSP90 (HSP90 complex) that forms a stress-sensitive complex with HSF1. Cell 94, 471-80.

Zou, Y., Zhu, W., Sakamoto, M., Qin, Y., Akazawa, H., Toko, H., Mizukami, M., Takeda, N., Minamino, T., Takano, H. et al. (2003). Heat shock transcription factor 1 protects cardiomyocytes from ischemia/reperfusion injury. Circulation 108, 3024-30.

Zuo, J., Rungger, D. and Voellmy, R. (1995). Multiple layers of regulation of human heat shock transcription factor 1. Mol Cell Biol 15, 4319-30.

# CHAPTER 2

# *EMPTY PERICARP2* ENCODES A NEGATIVE REGULATOR OF THE HEAT SHOCK RESPONSE AND IS REQUIRED FOR MAIZE EMBRYOGENESIS[1]

[1]Fu S, Meeley R, and Scanlon MJ. Empty pericarp2 encodes a negative regulator of the heat shock response and is required for maize embryogenesis. Plant Cell. 2002 Dec;14(12):3119-32. 

## Abstract

The heat shock response (HSR) is an evolutionarily conserved molecular/biochemical reaction to thermal stress that is essential to the survival of eukaryotic organisms. Recessive, *Mutator*-transposon mutations at the maize *empty pericarp2* (*emp2*) locus lead to dramatically increased expression of *heat shock protein* (*hsp*) genes, retarded embryo development, and early-staged abortion of embryogenesis. The developmental timing of emp2 mutant embryo lethality is correlated with the initial competency of maize kernels to invoke the HSR. Cloning and sequence analyses reveal that *emp2* gene encodes the maize orthologue of HEAT SHOCK BINDING PROTEIN1 (ZmHSBP1), first-described in animals as a negative regulator of the HSR. The *emp2* is a null mutation at *Zmhsbp1* and the first HSR negative regulator identified in plants. Despite the recessive emp2 phenotype, steady state levels of *emp2* transcripts are abundant in mutant kernels and the predicted coding region is unaffected. These expression data suggest that *emp2* transcription is feedback regulated, whereas S1 nuclease mapping suggests that emp2 mutant transcripts are 5' truncated and non-translatable. In support of this model, immunoblot assays reveal that EMP2 protein does not accumulate in mutant kernels. The data implicate a model whereby an unattenuated HSR results in the early abortion of emp2 mutant embryos. Furthermore, the developmental retardation of emp2 mutant kernels prior to the HSR implicates an additional role for EMP2 during embryo development, distinct from the HSR.

## Introduction

Eukaryotic cells are subjected to a variety of environmental challenges and stresses, which demand rapid detection and effective responses in order to ensure survival of the organism. Exposure to heat shock induces alterations in the conformation of cellular proteins, which if left unchecked, lead to protein denaturation or aggregation, and cell death (reviewed in Schleshinger et al, 1982; Vierling, 1991; Morimoto, 1998; Schoffl et al., 1998; Santoro, 2000). In response to elevated temperature the transcription and translation of many cellular proteins is repressed or arrested, whereas the expression of a small subset of specialized heat shock proteins (HSP's) is preferentially elevated. The HSP's are molecular chaperonins that regulate protein homeostasis and membrane fluidity, and ultimately prevent or delay cell death during heat stress. This physiological response to thermal stress, termed the heat shock response (HSR), is one of the most evolutionarily conserved biochemical pathways in nature. Most plant tissue and cells are competent to induce the heat shock response during thermal stress. However, two stages in the plant life cycle, pollen germination and early embryogenesis (i.e. prior to cotyledon formation) are notable for their inability to invoke the full, heat shock response (Vierling, 1991; Schoffl, et al., 1998; Schrauwen et al., 1986; Pitto, et al., 1983). As a result, these tissues are especially sensitive to thermal stress.

The promoter regions of *hsp* genes contain a cis-regulatory sequence (5'-nGAAn-3') termed the heat shock element (HSE) that is required for the transcriptional up-regulation of *hsp* genes during thermal stress (Pelham, 1982; Amin et al., 1988; Barros et al., 1992; Fernandes et al., 1994). Typically, three copies of the HSE pentamer ensure efficient transcriptional activation of a *hsp* gene, whereas additional HSE's confer higher levels of promoter activity (Xiao et al., 1991). The sequence of the HSE is extremely conserved from yeast to mammals to higher plants,

and predicts the structural conservation and ancient origin of the corresponding regulatory proteins. Stress-induced transcription of *hsp* genes requires the mobilization and activation of HEAT SHOCK FACTORs (HSF), which bind to the HSE's of *hsp* genes and regulate their transcription (reviewed in Wu, 1995). Yeast and *Drosophila* harbor a single HSF, however most eukaryotes have redundant and tissue specific versions of HSF. Plant genomes, in particular, contain complex HSF families. The *Arabidopsis* genome contains 21 versions of HSF, whereas 24 copies are present in rice (Nover et al., 2001; Goff et al., 2002). At least six maize *hsf* genes are annotated in the public EST database (Guo et al., 2000); the discovery of additional maize HSF's is likely following sequencing of the maize genome. Promotion of *hsp* gene transcription requires HSF trimerization, which is mediated by oligomerization domains (HRA and HRB) comprised of hydrophobic, heptad repeat residues in HSF monomers (reviewed in Wu, 1995). Plant HSFs comprise three classes (A, B, C) based on the length of the linker region between the oligomerization domains (HRA/HRB) and the DNA binding domain (DBD), and the number of residues inserted between HRA and HRB. Accumulated evidence indicates that the multiple plant HSF's have evolved functional diversity, although relatively little is known concerning the regulation of diverse HSF functions (Nover, 2001).

Upon the attenuation of heat shock response, the HSP's (mainly HSP70) bind and thereby inhibit the transcriptional activity of the HSF trimers (Mosser et al., 1993). In addition, the recently identified HEAT SHOCK FACTOR BINDING PROTEIN1 (HSBP1) also binds to the active-trimerized form of HSF (Satyal et al., 1998). HSBP1 is a small protein with characteristic hydrophobic, heptad repeats in the central region. The heptad repeats of HSBP1 interact with the hydrophobic oligomerization domains (HRA and HRB) of HSF1; this interaction correlates with disassembly of the HSF trimers and attenuation of the heat shock transcriptional response (Satyal

et al., 1998). These findings are consistent with a role of HSBP1 during negative regulation of the heat shock response.

Here we describe the cloning of *empty pericarp2,* which encodes a maize orthologue HSBP1. Null mutations in *emp2* result in upregulated expression of maize *hsp* genes, correlated with embryo and kernel abortion at early stages of embryogenesis. Curiously, *emp2* transcripts are over abundant in recessive, emp2 mutant kernels. Furthermore, although the coding region of the emp2-R transcript is normal, mutant transcripts are 5' truncated and mutant kernels accumulate no comparable amount of EMP2 protein. These data contribute to a model in which *emp2* expression is feedback regulated, and 5' UTR of *emp2* transcripts are essential for their efficient translation. Moreover, the timing of *hsp* transcript accumulation and embryo abortion in emp2 kernels is correlated with developmental competency to elicit the HSR in maize kernels (Schoffl et al., 1998). These accumulated data suggest that lethality of emp2 mutant embryos is due to an unattenuated HSR, and identify *emp2* as a null phenotype for HSBP function in maize. In addition, the developmental retardation of emp2 mutant kernels prior to implementation of the HSR reveals a role for EMP2 during maize development, exempt from the HSR.

## Results

### *empty pericarp2* is an embryo-lethal, defective kernel mutation

The *empty pericarp2* defective kernel mutation of maize is a recessive, lethal mutation required for both endosperm and embryo development (Scanlon et al., 1994; Scanlon et al., 1997). At maturity, emp2 mutant kernels contain little if any endosperm or embryo structures (Figure 2.1A). Despite the empty pericarp phenotype of mature mutant kernels, endosperm

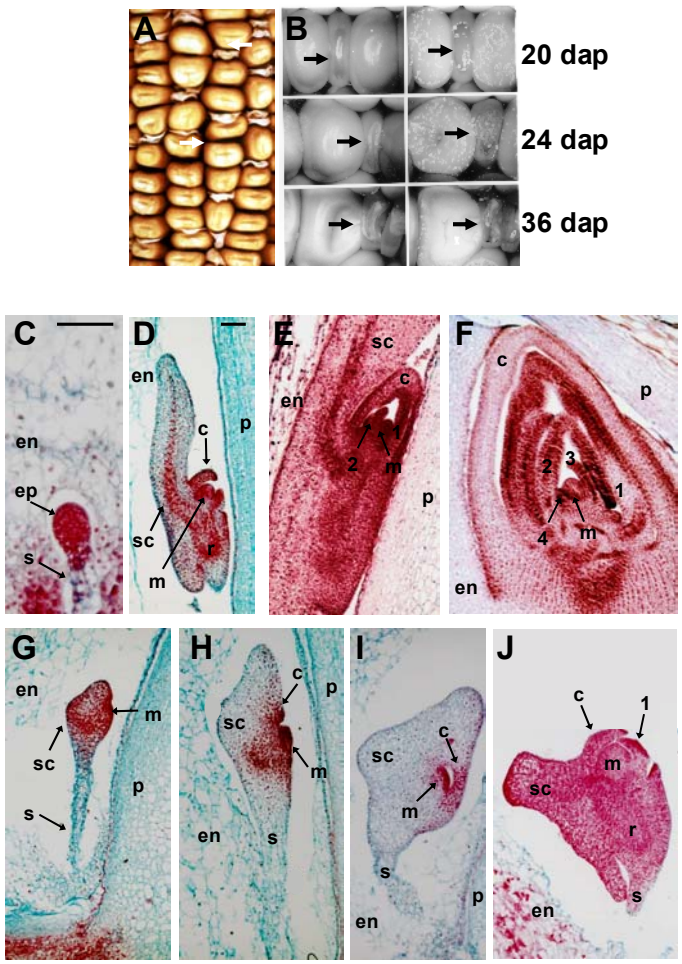


**Figure 2.1** Mutant emp2 kernels abort early in development. (**A**). Self-pollinated ears of *Emp2/emp2-R* heterozygous plants segregate 1/4 collapsed, defective kernel phenotypes. (**B**). Endosperm development in emp2 mutant kernels. Although kernel filling does occur in earlier stages (20 and 24 dap) of emp2-R mutant seed, endosperm development is eventually aborted. At 36 dap, much of the endosperm material that has accumulated in mutant kernels has been re-absorbed, and the mutant kernels are collapsing. Developmental comparisons of non-mutant sibling embryos at 7 dap (**C**), 12 dap (**D**), 14 dap (**E**) and 24 dap (**F**) and emp2-R mutant embryos at 12 dap (**G**), 14 dap (**H**), 16 dap (**I**) and 24 dap (**J**) reveal that mutant kernels are variably blocked following the development of the coleoptile, or more rarely, first foliar leaf. Mutant embryo development is also retarded as compared to non-mutant siblings, and in no

(**Figure 2.1** legend continued) cases did embryogenesis proceed further than the formation of a single leaf primordium. At 12 dap the non-mutant embryo (**D**) has no suspensor, and has formed a coleoptile, root pole and shoot meristem. In contrast, the 12 dap emp2 mutant embryo is just initiating a shoot meristem and has retained the suspensor (**G**). At 14 dap non-mutant siblings have developed 2 leaf primordia (**E**), whereas the emp2 mutant is just initiating the coleoptile (**H**). Necrosis and tissue collapse commences at 16 dap in mutant kernels (**I**). At 24 dap the non-mutant embryo has developed four leaf primordia (**F**). The 24 dap emp2 mutant sibling embryo has initiated a coleoptile and single leaf primordium, however the embryo is collapsing and becoming necrotic (**J**). It is noted the majority of emp2 mutant kernels examined had not developed leaf primordia, but arrest development at the coleoptilar stage. en = endosperm; s = suspensor; p = pericarp; sc =- scutellum; m = shoot apical meristem; r = root meristem; c = coleoptile; 1, 2, 3, 4 designate leaf primordia at various stages of development, wherein 1 = the youngest primordium.

development does progress (albeit in retarded fashion) beyond early stages before development is aborted (Figure 2.1B). The scarce endosperm material that does form in mutant kernels is either re-absorbed or becomes necrotic before kernel maturity. Likewise, embryogenesis in emp2 mutant kernels proceeds until the coleoptilar stage, or more rarely to the 1st leaf stage, whereupon development is arrested and the mutant embryos eventually decompose (Figure 2.1C-J; Scanlon et al., 1997). Close examination reveals that emp2 mutant embryo development is severely retarded at all stages in comparison to wild type, although mutants do form a SAM, a coleoptile (portion of the maize cotyledon; Weatherwax, 1920), and in some cases a leaf primordium prior to their eventual abortion (Figure 2.1H-J). Therefore, EMP2 functions very early in kernel development, and is required for progression beyond the coleoptilar stage/stage1 of maize embryogenesis. Genetic analyses mapped the *emp2* locus to the long arm of chromosome 2, whereas dosage analyses suggest that the *emp2-R* mutation is a fully recessive, null allele (Scanlon et al., 1994; 1997). Culturing of mutant embryos explanted from emp2 kernels at 12, 14, 16, 18, and 20 days after pollination (DAP) fails to rescue the embryo-lethal phenotype (Scanlon et al., 1997), indicating that the emp2 lesion is not a nutritional deficiency.

**Cloning of the *emp2-R* mutation via transposon tagging**

The *empty pericarp2* reference mutation, *emp2-R,* was discovered in maize lines that were mutagenized with *Mutator* transposons (Scanlon et al.,1994). A 3 kb *Mu1*-tagged *Eco*RI restriction fragment tightly-linked to the *emp2-R* mutation (Figure 2.2A) was cloned into bacteriophage lambda. A 550 bp *Eco*RI-*Bgl*I fragment, Probe 1, is contained within the original cloned fragment, flanking the *Mu1* element (Figure 2.3). This fragment was used as a single-copy probe in a Southern hybridization analysis to confirm that the cloned fragment is linked to *emp2-R* (data not shown). The *emp2-R* mutation was identified in the self-pollinated ear of a

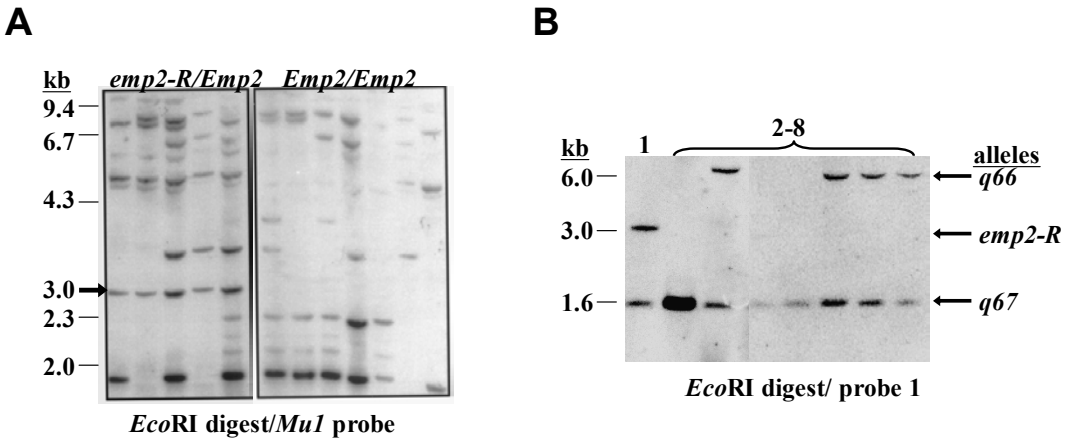


**Figure 2.2**. Southern analyses of clones linked to *emp2*. (**A**) A *Mu1* transposon-tagged *Eco*RI fragment (arrow) is linked to the *emp2-R* mutation. (**B**) Analyses of non-mutant siblings (lanes 2-8) of the original isolate harboring the *emp2-R* mutation segregate for non-mutant inbred (either inbred *q66* or *q67*) sized restriction fragments of clones linked to the *emp2-R* mutation *(*probe1, as described in the Materials and Methods). The *Mu1* transposon-tagged, 3 kb *emp2-R* linked *Eco*RI fragment is absent from non-mutant sibling DNA, indicating the *emp2-R* linked allele was not pre-existent in the genetic background that gave rise to the *emp2-R* mutation.

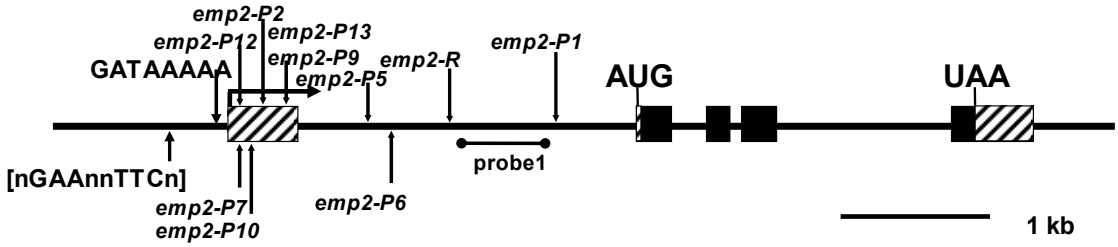


**Figure 2.3** Structural map of the *emp2* gene. The *emp2* gene is comprised of 4 introns and 5 exons (black boxes), including a long 5' UTR (hatched box). The locations of *Mutator* transposon insertions in the 5' UTR and intron corresponding to the known *emp2* mutant alleles are indicated. The putative TATA box (GATAAA) and transcriptional start site (large arrow) are shown, as well as the HSE promoter consensus sequence, located upstream of the TATA box. AUG = translational start site; UAA = translational stop.

single individual in a F1 family (hybrid Q66/Q67 that contained *Mutator* transposon activity) comprising 20 sibling plants (Scanlon et al., 1994), indicating that the mutation arose during gametogenesis in the *Mutator* parent. Sibling plants in this F1 family were examined to see whether the 3.0 kb *Mu1*-containing *Eco*RI fragment was present in this line prior to formation of the *emp2-R* mutation. If so, the 3.0 kb fragment would be present in one-half of the family members. Twenty sibling kernels of the single kernel that contained *emp2-R* were analyzed in Southern gel-blot hybridizations using probe 1 (Figure 2.2B). All twenty plants contained *Eco*RI fragments of the same size as those seen in standard Q66/Q67; none contained a 3.0 kb fragment. Therefore, a wild type allele of inbred Q67, a 1.6 kb *Eco*RI fragment, was modified by insertion of a 1.4 kb *Mu1* element. Moreover, insertion of this specific *Mu* transposon and the appearance of the *emp2-R* mutation are concomitant events, suggesting that the cloned fragment linked to *emp2-R* represents a portion of the *emp2* locus.

A 7.6 kb contiguous genomic clone containing sequences homologous to the 3 kb clone linked to *emp2-R* was identified from two distinct clones (comprising approximately 27 kb of genomic DNA) obtained from an inbred Mo17 maize genomic DNA library (Methods). Reverse genetic analyses were employed to prove that this 7.6 kb maize genomic interval contains the *emp2* locus. Oligonucleotide primers corresponding to genomic sequences throughout the *emp2*-linked contiguous sequence were used together with *Mutator* transposon-specific primers in the TUSC (Trait Utility System for Corn; Benson et al., 1995) reverse genetic analysis to identify nine additional *Mu*-transposon insertions within this cloned locus. Intriguingly**,** all ten *Mutator* insertions identified in emp2 mutant alleles are located within either the 5' untranslated region (UTR) or the first intron of the *emp2* gene (Figure 2**.**3; GenBank #AF494285), despite the fact that oligonucleotides primers were prepared from throughout the *emp2* gene. Complementation

analyses of *emp2-R* heterozygous plants and plants harboring the newly identified *Mu1* insertions (termed *emp2-PI*) revealed that all nine TUSC-derived insertions define kernel mutations that are allelic to *emp2-R*. These data indicate that the 7.6 kb contiguous clone contains a portion of the *emp2* locus.

**EMP2 is predicted to encode HEAT SHOCK FACTOR BINDING PROTEIN1 of maize, a negative regulator of the heat shock response**

Sequencing of the 7.6 kb contiguous *emp2* clone identifies regions of exact homology to a 480 bp cDNA clone isolated from maize seedling RNA**.** Northern gel-blot analyses (Figure 2.4) reveal that the *emp2*-homologous EST hybridizes to an approximately 700 bp transcript in maize tissues, indicating that the cDNA clone is not complete. Therefore, rapid amplification of cDNA ends (RACE, Clontech) was employed to isolate nearly full- length, *emp2* cDNA; the exact transcriptional start site was identified by S1 nuclease protection assays (Figure 6). These combined analyses reveal that the non-mutant *emp2* transcript is 760 bp long, excluding the polyA+ tail (GenBank #AF494284). Database searches and cDNA cloning indicate multiple polyadenylation sites are utilized in *emp2* transcripts, resulting in a broad hybridizing band in Northern gel-blot analyses (Figure 2.4; GenBank #AF494284). Alignment of genomic and cDNA clones reveals that the*emp2* gene is comprised of five exons and four introns (Figure 2.3).

The *emp2* cDNA clone is predicted to encode a 78 amino acid peptide that shows homology (approximately 36% identical and 60% similar amino acids over the full length protein, Figure 2.5) to the human HEAT SHOCK FACTOR BINDING PROTEIN. First identified in humans by its ability to bind to the trimerization domain of HSF1, analyses in *C. elegans* demonstrate that HSBP1 functions as a negative regulator of the heat shock transcriptional response (Satyal et al., 1998). Multiple lines of evidence suggest that EMP2 is as maize orthologue of HSBP1

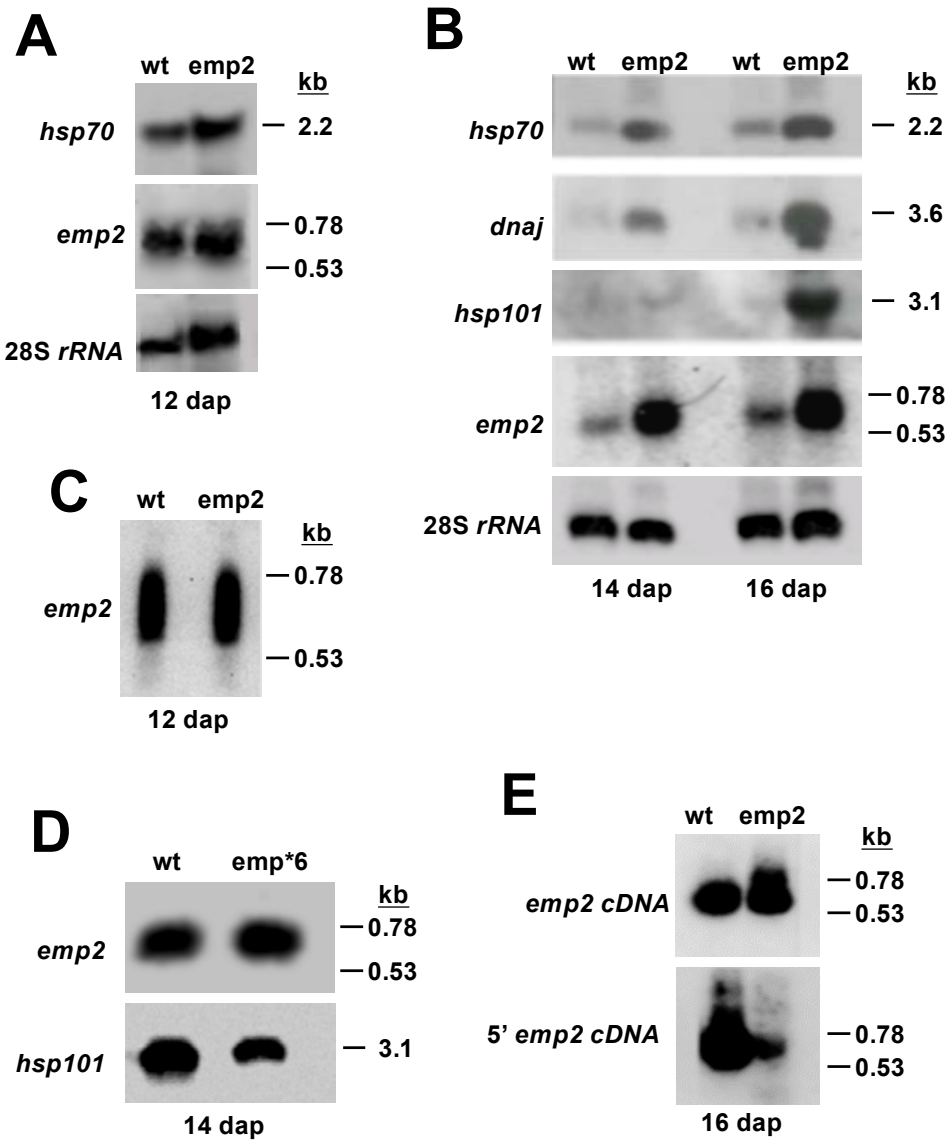


**Figure 2.4** Northern blot analyses of emp2 mutant kernels. (**A**) At 12 days after pollination (12 dap) no differences in *hsp70* or *emp2* transcript abundance are detected in non-mutant (wt) and mutant (emp2) kernels. All panels represent separate hybridizations to the same blot. (**B**) At 14 and 16 dap, transcripts homologous to the *heat shock* genes *hsp70, dnaj,* and *emp2* are overly abundant in emp2 mutant kernels, whereas *hsp101* transcripts accumulate at 16 dap. All panels

(**Figure 2.4** legend continued) represent separate hybridizations to the same blot. (**C**) Polyacrylamide RNA-gel blot hybridization reveals molecular weight heterogeneity for *emp2*-homologous transcripts in non-mutant and emp2 mutant 12 dap kernels. (**D**) Transcripts of *emp2* and *hsp101* are not upregulated in the defective kernel mutant emp*6. Both panels represent separate hybridizations to the same blot. (**E**) Abundant *emp2* transcripts are detected in poly A+ selected RNA using internal *emp2*-specific probes (emp2 cDNA), however the hybridization signal is much reduced in RNA from emp2 mutant kernels when the blot is stripped and rehybridized using only the 5' most 174 nucleotides of the emp2 cDNA (5' *emp2* cDNA) as probe. Note that more polyA+ RNA is loaded in the non-mutant (wt) lane.

(described below and in the following section). EMP2 is predicted to contain the conserved hydrophobic heptad repeat domains, and to form the characteristic coiled-coil structure (Figure 2.5A-D) found in animal HSBP1 (Satyal et al, 1998; Tai et al., 2002). Furthermore, the positions of both introns found in human *hsbp1* are absolutely conserved in *emp2* (Figure 2.5E), although *emp2* harbors two additional introns (Figure 2.5E) not found in animal *hsbp* genes.

EMPTY PERICARP2 is the first described HSBP-like protein in plants: homologous EST's are identified from five monocot species, eight eudicots and a single gymnosperm (Figure 2.5E). Interestingly, although a single *hsbp* isoform is identified in eudicots, two isoforms exist in monocots (Figure 2.5E). In addition, interspecific homologues of HSBP1 (or HSBP2) in grasses are more closely related than are HSBP1 and HSBP2 from the same species. Therefore, the duplication of the *hsbp* gene most likely occurred prior to the evolutionary divergence of monocot grass species. Moreover, of the two rice genes closest to animal HSBP (*Oshsbp1* and *Oshsbp2;* GenBank UniGene Os.9890, Os.1120) found in the entire, sequenced genome, neither rice gene is predicted to encode a protein with higher homology to animal HSBP1 than *emp2* and *Zmhsbp2* respectively (Figure 2.5E). In addition, the intron positions of maize *emp2* are completely conserved among rice and *Arabidopsis hsbp* genes (Figure 2.5E). Therefore, it is unlikely that there are additional, undiscovered maize *hsbp* genes that are more highly homologous to animal *hsbp1* than *emp2*.

**The emp2 mutant embryo exhibits an unattenuated heat shock response**

In order to understand the cause of emp2 mutant embryo abortion, we studied the steady state transcript abundance of the major heat shock proteins in mutant kernels. If EMP2 functions as a negative regulator of HSR in maize as it does in animals, it is predicted that loss of EMP2 EMP2 function may lead to un-attenuated heat shock response. Indeed, this is the case. Transcripts of

**A**

MDSDPSSQNPTDMTAFVQNLLGQMQTRFESMSQNIVSKIDEMGTKIDELEQSINDLKAEMGTETPVKKPDEPKPADSA

a d a d a d a d a d a d a d

**B**

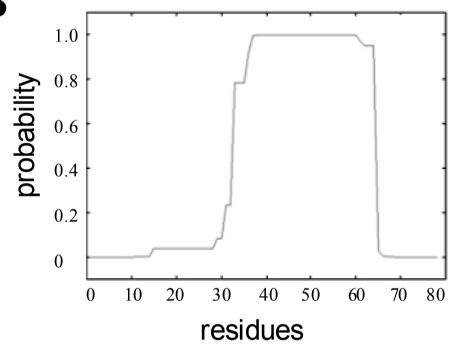


**C**

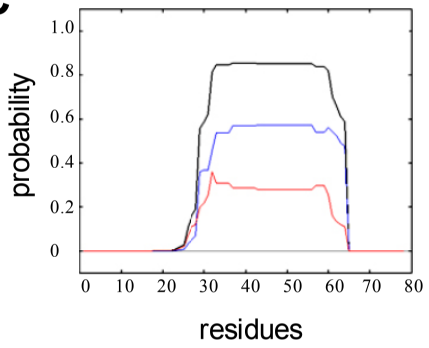


**D**

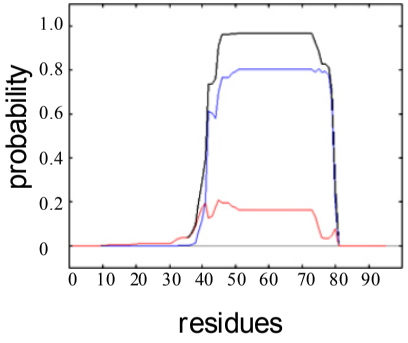


total probability
dimer probability
trimer probability

**E**

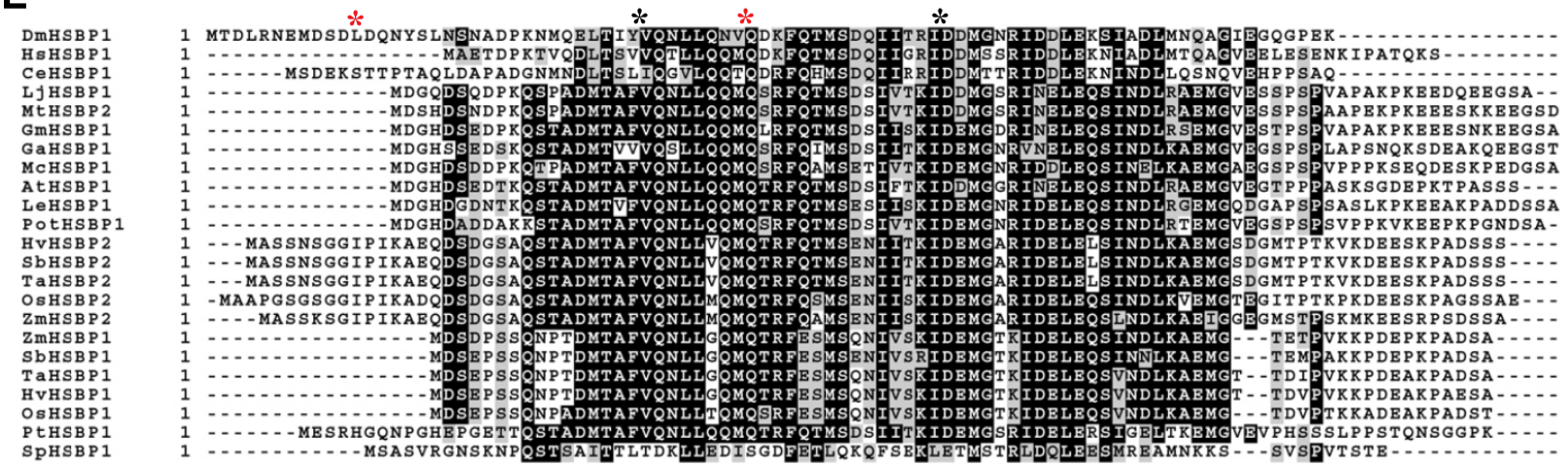

**Figure 2.5** EMP2 is homologous to animal HSBP1. (**A**) The predicted amino acid sequence of EMP2. EMP2 contains conserved arrays of hydrophobic (residues labeled **a** and **d**) heptad repeats. (**B**) Probability plot of the predicted EMP2 protein to form a coiled-coil structure using the software prediction application COILS and a window of 21 residues. Probability plot of the predicted EMP2 protein (**C**) and the predicted ZmHSBP2 protein (**D**) to form dimer and trimer multimers, as calculated by PAIRCOIL. (**E**) Alignment of the predicted amino acids of the EMP2 gene product (ZmHSBP1) and other HSBP homologues from plants and animals. Identical amino acid residues are in black, similar residues are shaded. The positions of introns conserved in human, maize, rice and *Arabidopsis hsbp* genes are indicated by the black asterisks; two additional introns conserved in plant *hsbps* are indicated by red asterisks. Two distinct HSBP-like proteins (HSBP1 and HSBP2) are identified in plants. Sequences were aligned with ClustalW and BOXSHADE.

*hsp70* and *DNAJ* genes are highly expressed in mutant kernels (but not in non-mutant sibling kernels) beginning at 14 dap; normal levels of transcript are seen at 12 dap (Figure 2.4A-B). In addition, transcripts of the maize *heat shock protein101* (*hsp101*) are also upregulated in emp2 kernels at 16 dap. Unlike *hsp70* and *dnaj*, which are upregulated at the onset of heat shock, *hsp101* is upregulated only after extended thermal stress (Queitsch et al., 2000). Thus, the over accumulation of *hsp101* transcripts indicates that emp2 mutant kernels are unable to attenuate the heat shock response. Furthermore, the timing of *hsp* transcript over accumulation is well-correlated with the developmental time point upon which maize embryos are first competent to elicit heat shock response (Schoffl, et al., 1998) and precedes the emp2 mutant embryo necrosis at 16 dap (see Figure 2.1). Importantly, transcripts of *emp2* and *hsp101* are not upregulated in 16 dap kernels homozygous for the unlinked, defective kernel mutation *empty pericarp*6* (Figure 2.4D), which also causes early-staged embryo abortion. Therefore, the pattern of *hsp* upregulation in emp2 mutant kernels is not simply a phenotype exhibited by defective kernel mutants as a class, nor a stress response to embryo abortion.

### ***Emp2*** **transcripts accumulate in homozygous, emp2 mutant kernels**

The expression pattern of *emp2* transcripts was analyzed in wild type and emp2 mutant tissues. *emp2* transcripts are detected in every non-mutant maize tissue examined, including developing kernels, roots, whole seedlings, leaves and vegetative shoot apices (maize vegetative shoot meristem and the youngest 5-6 leaf primordia). At 12 days after pollination (dap) no differences are detected in the *emp2* transcript size or abundance in non-mutant versus emp2 mutant seed (Figure 2.4A). At 14 dap and 16 dap however, there is a dramatic reduction in steady state transcript abundance in non-mutant kernels as compared to 12 dap (Figure 2.4A-B). This down-regulation of steady state*emp2* transcript coincides with the initial competency of

maize embryos to elicit the heat shock transcriptional response (Vierling, 1991; Schoffl, et al., 1998; Schrauwen et al., 1986; Pitto, et al., 1983) and with embryonic developmental arrest in emp2 mutant kernels. In contrast, emp2 mutant kernels at 14 dap and 16 dap exhibit significantly higher levels of *emp2* transcript than non-mutant sibling kernels (Figure 2.4B). Moreover, transcript abundance in mutant kernels at 14 and 16 dap is increased as compared to 12 dap mutant kernels (Figure 2.4A-B). In addition, sequence analyses of twenty individual cDNA clones obtained via hybridization to *emp2* probes indicate no cross-hybridization to *Zmhsbp2,* and demonstrate that the upregulated transcripts are *emp2*-specific.

Sequence analyses of cDNA prepared from *emp2* mutant transcripts reveal that the coding region of *emp2-R* mutant cDNA is normal. The apparent molecular weight of *emp2*-homologous transcripts is difficult to quantify from RNA-gel blots, because the transcripts migrate in a broad band on agarose gels (Figure 2.4A-B). Moreover, high-resolution polyacrylamide gel-hybridization reveals that *emp2* transcripts are of heterogeneous molecular weight (Figure 2.4C). Sequence analyses of thirteen emp2 mutant and seven non-mutant transcripts reveal that a variety of different polyadenylation sites are utilized in *emp2* transcripts (ranging from base pair 623 to 760; GenBank #AF494284), which contributes to transcript size heterogeneity. In addition, emp2 alleles exhibit no preference for any particular polyadenylation site(s).

### ***Mutator*** **transposon insertion in the 5' UTR region correlates with truncated *emp2* transcripts and embryo-lethal mutations**

A perplexing contradiction of the emp2-R phenotype (as well as emp2-P1) is the abundant accumulation of *emp2* transcripts (Figure 2.4B) that contain unaltered coding regions in kernels homozygous for null, recessive *emp2* mutations (Scanlon et al, 1994; 1997; this report). Northern gel-blot analyses of poly A+-selected RNA from 16 dap emp2-R mutant and sibling

kernels reveal that sequences contained within a 174 bp fragment comprising the 5'-end of the emp2-R cDNA are under-represented in mutant transcripts (Figure 2.4E). S1 nuclease protection analyses were employed to locate the predominant transcriptional start site in non-mutant kernels to 17 base pairs downstream from the putative TATA box (Figure 2.6A-B). In contrast, *emp2-R* mutant transcripts are 5' truncated, and prevalently initiate 146 bp downstream of the preferred transcriptional start site in non-mutant siblings (Figure 2.6C-D). Interestingly, the mutant transcriptional initiation site is located 23 base pairs downstream from a second TATA box-like sequence (TATACA). These data suggest that *Mutator* transposon insertion within the 5'UTR of *emp2* may cause alternative promoter utilization, perhaps resulting in an untranslatable transcript.

**emp2 mutant kernels do not accumulate EMP2 protein**

In order to test our prediction that the 5' truncated emp2 transcripts are not translated in emp2 mutant kernels, polyclonal antibodies were raised against predicted EMP2-specific antigens (see Materials and Methods) and utilized in immunoblot assays of proteins extracted from non-mutant and emp2 mutant kernels (Figure 2.7). The anti-EMP2 antibodies identified a single protein band of the approximate molecular weight predicted for *emp2*-encoded protein in 12 dap and 16 dap non-mutant kernels. In contrast, no immunoreactive proteins are detected in emp2 mutant kernels by Western blot (Figure 2.7). Therefore, emp2-R is a null mutant, and the 5'-end truncated transcript is associated with loss of EMP2 protein accumulation.

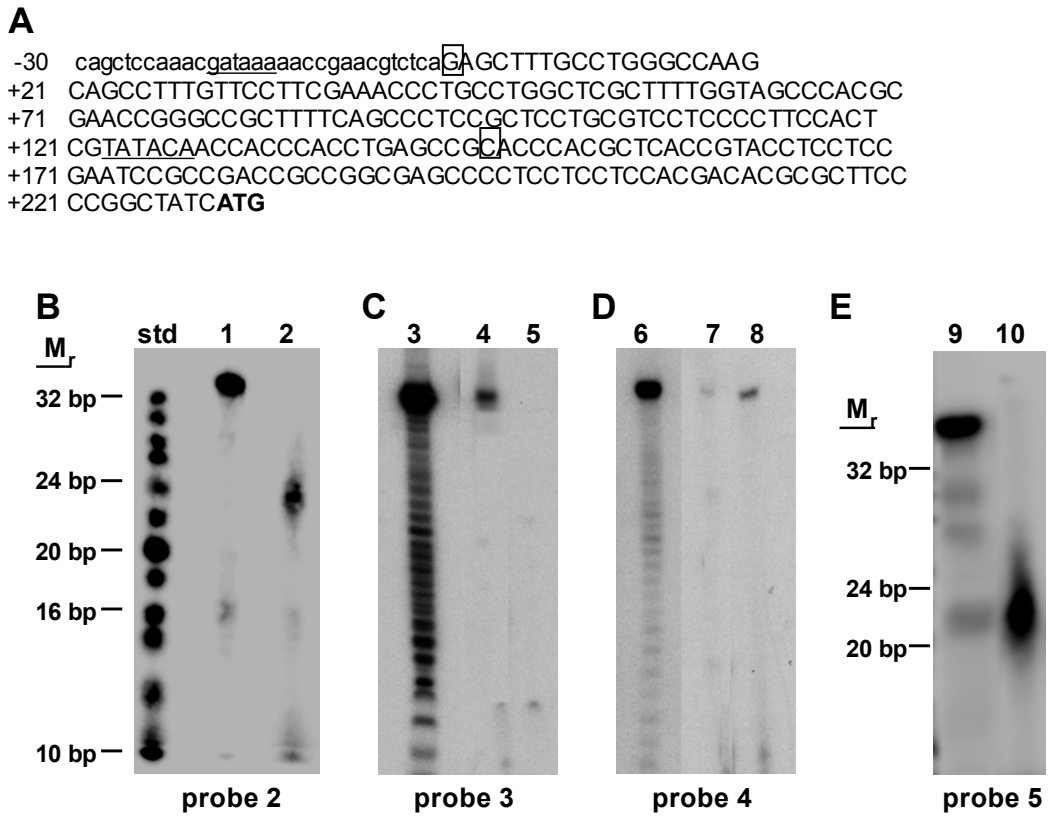


**Figure 2.6** S1 nuclease protection analyses of *emp2* transcripts. (**A**) The 5'-UTR sequence of *emp2* is shown in upper case, including 30 base pairs of promoter sequence (lower case). The putative upstream and downstream TATA boxes are underlined. The *emp2* transcriptional start sites, as mapped by S1 nuclease protection assays, in non-mutant (position +1; presented in [**B**]) and emp2 mutant (position +146; presented in [**E**]) kernels are boxed. (**B-E**) S1 nuclease protection assays of non-mutant (lanes 2, 4, 7) and emp2 mutant (lanes 5, 8, 10) transcripts reveal that the predominant transcripts in emp2 mutant kernels are 5' truncated. (**B**) Mapping of the transcription start site in the non-mutant by probe 2. A 24bp fragment of probe 2 is protected by *emp2* transcripts (lane 2). (**C**) Mutant transcripts are 5' truncated. Probe 3 is fully protected by non-mutant *emp2* transcripts (lane 4) but is not protected by *emp2* mutant transcripts (lane 5). (**D**) 3' transcripts are intact in emp2 mutant kernels. Probe 4 is fully-protected by *emp2*

(**Figure 2.6** legend continued**)** transcripts from both mutant (lane 8) and non-mutant (lane 7) kernels. (**E**) The transcription start site of emp2 mutant transcripts. A 22bp fragment of probe 5 is protected by emp2 mutant transcripts. Undigested *emp2* oligonucleotide probes are presented in lanes 1, 3, 6 and 9. The sequences of the *emp2* oligonucleotide probes (probe 2 = position -11 to +25; probe 3 = position +16 to +48; probe 4 = position +392 to +421; probe 5 = position +135 to +171) are described in the Methods, Table 1.

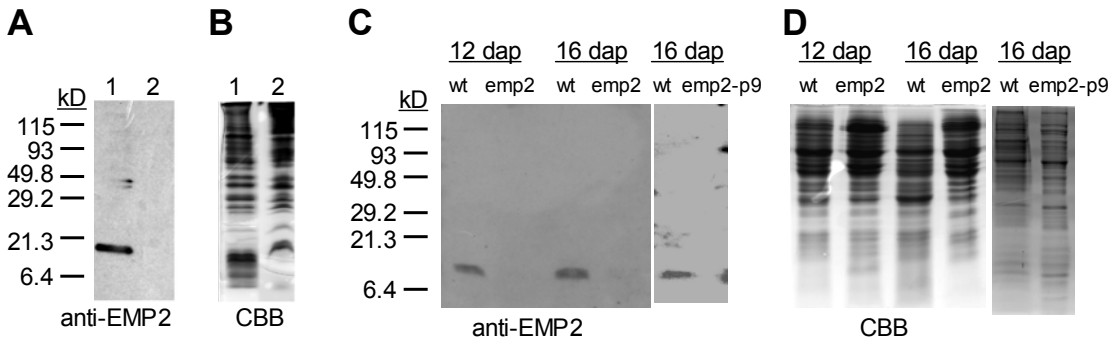


**Figure 2.7** EMP2 protein does not accumulate in null, emp2 mutant kernels. (A-B) Anti-EMP2 antibodies specifically recognize EMP2 fusion protein. Lane 1 contains *E. coli* protein extract including the bacterially-expressed EMP2 fusion protein. The predicted MW of the EMP2 fusion protein is approximately 17 kDa. Lane 2 contains extracts from bacterial strains in which *emp2* is cloned out of frame. (C-D) Analysis of 30 ug of protein extracted from non-mutant sibling (wt) and emp2 mutant kernels (emp2 and emp2-p9) at 12 dap and 16 dap. The predicted MW of the EMP2 protein is approximately 8.5 kDa. "anti-EMP2" designates immunoblots using an EMP2-specific antibody. "CBB" designates polyacrylamide gels stained with Coomassie brilliant blue.

## Discussion

### Abortion of emp2 mutant embryos is caused by an unattenuated heat shock response

*empty pericarp2* is an embryo-lethal, defective kernel mutation of maize (Scanlon et al, 1994; 1997). Embryogenesis in emp2 mutant kernels is aborted at the coleoptilar stage/stage1, followed by necrosis and re-absorption of kernel contents (Figure 2.1). Abortion of embryogenesis is preceded by an un-attenuated heat shock response in homozygous *emp2* embryos (Figure 2.4). Furthermore, both mutant embryo abortion and *hsp* transcript over-accumulation occur during or shortly after the coleoptilar stage of maize development, the developmental time-point upon which plant embryos become competent to invoke the heat shock response (Pitto et al., 1983; Vierling, 1991; Schoffl et al., 1998). These data indicate that the embryo abortion in emp2 mutant embryos is caused by un-attenuated heat shock response. The HSR is known to result in transcriptional and translational arrest of numerous plants genes (reviewed in Nagao et al., 1986; Vierling, 1991, Morimoto, 1991), including those affecting cellular metabolism (Simoes-Araujo et al., 2002) and cell wall/membrane biosynthesis (Li and Showalter, 1996; Iwahashi and Hosoda, 2000; Simoes-Araujo et al., 2002). In addition, the HSR blocks essential cellular processes such as DNA synthesis and cell cycle progression (Song et al., 2001 and references therein). Thus, following competency to invoke the HSR after the coleoptilar stage of development, an extended, unattenuated heat shock transcriptional response may trigger embryo abortion. Indeed, over expression of a single heat shock protein HSP70 in *Drosophila* has been shown to dramatically reduce the rate of cell division and growth (Feder et al., 1992).

**EMP2 is an essential negative regulator of the heat shock transcriptional response**

HSBP1 was first-described in animals as a negative regulator of the transcriptional activity of HSF1 during heat shock attenuation (Satyal et al., 1998). Herein we report that loss of EMP2 function results in an un-attenuated HSR and embryo lethality in maize kernels. In addition, the hydrophobic heptad repeat structure and the intron position are both conserved between EMP2 and animal HSBP1 (Figure 2.5). Taken together, these results suggest that EMP2 is the functional orthologue of HSBP1 in maize. However, *hsbp1* knockouts in *C.elegans* do not show reduced viability after exposure to heat stress. This discrepancy may indicate that EMP2 is an essential negative regulator of the HSR in maize, whereas redundant mechanism(s) of HSR attenuation may exist in *C.elegans*.

It has been demonstrated that the hydrophobic heptad repeats of HSBP1 interact with the oligomerization domain of HSF1 in animals. Whereas animals have one to four HSFs, plants may contain more than 20 (Nover, 2001). In addition, the oligomerization domains of animal and plant HSFs are divergent. Both class A and class C HSFs in plants have an expanded insertion of amino acid residues between the HRA and HRB domain. The extended distance between HRA and HRB in plant HSFs may make HSBP1 a necessary regulator of HSFs activity. Furthermore, there are two isoforms of HSBP in monocot grasses (Figure 2.5). Although the monocot HSBPs are extremely homologous in the heptad repeat region, HSBP2 has a distinct extension in the N-terminus as well as a longer C-terminal tail than HSBP1 (Figure 2.5E). These differences may modify the structure of HSBP and the functional interactions between the heptad repeats of HSBP and the oligomerization domain of a specific HSF(s). Indeed, HSBP2 is likely to form dimers exclusively as predicted by PAIRCOIL (Figure 2.5D), whereas EMP2/HSBP1is

more likely to form a mix of dimers and trimers. The co-existence of *emp2* and *Zmhsbp2* transcripts (data not shown) in developing embryos and the unattenuated HSR in emp2 mutant embryos further supports the notion that they are not functionally mutual replaceable *in planta*. Lastly, the divergent but partial overlapping expression pattern of *emp2/Zmhsbp1* (GenBank UniGene Zm.4289) and *Zmhsbp2* (GenBank UniGene Zm.3728) in maize indicates different mechanisms are governing the expression of *hsbp* paralogues. Taken together, we speculate the two homologues of *hsbp* found in monocots may have evolved diversified functions in respond to different upstream signals.

### *Mutator* transposon insertion correlates with the utilization of alternative *emp2* transcriptional start site

The *emp2-R* mutation is recessively-inherited and renders a null mutant phenotype (Scanlon et al, 1994; Scanlon et al., 1997; this report). Despite the null mutant phenotype, emp-R kernels accumulate overly abundant levels of *emp2* transcript (Figure 2.4). Furthermore, no *Mutator* transposon sequences are detected within the mutant transcripts, and the coding region of emp2-R mutant mRNA is intact (data not shown). Determination of the exact size of *emp2* transcripts via Northern gel-blot analyses is complicated by the utilization of diverse polyadenylation sites, resulting in wide variation in the length of the 3' UTR (Figure 2.4; Figure 2.5). However, S1 nuclease protection assays and Northern gel blot analyses reveal that the *emp2* transcriptional start site in mutant kernels is 5' truncated; *emp2-R* transcripts initiate approximately 146 base pairs downstream of non-mutant siblings mRNA (Figure 2.6). Western blot analyses account for the null emp2-R mutant phenotype, revealing that the 5' truncated emp2-R mutant transcripts yield no detectable EMP2 protein (Figure 2.7). We propose that the 5'UTR of the *emp2* transcript harbors element(s) important for its efficient translation. It has been demonstrated that,

in both *Drosphila* and *Homo sapiens,* a lengthy and intact 5' UTR is required for preferential translation of *hsp70* transcripts under stress conditions (Lindquist and Petersen, 1990; Hess and Duncan, 1996; Vivinus et al., 2001). If the 5'UTR of *emp2* plays a similar function as that of *hsp70*, this may provide a mechanism to regulate the accumulation of EMP2 in response to heat stress, noting that *emp2* is constitutively transcribed (data not shown).

Furthermore, the data suggest that the EMP2 gene product may be negatively feedback-regulated, such that the presence of functional EMP2 protein leads to a reduction in steady state levels of *emp2* transcript. In this way, the absence of functional EMP2 protein in mutant embryos may lead to over-accumulation of the non-functional, mutant *emp2* transcript. Additional, albeit speculative support for such a feedback mechanism is provided by the presence of an inverted pentanucleotide repeat (nGAAnnCTTn) with identity to the consensus HSE promoter element located 400 bp upstream from the transcriptional start site of the *emp2* gene (Figure 2.3). Therefore, it is possible that *emp2* transcription can be enhanced by HSF binding to this HSE, and thus may be influenced by feedback mechanisms during attenuation of the heat shock response.

### *Mutator* transposons preferentially insert into the 5' region of *emp2* mutant alleles

The *emp2* locus is defined by 10 independent *Mu* transposon insertions, all of which are located in the 5' UTR and/or the first intron (Figure 2.3). In addition, reverse genetic analyses identify five additional transposon insertions in this region of *emp2,* although complementation tests of these insertion stocks are not yet completed. Therefore, despite that fact that *emp2*-gene specific primers were prepared from several, distinct regions of the *emp2* locus, *Mu* insertions were identified only in 5' genic regions. Previous surveys have also suggested a "preference" for *Mu* transposon insertion in 5' promoter regions of maize genes (Dietrich et al., 2002), although

no mechanistic explanation accounting for this insertion site bias has been demonstrated. Nonetheless, these data suggest that genomic sequences present in the 5' UTR, and within the first intron especially, may be important for directing the correct initiation site of *emp2* transcripts.

**EMP2 may provide additional functions beyond regulation of the heat shock response**

Our results indicate that EMP2 is a negative regulator of HSR during attenuation, and unlike HSBP1 in *C.elegans*, ZmHSBP1 function is required for embryo viability. Moreover, our results indicate that EMP2 performs an important developmental function(s) outside the realm of the heat shock response. Embryogenesis in emp2 mutant kernels is severely retarded at 12 dap (Figure 2.1), well before maize kernels are competent to invoke the HSR (i.e., at the coloeoptilar stage; reviewed in Vierling et al., 1991). Moreover, no abnormal accumulation of *hsp* gene transcripts is observed in mutant kernels before 14 dap (Figure 2.4). Thus, the developmental retardation of emp2 mutant indicates an additional role (i.e. beyond the regulation of *hsp* gene regulation) for EMP2 in very early stages of maize development. The *emp2* mutation provides a powerful genetic tool in order to investigate the expanded role of HSBP protein during maize embryogenesis.

## Materials and Methods

**Isolation and propagation of defective kernel mutants**

The *empty pericarp2* mutation was identified in a self-pollinated F1 plant that was generated via outcrossing the maize hybrid stock Q66/Q67 as female to plants containing active *Mutator* transposons (tagging scheme described in Scanlon et al., 1994). A specific F1 plant was found to be heterozygous for a *dek* mutation, designated *emp2-R*, by observing normal and defective

kernels on the self-pollinated ear segregating at the ratio of 3:1. The *emp2-R* mutation was mapped to chromosome 2L:91 and shown to define a previously undescribed maize locus. Because *emp2-R* homozygous kernels are inviable, the mutation was propagated by outcrossing *emp2-R/Emp2* plants to the maize inbred lines B73 or Q66 lines as described (Scanlon et al., 1994; Scanlon et al., 1997).

**Histology analysis of mutant maize kernel phenotypes**

Whole maize kernels were dissected from self-pollinated, heterozygous (*Emp2/ emp2-R*) ears and fixed in paraformaldehyde as described (Scanlon and Freeling, 1998). Samples were sectioned at 10 um and mounted on slides as described. Following deparaffinization, slides were stained in fast green or safranin/fast green as described (Sylvester and Ruzin, 1994).

**DNA gel-blot analyses**

Maize genomic DNA was isolated from immature ears or 7 day-old seedlings and analyzed by DNA gel blot hybridization analysis as described previously (James et al., 1995). Hybridization probes were as follows. Probe Mu1 is the 960 bp *Mlu*I fragment internal to transposon *Mu1* (Barker et al., 1984). Probe 1 was obtained from the *Mu*-tagged genomic clone, a 550 bp *Bgl*I-*Eco*RI restriction fragment adjacent to the *Mu1* insertion contained within *emp2-R* (Figure 2.4). Gel -purified double stranded DNA restriction fragments used as hybridization probes were radioactively labeled by random primer extension. In all instances labeled DNA probes were separated from free nucleotides by size exclusion chromatography using Sephadex G-50 (Sigma).

**Cloning of maize genomic DNA fragments linked to emp2**

DNA was isolated from the immature second ear of an *emp2-R/Emp2* plant. Approximately 150 ug of genomic DNA was digested with *Eco*RI, and fragments were fractionated by

electrophoresis in 0.8% agarose gels (Gibco ultra grade agarose, BRL, Bethesda, MD). Fragments of the size range 2.5 kb to 4.0 kb were isolated by electroelution, purified by phenol extraction, and concentrated by ethanol precipitation. These fragments were ligated into *Eco*RI-digested phage lambda vector NM1149 at an approximate molar ratio of 1:1, packaged into bacteriophage particles (Giga-pack gold II packaging kit, Stratagene Cloning Systems) used to infect *Escherichia coli* strain C600 *hfl.* The library was screened by standard plaque hybridization using probe MJ960, and a single hybridizing plaque was identified among approximately 6 x $10^4$ total plaques. Following isolation of DNA from the *Mu1* hybridizing recombinant bacteriophage isolate, the maize genomic DNA inserts were subcloned into the vector pBR322 to form plasmid pMS1.

Two separate genomic clones containing the full length, *emp2* gene were obtained by screening a Mo17 maize genomic library (Stratagene, La Jolla, CA) with probes linked to *emp2* genomic and cDNA clones (Figure 3). Both clones were sequenced to identify a 7.6kb contiguous region; the complete genomic sequence of *emp2* is deposited in GenBank, #AF494285).

Furthermore, the positions of *Mutator* transposon insertions in all *emp2* alleles (Figure 3) were determined by sequencing PCR products amplified with primers specific to the terminal inverted repeat of *Mu* and the *emp2* genomic DNA (see Table 2.1). The insertion positions are deposited to GenBank #AF494285.

**Maize transcript analyses**

For preparation of total RNA, 4 g of maize tissue was ground in liquid nitrogen with a mortar and pestle and thawed in Trizol™ lysis buffer (Gibco-BRL)). Following extraction in chloroform, the RNA was precipitated with ethanol and resuspended in $H_2O$. Yields of total

**Table 2.1 Oligonucleotide primers used in this study**

| Name | primer region | primer sequence |
|---|---|---|
| Probe 2 | –11 to +25 of emp2 cDNA | GGCAGGGTTTCGAAGGAACAAAGGCTGCTTGGC |
| Probe 3 | 16 to 48 of emp2 cDNA | GCGTCTCAGTGCCCATCTCAGCTTTGAGATCG |
| Probe 4 | 392 to 421 of emp2 cDNA | GGCTGCTTGGCCCAGGCAAAGCTCTGAGACGTTCGG |
| Probe 5 | 135-171 of emp2 cDNA | GGAGGAGGTACGGTGAGCGTGGGTGCGGCTCAGGTGG |
| F1 | 297-316 of emp2 cDNA | TCGAACCTTGTTTGCATCTG |
| R1 | 524-545 of emp2 cDNA | CAGATACGATCACGTACTGCTGA |
| F2 | 1-21 of of emp2 cDNA | AGAGCTTTG CCTGGGCCAA G |
| R2 | 155-174 of emp2 cDNA | TTCGGAGGAGGTACGGTGAG |
| F3 | 3367-3388 of Zmdnaj | TGCAAGGCTC TCGAGACAGT AC |
| R3 | 3687-3666 of Zmdnaj | CTTGCGAGGT CGATTCAGCT TC |
| R4 | 281-308 of emp2 cDNA | TGTTTGCATCTGTCCAAGGAGGTTCTGG |
| R5 | 234-263 of emp2 cDNA | TGTTGGGTTCTGTGATGATGGATCTGAATC |
| F6 | 1868-1895 of emp2 genomic DNA | CCAATGCCGTCTCTAATCACAGCTCCAA |
| R6 | 2030-2057 of emp2 genomic DNA | TCAGGTGGGTGGTTGTATACGAGTGGAA |
| F7 | 5956-5982 of emp2 genomic DNA | TGACTCTGCCTAACTTGGGTGTAACCC |
| R7 | 6425-6452 of emp2 genomic DNA | CCACTCCACAAGTCGAGGATATTCGTGT |

RNA isolated by this procedure typically ranged from 500 to 875 ug/g fresh tissue weight. Polyadenylated RNA was selected by the PolyA tract™ mRNA isolation system (Promega Cat#Z5200). Procedures for northern blotting and hybridization of total maize RNA from agarose gels are described by Seeley et al., (1992). Procedures for polyacrylamide gel-blot analyses of RNA are those described by Thompson et al., (1992).

Northern gel-blot hybridizations utilizing oligonucleotide probes were performed as described by Thompson and Meagher, 1990. For use as an RNA loading control, a 26 base pair oligonucleotide probe homologous to the soybean 18S rRNA gene (Tanzer and Meagher, 1994) was used as a hybridization probe. The *emp2* cDNA probe was amplified from the intact *Emp2* cDNA clone utilizing the F1 and R1 oligonucleotide primer pairs (Table 2.1); the predicted PCR product corresponds to nucleotides 297 to 545 of the emp2 cDNA. The 5' *emp2* cDNA probe is comprised of the first 174 base pairs of the*emp2* cDNA, and was obtained by PCR amplification using primers F2 and R2 (Table 2.1). The maize*hsp101* cDNA was a gift from T. Young (U.C. Riverside) andthe maize *hsp70* cDNA clones were provided by P. Rogowsky (Lyon, France). The cDNA probe corresponding to 320 base pairs from 3' end of the maize *dnaJ* gene (Genbank accession #AAF053468) was amplified from maize kernel cDNA utilizing the PCR primers of F3 and R3 (Table 1). 5'-Rapid Amplification of cDNA Ends (5'-RACE) was carried out according to recommended protocols of the Marathon™ cDNA Amplification Kit (Clontech, Catalog#K1802-1) utilizing the *emp2*-specific primers R4 and R5 (Table 2.1). SMART™ PCR cDNA libraries were constructed from 1μg of total RNA from emp2 mutant and non-mutant kernels collected 16 days after pollination according to the manufactures recommended protocol (Clontech, Catalogue#K1052-1). Approximately 300,000 individual plaques were screened with radiolabeled *emp2* cDNA probe (Table 2.1).

S1 nuclease protection assays were performed using end-labeled oligonucleotide probes (Table 2.1) as described (Goldrick et al., 1996). Probe 2 and probe 3 (see Table 2.1) of the *emp2* cDNA were used to quantify the abundance of 5' and 3' transcripts respectively in non-mutant and emp2 mutant kernels. Probe 4 and probe 5 (Table 2.1) were utilized to map the *emp2* transcription start sites emp2 mutant kernels.

**Antibody production, recombinant protein expression, and immuno-analyses**

*Emp2* cDNA clones in phage lambda were directly converted intro *E.coli* via one step excision. The EMP2 recombinant proteins were expressed in the *LacZ* frame of vector pTriplEx (Clontech). Constructs with *emp2* cDNAs (+157 to end) cloned into the *Sfi*I site in frame with the *LacZ* translation initiation site were used for EMP2 recombinant protein expression, whereas the out of frame *emp2* construct (+20 to end) served as negative control. The predicted MW of the bacterially expressed 158 residue EMP2 fusion protein is approximately 17 kDa. Total cellular proteins of *E.coli* were extracted as described (Sambrook et al, 1989), and used in immunoblots to test the anti-EMP2 antisera. The EMP2 polyclonal antibodies were generated (Biosource International) against the last 13 residues of EMP2, with a Cys residue added to the N terminal (N-CVKKPDEPKPADSA-C). This sequence of residues in the predicted EMP2 protein is not present in the predicted protein encoded by *Zmhsbp2*. Immunoblot analyses were carried out according to the manufactures recommendation (ECL$^{TM}$, Amersham-Pharmacia) using a 1/300 dilution of crude serum as the primary antibody.

Maize kernels were ground in liquid nitrogen, rinsed with PBS and resuspended in soluble protein extraction buffer (20 mM Tris-HCl, 2mM EDTA, 1 mM PMSF, 200 mM NaCl. PH8.0). Cellular debris was pelleted by centrifugation at 1000g for three minutes. Protein gel

electrophoresis, transfer and coomassie blue staining were carried out according to standard methods (Sambrook et al., 1989). Thirty micrograms of protein were loaded in each lane.

**Computational and database analysis**

The EST and cDNA sequences were translated by ORF finder (http://www.ncbi.nlm.nih.gov/gorf/gorf.html). Secondary structure of EMP2 and ZmHSBP2 were predicted using COILS (http://www.ch.embnet.org/software/COILS_form.html), and the probabilities of multimerization were calculated by PAIRCOIL (http://parrot.lcs.mit.edu/cgi-bin/paircoil). The multiple alignment was performed utilizing ClustalW and BOXSHADE (http://dot.imgen.bcm.tmc.edu: 9331/multi-align/Options/clustalw.html). Sequences examined are (species names, Genbank accession numbers in parenthesis): AtHSBP1 (*Arabidopsis thaliana* , AV534620), CeHSBP1 (*Caenorhabditis elegans,* Q9u3b7), DmHSBP1 (*Drosophila melanogaster,* Q9vk90), GaHSBP1 (*Gossypium arboreum* , BF277371), GmHSBP1 (*Glycine max,* BF324235), HsHSBP1 (*Homo sapiens,* O75506), HvHSBP1 (*Hordeum vulgare,* AL509946), HvHSBP2 (*Hordeum vulgare,* BG344770), LeHSBP1 (*Lycopersicon esculentum* , AW624356), LjHSBP1(*Lotus japonicu*s, AW428820), McHSBP1 (*Mesembryanthemum crystallinum*, BE034188), MtHSBP1 (*Medicago truncatula* , AL381382), OsHSBP1(*Oryza sativa,* AU075659), OsHSBP2 (*Oryza sativa,* BE040146), PotHSBP1 (*Populus balsamifera subsp. trichocarpa,* AI166489), PtHSBP1 (*Pinus taeda,* BG039770), SbHSBP2 (*Sorghum bicolor,* AW746844), SbHSBP1 (*Sorghum bicolor,* BG411743), SpHSBP1 (*Schizosaccharomyces pombe,* O14330), TaHSBP1 (*Triticum aestivum,* BG606102), TaHSBP2 (*Triticum aestivum,* BE442689), ZmHSBP1 (*Zea mays,* AF494284), ZmHSBP2 (*Zea mays*, BG840671).

In order to determine the intron-exon border of *hsbp*'s, cDNA sequences were aligned against genomic sequences by BLAST 2 SEQUENCES (http://www.ncbi.nlm.nih.gov/blast/bl2seq/bl2.html). Genes whose intron positions determined are (GenBank accession numbers of cDNA and genomic DNA in parenthesis): *Hshsbp1* (AF068754, NT_010422.9), *Zmhsbp1* (AF494284, AF494285), *Athsbp1* (AV534620, Z97339), *Oshsbp1* (AU075659, AAAA01003466.1), *Oshsbp2* (BE040146, AAAA01000162.1).

**Acknowledgements**

We thank A. Myers and M. James for guidance and assistance during the early stages of this work. We thank T. Young for the *hsp101* clone, P. Rogowsky for the *hsp70* clone and R. Meagher for the rRNA oligonucleotide probe. We also thank Drs. R. K. Dawe, R. Meagher, L. Pratt and Z-H. Ye for helpful discussions.

## References

Abravaya, K., Phillips, B. and Morimoto, R. I. (1991) Attenuation of the heat shock response in HeLa cells is mediated by the release of bound heat shock transcription factor and is modulated by changes in growth and in heat shock temperatures. Genes & Dev. 5: 2117-2127.

Baler, R., Welch, W. J. and Voellmy, R. (1992) Heat shock gene regulation by nascent polypeptides and denatured proteins: hsp70 as a potential autoregulatory factor. *J. Cell Biol.* 117: 1151-1159.

Barker, R. F., Thompson, D. V., Talbot, D. R., Swanson, J. and Bennetzen, J. L. (1984). Nucleotide sequence of the maize transposable element *Mu1*. Nucl Acids Res 12, 5955-5967

Barros, M. D., Czarnecka, E. and Gurley, W. B. (1992) Mutational analysis of a plant heat shock element. Plant Molec. Biol. 19: 665-675.

Bensen, R. J., Johal, G. S., Crane, V. C., Tossberg, J. T., Schnable, P. S., Meeley, R. B., and Briggs, S. B. (1995). Cloning and characterization of the maize An1 gene. Plant Cell 7, 75–84

Cotto, J. S., Kline, M. and Morimoto, R. I. (1996) Activation of heat shock factor 1 DNA binding precedes stress-induced serine phosphorylation. Evidence for a multistep pathway of regulation. J. Biol. Chem. 271: 3355-3358.

Dietrich, C. R., Cui, F., Packila, M. L., Li, J., Ashlock, D. A., Nikolau, B. J. and Schnable, P. S. (2002). Maize Mu Transposons Are Targeted to the 5' Untranslated Region of the gl8 Gene and Sequences Flanking Mu Target-Site Duplications Exhibit Nonrandom Nucleotide Composition Throughout the Genome. Genetics 160, 697-716

Feder, J. H., Rossi, J. M., Solomon, J., and Solomon, N. and Lindquist, S. (1992). The consequences of expressing *hsp70* in *Drosophila* cells at normal temperatures. Genes and Dev, 6, 1402-1413.

Fernandes, M., O'Brien, T. and Lis, J. T. (1994) Structure and regulation of heat shock promoters. In *The Biology of Heat Shock Proteins and Molecular Chaperones*. Ed. R. I. Morimoto, A. Tissieres and C. Georgopolis, pp. 375-393. Cold Spring Harbor, Cold Spring Harbor Laboratory Press.

Gai, X., Lal, S., Xing, L., Brendel, V. & Walbot, V. (2000). Gene discovery using the maize genome database ZmDB. Nucl. Acids Res. 28, 94-96.

Goff, S. A., Ricke, D., Lan, T. H., Presting, G., Wang, R., Dunn, M., Glazebrook, J., Sessions, A., Oeller, P., Varma, H., Hadley, D., Hutchison, D., Martin, C., Katagir,i F., Lange, B. M., Moughamer, T., Xia, Y., Budworth, P., Zhong, J., Migue,l T., Paszkowski, U., Zhang, S., Colbert ,M., Sun, W. L., Chen, L., Cooper, B., Park, S., Wood, T. C., Mao, L., Quail, P., Wing, R., Dean, R., Yu, Y., Zharkikh, A., Shen, R., Sahasrabudhe, S., Thomas, A., Cannings, R., Gutin, A., Pruss, D., Reid, J., Tavtigian, S., Mitchell, J., Eldredge, G., Scholl, T., Miller, R.. M, Bhatnagar, S., Adey, N., Rubano, T., Tusneem, N., Robinson, R., Feldhaus, J., Macalma, T., Oliphan, T A., Briggs, S. (2002). A draft sequence of the rice genome (*Oryza sativa* L. ssp. *japonica*). Science 296, 92-100.

Goldrick, M., D. Kessler, and M. Winkler. 1996. Analysis by nuclease protection. In A laboratory guide to RNA (ed. P. Krieg), pp. 105-131. Wiley-Liss, New York, NY.

Hensold, J. O., Hunt, C. R., Calderwood, S. K., Housman, D. E. and Kingston, R. E. (1990) DNA binding of heat shock factor to the heat shock element is insufficient for transcriptional activation in murine erythroleukemia cells. Mol. Cell. Biol. 10: 1600-1608.

Hess, M. A. and Duncan, R. F. (1996) Sequence and structure determinants of Drosophila Hsp70 mRNA translation: 5'UTR secondary structure specifically inhibits heat shock protein mRNA translation. Nucleic Acids Res.15: 2441-2449.

Hubel, A. and Schoffl, F. (1994) Arabidopsis heat shock factor: characterization of the gene and recombinant protein. Plant Mol. Biol. 26: 353-362

Iwahashi, Y. and Hosoda, H. (2000). Effect of heat stress on tomato fruit protein expression. Electrophoresis 21: 1766-1771.

James, M. G., Robertson D. S. and Myers A. M. (1995). Characterization of the maize gene *sugary1*, a determinant of starch composition in kernels. Plant Cell 7: 417-429

Kline, M. P. and Morimoto, R. I. (1997) Repression of the heat shock factor1 transcriptional activation domain is modulated by constituitive phosphorylation. Mol. Cell. Biol. 17: 2107-2115.

Li, S. X. and Showalter, A. M. (1996). Cloning and developmental/stress-regulated expression of a gene encoding a tomato arabinogalactan protein. Plant. Mol. Biol. 32: 641-652.

Lindquist, S. and Petersen, R. (1990). Selective translation and degradation of heat -shock messenger RNAs in *Drosophila*. Enzyme 44:147-166.

Marrs, K. A., Casey, E. S., Capitant, S. A., Bouchard, R. A., Dietrich, P. S., Mettler, I. J. and Sinibaldi, R. M. (1993) Characterization of two maize hsp90 heat shock protein genes: expression during heat shock, embryogenesis, and pollen development. Developmental Genetics 14:27-41.

Morimoto, R. I. (1991). Heat shock: the role of transient inducible responses in cell damage, transformation, and differentiation. Cancer Cells 8: 295-301.

Morimoto, R. I. (1998) Regulation of the heat shock response: cross talk between a family of heat shock factors, molecular chaperones, and negative regulators. Genes & Dev. 12: 3788-3796.

Mosser, D. D., Duchaine, J. Massie, B. (1993). The DNA-binding activity of the heat shock transcription factor is regulated *in vivo* by hsp70. Mol. Cell. Biol. 13, 5427-5438.

Nagao, R. T., Kimpel, J. A., Vierling, E. and Key, J. L. (1986). The heat shock response: a comparative analysis. pp. 384-438 In *Oxford surveys of Plant Molecular and Cell Biology,* edited by B. J. Miflin. Oxford Press, Oxford..

Nover, L., Bharti, K., Doring, P., Mishra, S. K., Ganguli, A. and Scharf, K-D. (2001). *Arabidopsis* and the heat stress transcription factor world: how many heat stress transcription factors do we need? Cell Stress & Chaperones 6, 177-189.

Pelham, H. R. B. (1982) A regulatory upstream promoter element in the *Drosophila* hsp70 heat shock gene. Cell 46: 959-961.

Pitto, L., LoSchiavo, F., Giuliano, G. and Terzi, M. (1983) Analysis of heat shock protein pattern during somatic embryogenesis of carrot. Plant Mol. Biol. 2: 231-237.

Prandl, R., Hinderhofer, K., Eggers-Schumacher, G. and Schoffl, F. (1998) HSF3, a new heat shock factor from *Arabidopsis thaliana,* derepresses the heat shock response and confers thermotolerance when overexpressed in transgenic plants. Mol. Gen. Genet., 258: 269-278.

Queitsch, C., Hong, S. W., Vierling, E. and Lindquist, S. (2000). Heat Shock Protein 101 Plays a Crucial Role in Thermotolerance in Arabidopsis . Plant Cell 12, 479-492.

Sambrook J., Fritsch, E. F. and Maniatis, T. (1989) Molecular cloning. A laboratory manual. Ed. 2nd Cold Spring Harbor, NY. Cold Spring Harbor Laboratory.

Santoro, M. G. (2000) Heat shock factors and the control of the stress response. Biochem. Pharm. 59: 55-63.

Sarge, K. D., Murphy, S. P. and Morimoto, R. I. (1993) Activation of heat shock gene transcription by heat shock factor1 involves oligomerization, acquisition of DNA-binding activity, and nuclear localization and can occur in the absence of stress. Mol. Cell. Biol. 13: 1392-1407.

Satyal, S. H., Chen, D., Fox, S. G., Kramer, J. M. and Morimoto, R. I. 1998) Negative regulation of the heat shock transcriptional response by HSBP1. Genes & Devel. 12: 1962-1974.

Seeley, K. A., Byrne, D. J. and Colbert, J. T. (1992). Red light independent stability of oat phytochrome mRNA *in vivo*. Plant Cell 4: 29-38.

Scanlon, M. J. and Freeling, M. (1998). The narrow sheath leaf domain deletion: a genetic tool used to revea developmental homologies among modified maize organs. *The Plant J*. 13: 547-561.

Scanlon, M. J., Stinard, P. S., James, M. G., Myers, A. M. And Robertson, D. S. (1994) Genetic analysis of 63 mutations affecting maize kernel development isolated from *Mutator* stocks. Genetics 136: 281-294.

Schleshinger, M. J., Ashburner, M. and Tissieres, A. (1982) *Heat shock, from Bacteria to Man*. Cold Spring Harbor, Cold Spring Harbor Laboratory Press.

Schoffl, F., Prandl, R. and Reindl, A. (1998) Regulation of the heat shock response. Plant Phys. 17: 1135-1141.

Schrauwen, J. A. M., Reijnen, W. H., DeLeeuw, H. C. G. M. and van Herpen, M. M. A. (1986) Response of pollen to heat stress. Acta Bot. Neerl. 35: 321-327.

Sheridan, W. F. and Neuffer, M. G. 1980. Defective kernel mutants of maize II. Morphological and embryo culture studies. Genetics 95: 945-960.

Simoes-Araujo, J. L., Rodriques, R. L., de A. Gerhardt, L. B., Mondego, J. M. C., Alves-Ferreira, M., Rumjanek, N. G. and Margis-Pinheiro, M. Identification of differentially expressed genes by cDNA-AFLP technique during heat stress in cowpea nodules. FEBS Letters 515: 44-50.

Song, J., Takeda, M. and Morimoto, R. I. (2001). Bag1-Hsp70 mediates a physiological stress signalling pathway that regulates Raf-1/ERK and cell growth. Nature Cell Biol. 3, 276-282.

Sylvester, A. W. and Ruzin, S. E. (1994). Light microscopy I: Dissection and microtechnique. In: *The Maize handbook* (Freeling, M. and Walbot, V. eds.) New York: Springer-Verlag. pp. 83-94.

Tai, Li-J., McFall, S. M., Huang,K., Demeler, B., Fox, S. G., Brubaker, K., Radhakrishnan, I. and Morimoto, R. I. (2002). Structure-function analysis of the HEAT SHOCK FACTOR BINDING PROTEIN reveals a protein composed solely of a highly conserved and dynamic coiled-coil trimerization domain. J. Biol. Chem. 277: 735-745.

Tanzer, M. M. and Meagher, R. B. (1994) Faithful degradation of soybean *rbc*S mRNA in vitro. Mol. Cell. Biol. 14:2640-2650.

Thompson, D. M. and Meagher, R. B. (1990) Transcriptional and post-transcriptional processes regulate the expression of RNA encoding the small subunit of ribulose-1, 5-*bisphosphate carboxylase* differently in petunia and in soybean. Nucleic Acids Res. 1:83621-3629.

Thompson, D. M., Tanzer, M. M. and Meagher, R. B. (1992) Degradation Products of the mRNA Encoding the Small Subunit of Ribulose-1,5-Bisphosphate Carboxylase in Soybean and Transgenic Petunia. Plant Cell 4: 47-58.

Vivinus, S., Baulande, S., van Zanten, M., Campbell, F., Topley, P., Ellis, J. H., Dessen, P. and Coste, H. (2001) An element within the 5' untranslated region of human Hsp70 mRNA which acts as a general enhancer of mRNA translation. Eur J Biochem. 268: 1908-17.

Vierling, E. (1991) The roles of heat shock proteins in plants. Annu. Rev. Plant Physiol. Mol. Biol. 42: 579-620.

Weatherwax, P. (1920) Position of the scutellum and homology of coleoptile in maize. *Bot. Gaz.* 69: 179-182.

Wu, Carl (1995). Heat shock transcription factors: structure and regulation. Ann. Rev. Cell. Dev. Biol. 11, 441-469.

Xiao, H., Perisic, O. and Lis, J. T. (1991) Cooperative binding of *Drosphila* heat shock factor to arrays of a conserved 5 bp unit. Cell 64: 585-593.

# CHAPTER 3

# CLONAL MOSAIC ANALYSIS OF *EMPTY PERICARP2* REVEALS NON-REDUNDANT FUNCTIONS OF THE DUPLICATED HEAT SHOCK FACTOR BINDING PROTEINS DURING MAIZE SHOOT DEVELOPMENT[1]

[1] Fu. S. and Scanlon. MJ. Clonal mosaic analysis of *empty pericarp2* reveals non-redundant functions of the duplicated HEAT SHOCK FACTOR BINDING PROTEINs during maize shoot development. In press in Genetics. The material is copyrighted by Genetics Society of America, reprinted here with permission (see APPENDICES B).

**Abstract**

The paralogous maize proteins EMPTY PERICARP2 (EMP2) and HEAT SHOCK FACTOR BINDING PROTEIN2 (HSBP2) each contain a single recognizable motif: the coiled coil domain. EMP2 and HSBP2 accumulate differentially during maize development and heat stress. Previous analyses revealed that EMP2 is required for regulation of *heat shock protein* (*hsp*) gene expression and also for embryo morphogenesis. Developmentally abnormal emp2 mutant embryos are aborted during early embryogenesis. In order to analyze EMP2 function during post embryonic stages, plants mosaic for sectors of emp2 mutant tissue were constructed. Clonal sectors of emp2 mutant tissue revealed multiple defects during maize vegetative shoot development, but these sector phenotypes are not correlated with aberrant *hsp* gene regulation. Furthermore, equivalent phenotypes are observed in emp2-sectored plants grown under heat stress and non-stress conditions. Thus, the function of EMP2 during regulation of the heat stress response can be separated from its role in plant development. The discovery of emp2 mutant phenotypes in post embryonic shoots reveals that the duplicate genes *emp2* and *hsbp2* encode non-redundant functions throughout maize development. Distinct developmental phenotypes correlated with the developmental timing, position, and tissue layer of emp2 mutant sectors, suggesting that EMP2 has evolved diverse developmental functions in the maize shoot.

## Introduction

EMPTY PERICARP2 (EMP2) of maize is a small, evolutionarily conserved protein comprised solely of a central coiled coil domain (FU et al., 2002). Consisting of two to five amphipathic alpha helices that are twisted to form a super coil, the coiled-coil motif is a dominant feature in many protein::protein interactions (BURKHARD et al., 2001; YU, 2002). EMP2 homologous proteins are found throughout the eukaryotic domain, and were first identified in humans as the HEAT SHOCK FACTOR BINDING PROTEIN1 (HSBP1) via binding interactions with HEAT SHOCK FACTOR1 (HSF1) protein (FU et al., 2002; SATYAL et al., 1998; TAI et al., 2002). HSF1 is a transcription factor that induces the expression of a wide range of *heat shock protein* genes (*hsp*) during thermal stress (PIRKKALA et al., 2001; WIEDERRECHT et al., 1988). This heat-induced, upregulated transcription of *hsp*s and other chaperonins is termed the heat shock transcriptional response (HSTR), and is likewise an extraordinarily conserved phenomenon in nature (GURLEY and KEY, 1991; LINDQUIST, 1986; MORIMOTO, 1998). Previous analyses in humans and *C. elegans* suggest that HSBP1 binds to and inactivates animal HSF1 during attenuation of the heat shock response (SATYAL et al., 1998). These studies suggest that the coiled-coil domain of HSBP1 plays an integral role during mediation of protein::protein interaction with animal HSF1, although no mutant phenotype is observed in null mutations of *hsbp1* in *C. elegans* (SATYAL et al., 1998; TAI et al., 2002).

Two HSBP homologous are present in maize: EMP2 and HSBP2. Preliminary investigations of EMP2 suggest a conserved function in HSTR regulation during maize embryogenesis (FU et al., 2002). Loss of function emp2 mutants exhibit early-staged embryo abortion. The developmental timing of emp2 embryo lethality correlates with the initial competency of maize embryos to invoke the HSTR, and with over expression of *hsp* transcripts. However, emp2 mutant embryos display aberrant morphology throughout their abbreviated development, well before *hsp* over-expression and prior to embryonic abortion. Thus, an additional developmental function(s) of EMP2 is implied, outside of its role in HSTR regulation.

In this report, we demonstrate that the accumulation of the maize paralogues EMP2 and HSBP2 is differentially regulated in embryos and leaves. In order to investigate whether the paralogues function non-redundantly during post-embryonic maize development, clonal sectors of emp2 mutant tissue were generated in developing maize shoots against a heterozygous non-mutant background. In contrast to the phenotype seen in emp2 mutant embryos, EMP2 is not required for normal regulation of *hsp* gene expression in leaves. Furthermore, numerous developmental mutant phenotypes correlate with emp2 mutant sectors in the maize vegetative shoot. Thus, this clonal sector analysis has successfully separated the function of EMP2 in HSTR regulation from its unrelated function(s) during maize shoot development. These data suggest that the EMP2 coiled coil motif has been recruited to mediate additional protein-protein interaction(s) during the evolution of maize shoot development, and that EMP2 and HSBP2 perform non-redundant functions during post-embryonic as well as embryonic development.

## Materials and Methods

### Maize transcript and protein analyses

Total RNA from maize tissue was prepared by Trizol lysis buffer (Gibco BRL, Bethesda, MD) according to the manufacturer's recommendation. Total RNA concentrations were quantified by spectrophotometry. For use in Northern gel-blots, 5μg of total RNA was loaded in each lane. Gene specific probes for a 18kDa maize *hsp* EST contig (Plant GDB *Zmtuc03-08-11.14919*) were PCR amplified using the primer pair: 5'-CAT CAC AAA GCT CCA AAC CCA GCA-3' and 5'-GCC CAA GAC CAT CGA GAT TAA GGT-3'. A 0.7kb *Eco*RI-*Xho*I digestion fragment of *Zmhsp101* cDNA (gift from Dr. Gallie, UC Riverside) was used as a gene-specific probe. Immunoblot analysis of EMP2 protein accumulation in emp2 null sectored and non-sectored leaves were carried out as described previously (FU et al., 2002).

**Antibody production, Recombinant Protein Expression, Immunoblot Analysis and Immunolocalization:**

Soluble proteins from maize tissues were prepared as described previously (Fu et al., 2002). Recombinant proteins of EMP2 and HSBP2 were expressed separately in the pTriplEx vector (Clontech) and in the pBAD TOPO TA vector (Invitrogen) according to the manufacture's recommendations. Bacterial protein preparation, protein gel electrophoresis, transfer and coomassie blue staining (Brilliant Blue R350) were performed according to standard methods (Sambrook and Russel., 2001). Thirty micrograms of total protein were loaded per lane.

Rabbit anti-EMP2 (described in Fu et al., 2002) and anti-HSBP2 specific polyclonal antibodies were produced and affinity purified by BioSource Intl. (Camarillo, CA). The specificities of the purified antibodies were assayed by ELISA and Western gel-blotting against unique multiple antigenic peptides (MAP) and recombinant proteins of HSBP2. The dilutions used for primary antibodies in Western gel -blot assays were 1/3000 (anti-EMP2) and 1/2000 (anti-HSBP2). Fixation, paraffin embedment, sectioning and immunolocalization of EMP2 antigen in maize kernels were carried out as described (Sylvester and Ruzin, 1994). The affinity purified anti-EMP2 polyclonal antibodies were used as the primary antibodies at 1/100 dilution; the secondary antibodies were either goat anti-rabbit IgG -AP conjugated at 1/500 dilution (Promega, Madison, WI) or fluorescein isothiocyanate (FITC))–conjugated goat anti–rabbit antibody at 1/30 dilution (Jackson ImmunoResearch, West Grove, PA). The images were obtained using a Zeiss Axioplan II equipped with a Southern Micro Instruments (Pompano Beach, FL) CCD camera.

**Genetic stocks, sector generation, stress treatment and analyses**

Maize stocks heterozygous for the *emp2-R* (reference allele; Scanlon et al., 1997; Fu et al., 2002; previous designation *emp2-1047,* Scanlon et al., 1994) in coupling with the albino mutation *w3* were obtained by crossing plants of the genotypes *W3, Emp2/W3, emp2-R* by *w3, Emp2/W3, Emp2*. One quarter of the kernels obtained from this cross will be w3*, Emp2/ W3, emp2-R*. Plants of this genotype were identified by the segregation of both white and emp mutant kernels on self-pollinated ears; these plants were also out-crossed to B73. The progeny were subjected to an additional round of self-pollination and outcrossing, in order to identify individual plants that harbored the *emp2* and *w3* mutations in coupling. Outcross progeny of the *w3, emp2-R* heterozygous mutant parents were utilized for clonal analyses. All white sectored plants utilized in this report were analyzed by genomic PCR (FU et al., 2002), in order to verify that they harbored the *emp2-R* mutation.

A total of 9,000 seeds were imbibed overnight, germinated for two days and subsequently irradiated at 1250-1500 rads utilizing cobalt 60 and average energy 1.25 MeV. Following radiation 6,000 seedlings were field planted, 2,000 seedlings were grown at 25°C in the greenhouse, and an additional 1,000 seedlings were subjected to daily heat stress treatments (36°C or 42°C, for two hours).

Single-leaf sectors appeared on juvenile leaves only, and were harvested before plant maturity. In contrast, multiple leaf sectors were harvested at plant maturity. All sectored plants were genotyped by PCR. Hemizygous, *w3*, *emp2/-* sectored plants were analyzed to determine the tissue layers occupied by the sectors; phenotypes were scanned, photographed or photocopied as described (SCANLON, 2000).

The position and width of each leaf sector was recorded relative to the lateral vein number at which the sectored started, and how many lateral veins the sector spanned relative to the number of total lateral veins contained within the half leaf. The lateral vein data were used to extrapolate positions of sectors on mature leaves back to the leaf primordium (Figure 3.1B and legend), because lateral veins are evenly spaced in young primordia (Sharman, 1942). When mixed cell layer sectors were encountered, only the sector portion that occupied the full L2-derived layer was mapped in Figure 3.5. In those cases wherein a narrow leaf phenotype was associated with a sector, the vein number on the non-phenotypic side of the leaf was used as the total vein number. Leaf primordia were assumed to be uniform in size, comprising 40 units in length from midrib to margin (Figure 3.1B). The overall distribution of sector positions on leaf primordia is presented as overlaying solid lines, with their positions and lengths correlated to the location and width of each sector. Consequently, a two dimensional plot was derived to describe the correlation of narrow leaf phenotypes with the lateral location of sectors extrapolated to the leaf primordium.

The methodology used to extrapolate meristematic leaf sectors onto the circumference of the SAM is essentially the same as described previously (Figure 3.1 and legend, SCANLON, 2000). The only modification is that the half circumference of the SAM is represented by a solid straight bar of 40 units in width, with 0 and 40 anchored for the midrib and marginal flanks of the SAM. For example, if 5 cm in girth stem contains a sector that initiates 1.5cm away from the midrib and extends 0.5 cm laterally, the sector is represented by a solid line extending from position 24 to position 32 in Figure 3.6. Sectored leaves were categorized according to developmental stage (middle and adult) according to the same criteria described in SCANLON (2000).

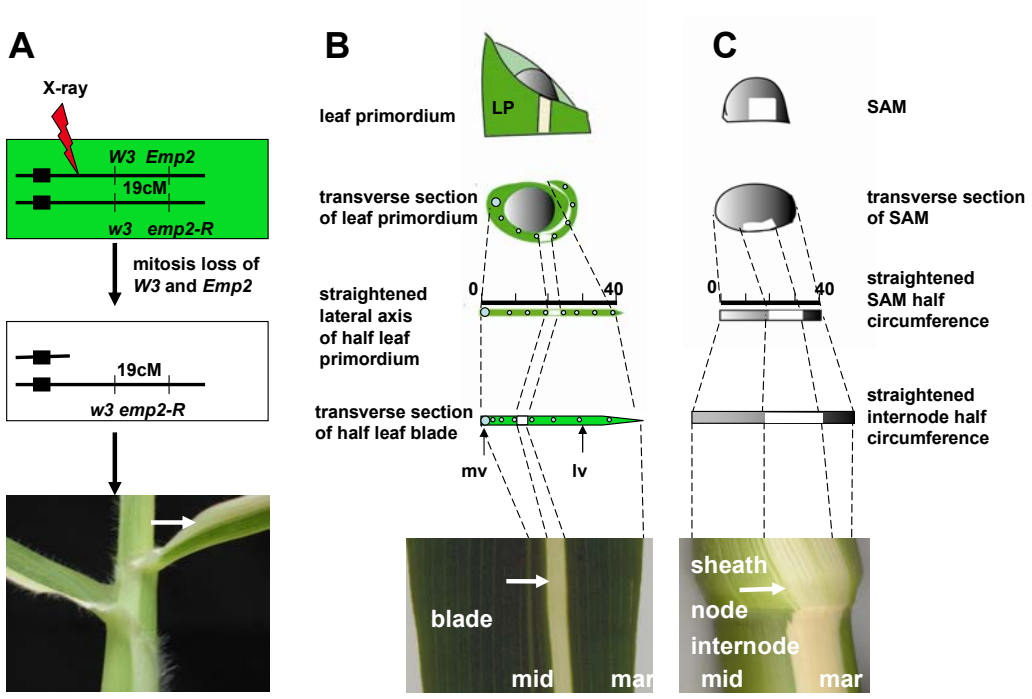


**FIGURE 3.1** Generation and analyses of albino-marked emp2 hemizygous sectors. (A) Cartoon of a maize cell (top) heterozygous for the *emp2-R* and *w3* mutations in coupling on chromosome 2 (black rectangles = centromere). X-ray induced random chromosome breakage of the nonmutant chromosome proximal to the *W3* locus leads to clonal loss of the nonmutant *W3* and *Emp2* alleles in albino progeny cells (middle). Thus, sectors of albino tissue mark the clonal loss of EMP2 function (bottom). (B) Methodology used to estimate the position of emp2 mutant sectors on leaf primordia (top) via extrapolation of the sector position on mature leaves (bottom). As described in the Materials and Methods, the lateral axis of a half-leaf primordium (LP) was graphically subdivided into 40 equal increments; these increments were later correlated to the positions of lateral veins (lv) counted on the mature, sectored leaf. (C) Methodology used to estimate the lateral position of sectors within the shoot apical meristem (SAM) via extrapolation of the position of sectors within the internode of mature plants. See Materials and Methods for

(**FIGURE 3.1** legend continued) further details. mid = midrib domain; mar = margin; mv = midvein.

**Heat treatment of maize plants for transcript analyses**

Plants used for transcript analysis of *emp2*, *hsbp2* and various maize *hsps* [*hsp101, hsp18, hsp82, hsp70, dnaj,* and two additional small *hsps* identified from maize ESTs deposited in the public database (http://www.plantgdb.org/)] were grown continuously under 25°C, heat-shifted to either 36°C or 42°C for 2h, followed by recovery at 25°C. Sectors and adjacent unsectored tissues were periodically sampled for analysis of maize *hsp* transcripts by Northern gel-blot analyses as described (FU et al., 2002).

## Results

**The homologous proteins EMP2 and HSBP2 show differential accumulation in maize embryos and leaves**

RT-PCR and Northern gel-blot analyses revealed that *emp2* and *hsbp2* are both expressed constitutively in all tissues examined. However, Western analyses using gene product-specific antibodies (see Materials and Methods) indicate that the EMP2 and HSBP2 proteins accumulate differentially in maize embryos and leaves (Figure 3.2). Specifically, EMP2 protein is more abundant in 16 day after pollination (DAP) embryos than in mature leaves, whereas HSBP2 protein is less abundant in embryos than in leaves. Also, whereas EMP2 protein levels are not heat inducible in leaves, accumulation of HSBP2 protein is induced in the maize leaf following incubation for 2h at 36°C and 42°C (Figure 3.2).

Immunohistolocalization analyses reveal that EMP2 protein accumulates in the nuclei, and to a lesser extent in the cytoplasm, of maize embryonic cells (Figure 3.3E). No tissue-specific localization of EMP2 protein is observed; equivalent levels of protein are detected in all embryonic cell types, including the scutellum, and organs of the root and shoot pole. In addition, longitudinal and transverse sectioning of maize embryos revealed no compartmentalized

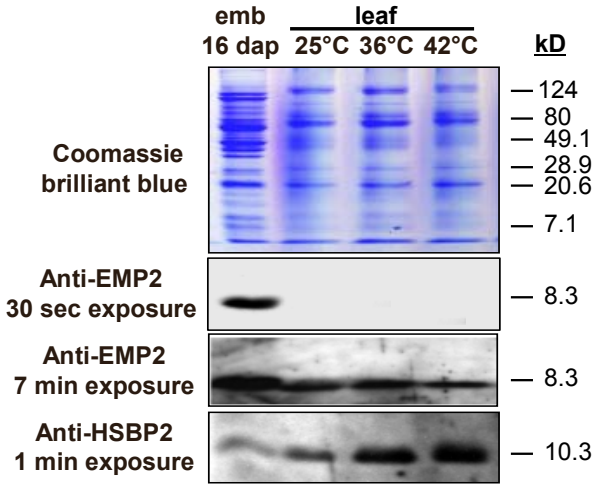


**Figure 3.2** EMP2 and HSBP2 show differential accumulation and responses to heat stress. Western gel-blot analyses reveal that EMP2 protein preferentially accumulates in 16 day after pollination (DAP) embryos (emb) and is not heat inducible in mature leaves. In contrast, the paralogue HSBP2 preferentially accumulates in leaves rather than embryos, and accumulation of HSBP2 is induced following heat treatment of leaves.

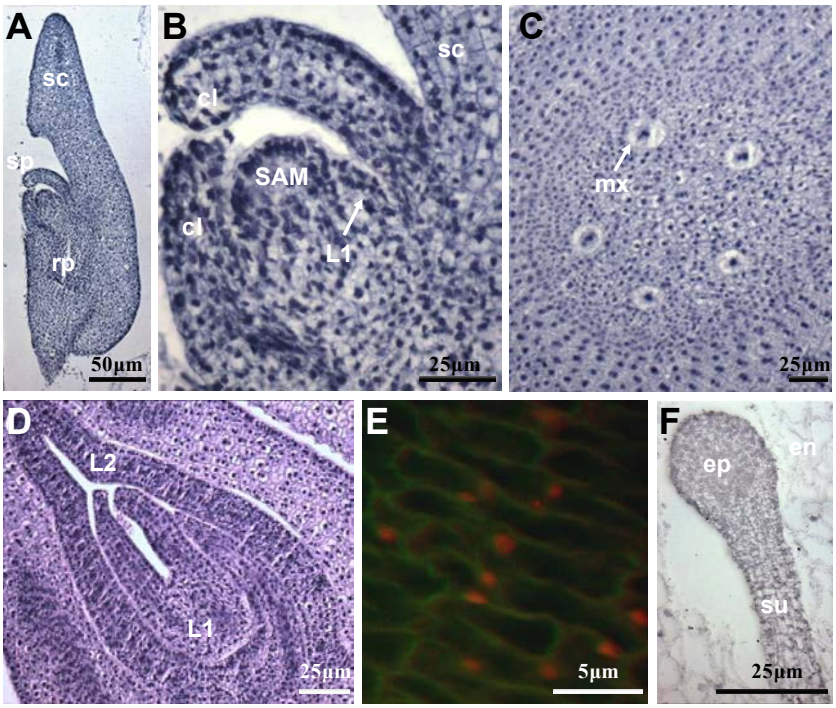


**Figure 3.3** Tissue and cellular localization of EMP2 protein. (A) Immunolocalization of EMP2 protein in maize embryos. Longitudinal section of a maize 14 DAP embryo reveals accumulation of EMP2 protein (dark blue) throughout the embryo, including the scutellum (sc), shoot pole (sp) and root pole (rp). (B) Close up of the shoot pole of the embryo shown in (A) reveals equivalent accumulation of EMP2 protein in the SAM, coleoptile (cl), leaf primordium (L1) and scutellum (sc). Transverse sections of the root (C) and shoot (D) of a 24 DAP maize embryo show even accumulation of EMP2 proteins throughout the lateral axes of the embryo. (E) Merged UV fluorescence/light micrograph analyses of subcellular localization of EMP2 protein (red) in 14 DAP pericarp cells reveals accumulation predominately in the nucleus although faint signals are detected outside the nucleus. Cell walls autofluoresce green. (F) 12 DAP emp2 null mutant embryo does not accumulate EMP2 protein. ep = embryo proper; en equals endosperm; su = suspensor.

accumulation of EMP2 proteins within the shoot apical meristem (SAM) or in leaf primordia (Figure 3.3B-D).

**Analyses of EMP2 function in the post-embryonic shoot: generation of EMP2 loss of function clonal sectors**

The embryo lethality of the homozygous emp2 mutants precludes traditional genetic analyses of EMP2 function in the post-embryonic shoot. In order to study the function of EMP2 beyond embryogenesis, a clonal mosaic analysis was performed in which the *emp2-R* mutation was exposed in hemizygous, albino-marked sectors (*w3*, *emp2-R*/-,-) in a non-mutant (*w3*, *emp2-R*/*W3*, *Emp2*) genetic background by X-ray induced random chromosome breakage proximal to the *W3* locus (Figure 3.1). Previous mosaic analyses utilizing the *w3* albino marker confirmed that aside from albinism, hemizygous clonal sectors of w3 mutant leaf tissue do not alone cause disturbances in shoot morphological development (FOSTER et al, 1999; SCANLON, 2000). Therefore, developmental abnormalities associated with albino emp2-null mutant sectors enable phenotypic analyses of EMP2 function(s) in adult maize shoots. The cell autonomy, organ/tissue layer specificity, and developmental timing of EMP2 function in the shoot may also be inferred from clonal analysis.

Western gel blot analyses confirmed that no EMP2 protein is detectable in emp2 null albino sectors, although EMP2 does accumulate in sectors hemizygous for the non-mutant *Emp2* allele (Figure 3.4). These data reveal that the *emp2-R* allele is a null mutation in maize leaves as well as in embryo, although the paralogous protein HSBP2 accumulated to equivalent levels in both emp2 null and non-mutant albino sectors (data not shown). Therefore, the accumulation of EMP2 and HSBP2 is not co-regulated in maize leaves.

**Expression of heat shock protein (*hsp*) genes is unaffected within emp2 mutant leaf sectors**

In order to decipher whether EMP2 functions to regulate *hsp* expression in the post-embryonic shoot (as it does in maize embryos, FU et al., 2002), transcript levels of seven different maize *hsps* (including *hsp101, hsp18, hsp82, hsp70, dnaj,* and two additional small *hsps* identified as

ESTs; LUND et al., 1998; MARRS et al., 1993; NIETO-SOTELO et al., 2002; VIERLING et al., 1989; YOUNG et al., 2001) were analyzed via RNA gel-blots before, during, and after heat stress in both mutant sectored and adjacent wild type unsectored leaf tissues. Sectors of emp2 mutant tissue had no effect on the accumulation of any of the *hsp* transcripts analyzed; the data for *hsp101* and *hsp18* are shown in Figure 3.5. When grown at non-stress temperatures (25°C), transcripts of *hsp101*and *hsp18* in emp2 null sectors and in adjacent unsectored tissues are not detected (Figure 3.5). However, after plants were heat shocked at 42°C for 2 hours, accumulation of *hsp* gene transcripts was induced equivalently in both unsectored and emp2 -null sectored leaf tissues. Notably, restoration of non-stress temperature corresponded with the prompt (within 2h) attenuation of *hsp* transcription in both emp2 null sectored and non-mutant leaf tissue (Figure 3.5). Thus, whereas EMP2 is required for correct *hsp* gene regulation in maize embryos (FU et al., 2002), this function of EMP2 is dispensable in maize leaves. As elaborated below, these analyses have successfully separated the *hsp* gene regulatory function of EMP2 from its role in plant development.

**Clonal sectors of loss of EMP2 function in the maize shoot correlate with diverse developmental defects**

In order to investigate the function(s) of EMP2 during post-embryonic shoot development, a total 117 sectored plants (encompassing 245 leaves) out of greater than 6000 irradiated seedlings were examined. Among them, 98 sectors (encompassing 188 total leaves) were genotyped as em*p2-R/-* via PCR analysis, while the remaining sectors were *Emp2*/-. No developmental phenotype was observed in any hemizygous sectors from *Emp2*/*Emp2* plants (data not shown), while 48 of the emp2/- sectors were associated with developmental defects (Table 3.1-5, Figure 3.6). As described above (Figure 3.5), none of the emp2-R/-null albino sectors showed aberrant *hsp* gene expression at ambient temperature, during heat shock, or after recovery from heat shock. Moreover, equivalent developmental phenotypes were observed in field-grown emp2 sectored plants, in plants grown in the greenhouse under non-heat shock conditions (< 25°C), as well as in

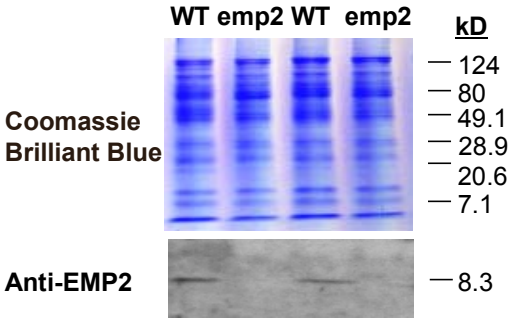


**FIGURE 3.4** The emp2/- mutant sectors do not accumulate EMP2 protein. Western gel-blot analyses reveal that EMP2 protein accumulated in the sectors that are hemizygous for the nonmutant *Emp2* allele (WT), but not in *emp2-R* hemizygous sectors (emp2).

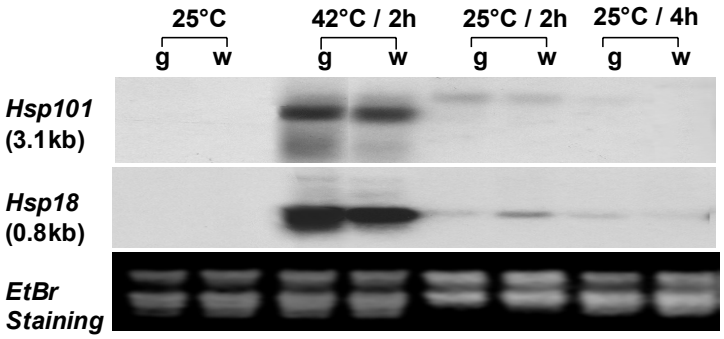


**FIGURE 3.5** The accumulation of maize heat shock protein transcripts is unaffected in sectors of emp2-null mutant leaf tissue. RNA gel-blot analyses of emp2 null sectored (w) and adjacent, nonmutant unsectored leaf tissue (g) reveal equivalent accumulation of both *hsp101* and *hsp18* transcripts before (25ºC) during (42ºC) and after (25ºC / 2h and 25ºC / 4h) heat stress.

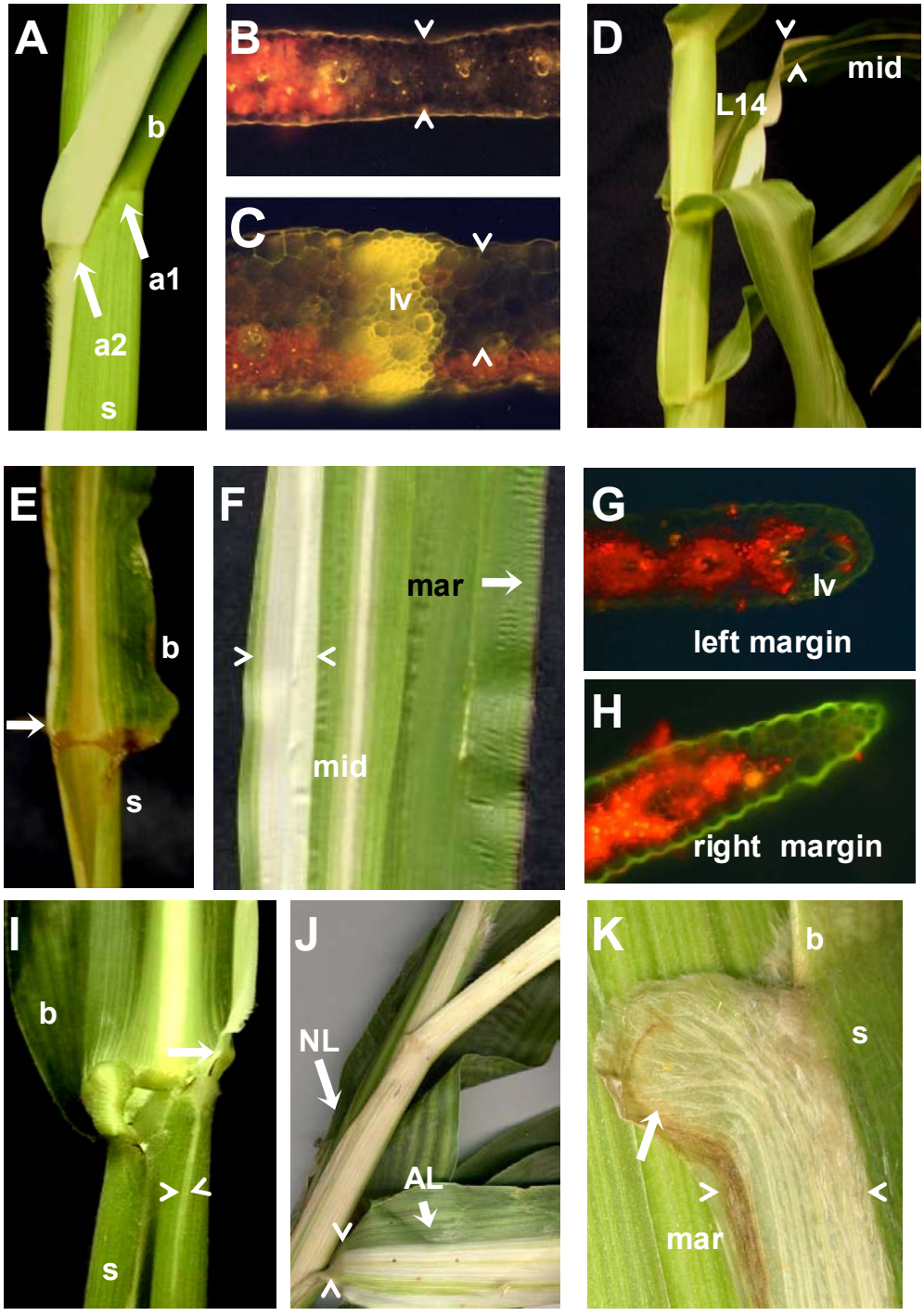


**FIGURE 3.6** Multiple developmental defects are associated with emp2 mutant sectors. (A) Sector #59; leaf #6. The ligule/auricle structure within the mutant sector is displaced proximally (a2, auricle) compared to the ligule/auricle structure in the unsectored portion of the leaf (a1, auricle). UV fluorescence micrographs (chlorophyll is red) reveal that ligule/auricle

(**Figure 3.6** legend continued) displacement phenotypes are associated with emp2 sectors (bordered by arrows) that were contained in all L2-derived tissue layers (B) and also in sectors confined to adaxial L2-derived tissues: sector #37; leaf #4 (C). (D) Sectors #66 and #67; leaf #14: Abnormal phyllotaxy of emp2 sectored leaves. Two leaves arose from the same node and in dechussate phyllotaxy, as opposed to the alternate phyllotaxy of adjacent leaves. Note that leaf 14 (L14) contains two independent emp2 sectors (arrows) straddling the midrib. (E-F) Sector #51; leaf 3 and sector #82; leaf #13: Emp2 mutant sectors lead to the deletion of a lateral leaf domain (arrow) in both the sheath(s) and blade (b). UV fluorescence micrograph of the left margin of the narrow leaf blade shown in (F) is blunted and chlorophyllic (G), whereas the nonmutant right margin of the same leaf (H) is tapered and non-chlorophyllic. (I) Sector #96; leaf #11: Partial narrow leaf emp2 mutant sector (arrows) in which the lateral domain deletion is localized to the leaf blade and the upper part of sheath only. (J) Sector #97; leaf #16: A narrow leaf emp2 sector in which an accessory leaf (AL, arrow) is attached to a narrow leaf (NL, arrow). (K) Sector #83; leaf #12: An emp2 mutant sector in which an abnormal outgrowth of sheath tissue is hypervascularized and the normal parallel vascular pattern is disrupted. b = blade; s = sheath; mid = midrib; mar = margin; lv = lateral vein.

**Table 3.1** emp2 mutant sectors and phenotypes

| phenotypes (# of affected leaves) | sector timing | | sector tissue layer | | | | |
|---|---|---|---|---|---|---|---|
| | meristematic | non-meristematic | L2 alone | L1-L2 | adaxial L2[f] | internal L2 alone | abaxial L2[f] |
| ligule/auricle displacement (11) | 2 | 9 | 6 | 3 | 2 | 0 | 0 |
| abnormal phyllotaxy (8) | 12[b] | 0 | 2 | 7 | 3[g] | 0 | 3[g] |
| narrow leaf (28) | 14[a] | 9 | 12 | 17 | 0 | 0 | 0 |
| narrow leaf with accessory leaf | 4 | 0 | 4 | 0 | 0 | 0 | 0 |
| narrow leaf with lobe growth | 2 | 0 | 0 | 2 | 0 | 0 | 0 |
| no phenotype (141)[e] | 8 | 45 | 34 | 28 | 13 | 2 | 11 |
| total sectored leaves (188)[e] | 32[c,d] | 63 | 52[c] | 53[d] | 18 | 2 | 14 |

[a] The fourteen meristematic sectors condition 20 narrow leaves.

[b] The twelve meristematic sectors condition 8 abnormal phyllotaxy leaves.

[c,d] Two sectors each ([c]: sector #77 and #89; [d]: sector #96 and #97) were associated with both narrow leaf phenotypes and abnormal phyllotaxy.

[e] Not all the emp2 mutant sectors on leaves have their tissue layer and developmental timing determined.

[f] includes sectors extended into the internal L2 layer.

[g] both the adaxial and abaxial L2 are sectored but not the internal layer.

**Table 3.2** Ligule/auricle emp2 sectors

| sector # (leaf #)[a] | sector type[b] | leaf stage[c] | lateral vein # | sector position[d] | tissue layer[e] | phenotype |
|---|---|---|---|---|---|---|
| 23(3) | non- meristematic | J | L6, R6 | R4-4.5 | wwwww | Y |
| 24(3) | non- meristematic | J | L6, R6 | L2-2 | wwwww | Y |
| 25(3) | non- meristematic | J | L6, R6 | R3-4 | wwwww | Y |
| 30(4) | non- meristematic | J | L8, R8 | L1-1.5 | GwwGG | Y |
| 37(4) | non- meristematic | J | L9, R9 | L3-5 | GwwGG | Y |
| 46(3) | non- meristematic | J | L8, R8 | L3-3.5 | GwwwG | Y |
| 52(6) | non- meristematic | J | L13, R10 | L1.5-2 | GwwwG | Y |
| 56(4) | non- meristematic | J | L12, R12 | R2-3 | GwwwG | Y |
| 59(5) | non- meristematic | J | L9, R10 | R7-E | GwwwG | Y |
| 65(14) | meristematic | A | L18, R18 | ND | ND | N |
| 65(15) | meristematic | A | L18, R18 | L4-4.1 | GwwwG | Y |
| 91(11) | meristematic | M | L22, R22 | ND | ND | N |
| 91(12) | meristematic | M | L22, R22 | R10.5-12 | GwwwG | Y |

[a] For plants harvested at maturity, six basal leaves were assumed to be lost.
[b] Sectors span more than one phytomer were categorized as meristematic while those restricted in a single phytomer were recognized as non-meristematic.
[c] Leaf stages categorized as: Juvenile leaf (J, leaf#1-#8), Middle stage leaf (M, leaf#9-#13) and Adult stage leaf (A, leaf#14 and beyond).
[d] The sector position relative to midvein is denoted as: L = left side of midvein; R = right side of midvein; E = leaf edge; ND = not determined.
[e] The transverse dimension of the leaf was divided into five designated layers: adaxial L1-derived ; adaxial L2-derived; middle L2-derived; abaxial L2-derived; abaxial L1-derived.and w = white emp2 null tissue; G = green non-mutant tissue; ND = not determined.

**Table 3.3** Abnormal phyllotaxy emp2 mutant sectors

| sector# (leaf#)[a] | sector type[b] | leaf stage[c] | lateral vein# | sector position[d] | tissue layer[e] | phenotype[f] |
|---|---|---|---|---|---|---|
| 67(11) | meristematic | M | L18, R18 | R(0.2-0.8) | wwwww | N |
| 67:66(12) | meristematic | M | L22, R22 | L(14-16.5) R(13-E) | wwwww | N |
| 66:67(13) | meristematic | M | ND | L(0-0.8) R(1.5-2.5) | wwwww | N |
| 67:66(14) | meristematic | M | L21, R22(SL31) | R(14-16) R(9.5-10.5) | wwwww | Y |
| 76(7) | meristematic | J | L7, R14 | L(5-6.5) | wwwww | N |
| 76(8) | meristematic | J | L12, R12 | R(4-6) | wwwww | N |
| 76:77(9) | meristematic | M | L17, R13 | L(3.5-4.5) R(13-13) | wwwww | N |
| 77:76(10) | meristematic | M | L19, R19 | L(4-4.5) R(5-7.5) | wwwww | Y |
| 85:84(13) | meristematic | M | L22, R22 | L(5-6.5) R(6.5-10) | wwwww | Y |
| 89:89(13) | meristematic | M | L20, R23 | L(12.5-E) R(ND) | wwwww | Y |
| 93:94(14) | meristematic | M-A | L17, R17 | L(2-7.5) R(14.5-E) | GwGwG | Y |
| 95:94(15) | meristematic | A | L16, R16 | L(0-1) R(6.5-8.5) | GwGwG | Y |
| 96(11) | meristematic | M | L18, R14 | L(14-14) | GwwwG | N |
| 96(12) | meristematic | M | L20, R20 | R(0.3-0.7) | GwwwG | N |
| 96(13) | meristematic | M | L20, R20 | L(ND) | GwwwG | N |
| 97:96(14) | meristematic | A | L13, R20 | L(13-13) R(0.5-1.5) | GwwwG | Y |
| 96:97(15) | meristematic | A | AL16, L9, R18 | AL(8-16) L(9-9) R(3-4) | GwwwG | Y |
| 97(16) | meristematic | A | L17, R9 | L(1-E) | GwwwG | N |
| 97(17) | meristematic | A | L11, R14 | R(6.5-E) | GwwwG | N |

[a] For plants harvested at maturity, six basal leaves were assumed to be lost.
[b] Sectors were categorized as meristematic sectors and non-meristematic sectors as described in Materials and Methods.
[c] Leaf stages categorized as: Juvenile leaf (J, leaf#1-#8), Middle stage leaf (M, leaf#9-#13) and Adult stage leaf (A, leaf#14 and beyond).
[d] The sector position relative to midvein is denoted as: L = left side of midvein; R = right side of midvein; E = leaf edge; SL = secondary leaf; AL = accessory leaf. SL is an independent leaf whereas AL designates an elaborated accessory leaf domain that is fused to a narrow leaf. When a sector starts and ends with the same lateral vein, this sectored lateral vein abuts leaf edge.
[e] transverse dimension of leaf is divided into five layers: adaxial L1-adaxial L2-middle L2-abaxial L2-abaxial L1. w = white emp2 null tissue; G = green non-mutant tissue; ND = not determined.

**Table 3.4** Narrow leaf emp2 sectors

| sector # (leaf #)[a] | sector type[b] | leaf stage[c] | #lateral vein | sector position (vein)[d] | internode girth | sector position (internode) [d] | tissue layer[e] | phenotype [f] |
|---|---|---|---|---|---|---|---|---|
| 1(5) | non-meristematic | J | L8, R4 | R 3-4 | ND | ND | GwwwG | narrow |
| 44(5) | non-meristematic | J | L12, R9 | R 3.5-4 | ND | ND | GwwwG | narrow |
| 47(4) | non-meristematic | J | L9, R8 | R 7-E | ND | ND | wwwww | partial |
| 51(3) | non-meristematic | J | L10, R7 | R 6-E | ND | ND | wwwww | narrow |
| 53(6) | non-meristematic | J | L13, R10 | R 4-4 | ND | ND | GwwwG | narrow |
| 55(5) | non-meristematic | J | L13, R10 | R 5.5-6 | ND | ND | GwwwG | narrow |
| 58(5) | non-meristematic | J | L10, R8 | R 8-E | ND | ND | wwwww | partial |
| 62(3) | non-meristematic | J | L7, R9 | L 5-6 | ND | ND | GwwwG | partial |
| 64(5) | non-meristematic | J | L9, R13 | L 7-E | ND | ND | wwwww | narrow |
| 68(10) | meristematic | M | L20, R17 | R 8.5-E | 8.8 | R 2.4-3.5 | GwwwG | narrow |
| 68(9) | meristematic | M | L17, R17 | L 3-3.5 | ND | ND | GwwGG | N |
| 70(11) | meristematic | M | L17, R23 | L 14-E | 7.1 | L 3.0-3.2 | wwwww | partial |
| 70(12) | meristematic | M | L23, R23 | R 1.5-2.5 | 8.2 | R 0.6 -0.8 | wwwww | N |
| 70(13) | meristematic | M | L17, R25 | L 13-E | 7.0 | L 2.5-3.0 | wwwww | partial |
| 70(14) | meristematic | A | L21, R21 | R 1.5-2.5 | ND | ND | wwwww | N |
| 70(15) | meristematic | A | L20, R20 | L 13-15 | 5.8 | L 2.2-2.3 | wwwww | N |
| 72(13) | meristematic | M | L22, R19 | L (ND) | 4.7 | L 2.0-2.2 | wwwww | partial |
| 72(14) | meristematic | A | L17, R19 | R 0.5-1 | 4.0 | R 1.0-1.1 | wwwww | N |
| 72(11) | meristematic | M | L13, R19 | L 12.5-E | 5.5 | L 2.2-2.3 | GwwwG | narrow, AL |
| 72(12) | meristematic | M | L22, R22 | R 0-0.5 | ND | ND | wwwww | N |
| 73(12) | meristematic | M | L22, R19 | L (ND) | 4.7 | L 1.1-1.4 | wwwww | N |
| 73(13) | meristematic | M-A | L17, R19 | R 5.5-15 | 4.0 | R 1.5-1.6 | wwwww | partial |
| 73(11) | meristematic | M | L22, R22 | R 5-7.5 | 5.3 | R 1.2-1.3 | wwwww | N |
| 74(12) | meristematic | M | L19, R19 | L 1-2 | ND | ND | wwwww | N |
| 74(13) | meristematic | M-A | L19, R17 | R 13.5-E | 4.5 | R 1.6-1.9 | wwwww | partial |
| 74(14) | meristematic | A | L13, R13 | R 10.5-E | ND | ND | GwwwG | N |
| 75(8) | meristematic | J | L7, R14 | L 7-E | ND | ND | wwwww | narrow, AV |
| 77(11) | meristematic | M | L17, R13 | R 13-13 | 5.9 | R 1.5-2.5 | wwwww | narrow |
| 77(12) | meristematic | M | L19, R19 | L 5-7.5 | 5.5 | L 1.5-1.6 | wwwww | N |
| 77(13) | meristematic | M | L20, R20 | L 5-7.5 | ND | ND | wwwww | N |
| 82(11) | meristematic | M | L16, R16 | R 11-11.5 | ND | ND | wwwww | N |
| 82(13) | meristematic | M | L17, R19 | L 11-E | ND | ND | wwwww | narrow |
| 83(11) | meristematic | M | L22, R22 | R 0.5-1 | 6.0 | R 0.1-0.2 | GwwwG | N |
| 83(12) | meristematic | M | L12, R22 | L 12-12 | ND | ND | wwwww | narrow, AV |
| 83(14) | meristematic | A | L18, R18 | L 15-E | 4.1 | L 1.9-2.0 | GwwwG | N |
| 89(13) | meristematic | M-A | L20, R23 | L12.5-E | 4.3 | L 1.6-2.1 | wwwww | partial |
| 92(13) | meristematic | M | ND | R1.5-2 | ND | ND | wwwww | N |

**Table 3.4** Narrow leaf emp2 sectors (continued)

| sector # (leaf #)[a] | sector type[b] | leaf stage[c] | #lateral vein | sector position (vein)[d] | internode girth | sector position (internode) [d] | tissue layer[e] | phenotype [f] |
|---|---|---|---|---|---|---|---|---|
| 92(14) | meristematic | M-A | L15, R19 | L12-E | ND | ND | wwwww | partial |
| 96(11) | meristematic | M | L14, R18 | L14-14 | ND | ND | wwwww | partial |
| 96(12) | meristematic | M | L20, R20 | R 0.3-0.7 | 6 | R 0.1-0.2 | GwwwG | N |
| 96(13) | meristematic | M | L20, R20 | L (ND) | 6 | L 2.8-3.0 | GwwwG | N |
| 96(14) | meristematic | A | L13, R20 | R 0.5-1.5 | 5.5 | R 0.1-0.3 | GwwwG | N |
| 96(15) | meristematic | A | (AL16) L9, R18 | AL 8-16, L 9-9 | 4.6 | R 1.6-2.3 | GwwwG | narrow, AL |
| 97(14) | meristematic | A | L13, R20 | L 13-13 | ND | ND | GwwwG | narrow |
| 97(15) | meristematic | A | (AL16) L9, R18 | R 3-4 | 4.6 | R 0.3-0.4 | GwwwG | N |
| 97(16) | meristematic | A | L17, R9 | R1-E | 4.0 | R 0.3-1.1 | GwwwG | narrow, AL |
| 97(17) | meristematic | A | L11, R14 | L6.5-E | 3.5 | L 1.0-1.4 | GwwwG | narrow |
| 98(12) | meristematic | M | L17, R17 | L(ND) | 3.2 | L 0.3-0.6 | GwwwG | N |
| 98(13) | meristematic | M | L17, R7 | R(ND) | 3.3 | R 1.0-1.2 | GwwwG | N |
| 98(14) | meristematic | A | L13, R13 | L(ND) | 2.8 | L 0.45-0.6 | GwwwG | N |
| 98(15) | meristematic | A | L12, R12 | R(ND) | 2.4 | R 0.5-0.6 | GwwwG | N |
| 98(16) | meristematic | A | L10, R10 | L(ND) | 2.0 | L 0.30-0.5 | GwwwG | N |
| 98(17) | meristematic | A | L9, R7 | R(ND) | 2.0 | R 0.5-1.2 | GwwwG | narrow, AL |

[a] For plants harvested at maturity, six basal leaves were assumed to be lost.
[b] Sectors span more than one phytomer were categorized as meristematic while those restricted in a single phytomer were recognized as non-meristematic.
[c] Leaf stages categorized as: Juvenile leaf The transverse dimension of the leaf was divided into five designated layers: adaxial L1-derived ; adaxial L2-derived; middle L2-derived; abaxial L2-derived; abaxial L1-derived.and w = white emp2 null tissue
[d] The sector position relative to the midvein is denoted as: L = left side of midvein; R = right side of midvein; E = leaf edge; AL = accessory leaf, ND = not determined.
[e] The transverse dimension of the maize leaf is divided into five layers: adaxial L1-adaxial L2-middle L2-abaxial L2-abaxial L1. w = white emp2 null tissue; G = green non-mutant tissue; ND = not determined.
[f] N = no narrow leaf phenotype; narrow = narrow leaf in both sheath and blade; np = narrow leaf only in the blade and upper sheath; AL = accessory leaf; AV = abnormal vasculature.

**Table 3.5** Non-phenotypic emp2 sectors

| sector # (leaf #)[a] | sector type[b] | leaf stage[c] | lateral vein # | sector position[d] | tissue layer[e] |
|---|---|---|---|---|---|
| 2(5) | non-meristematic | J | L8, R8 | L6-6.5 | GwwGG |
| 3(6) | non-meristematic | J | L12, R12 | L5-7 | GwwwG |
| 4(4) | non-meristematic | J | L10, R10 | R6.5-7.5 | wwwww |
| 5(5) | non-meristematic | J | L10, R10 | L0-0.5 | GGwwG |
| 6(6) | non-meristematic | J | ND | R0-1 | GwwGG |
| 7(6) | non-meristematic | J | L10, R10 | R6-8 | GwwwG |
| 8(3) | non-meristematic | J | L6, R6 | L2-3 | GGwGG |
| 10(4) | non-meristematic | J | L8, R5[f] | L1-2 | GwGGG |
| 11(5) | non-meristematic | J | L9, R9 | L6.5-7 | GwGwG |
| 12(4) | non-meristematic | J | L9, R9 | R5-6 | GwwwG |
| 13(5) | non-meristematic | J | L9, R9 | R6-8 | GwwwG |
| 14(4) | non-meristematic | J | L6, R7[f] | R1-2 | GGGwG |
| 15(5) | non-meristematic | J | L10, R10 | L4-5 | GwGGG |
| 16(4) | non-meristematic | J | L8, R8 | R7-E | GwwwG |
| 17(3) | non-meristematic | J | L12, R12 | R10.5-E | wwwww |
| 18(5) | non-meristematic | J | L9, R9 | L4-5 | wwwww |
| 19(5) | non-meristematic | J | L9, R9 | L7.2-7.8 | GwwwG |
| 20(5) | non-meristematic | J | L10, R10 | R6.5-7 | GwwwG |
| 21(4) | non-meristematic | J | L7, R7 | L5-5.5 | GGwGG |
| 22(4) | non-meristematic | J | L9, R9 | L6-7 | GwwGG |
| 26(4) | non-meristematic | J | L8, R8 | R4-5 | GGGwG |
| 27(4) | non-meristematic | J | L10, R10 | L1-1.8 | GwwGG |
| 28(4) | non-meristematic | J | L9, R9 | R5.5-6.5 | GwwwG |
| 29(4) | non-meristematic | J | L8, R8 | L3-4 | GwwGG |
| 31(3) | non-meristematic | J | L7, R7 | R2-2.5 | GwwwG |
| 32(3) | non-meristematic | J | L7, R7 | L4-4.5 | GwGwG |
| 33(4) | non-meristematic | J | L8, R8 | L5-6 | wwwww |
| 34(5) | non-meristematic | J | L10, R10 | L4-4.5 | GwwwG |
| 35(4) | non-meristematic | J | L11, R11 | L2-3 | GwwwG |
| 36(5) | non-meristematic | J | L12, R12 | R8-9 | GGGww |
| 38(4) | non-meristematic | J | L9, R9 | L3-4 | GwGGG |
| 39(4) | non-meristematic | J | L9, R9 | R7-7.5 | GGGwG |
| 40(3) | non-meristematic | J | L7, R7 | R6-7 | GwwwG |
| 41(3) | non-meristematic | J | L7, R7 | R3-3.5 | GGwwG |
| 42(3) | non-meristematic | J | L8, R8 | R5-5.5 | GwwwG |
| 43(5) | non-meristematic | J | L12, R9[f] | L1-1.5 | GwwwG |

**Table 3.5** Non-phenotypic emp2 sectors (continued)

| sector # (leaf #)[a] | sector type[b] | leaf stage[c] | lateral vein # | sector position[d] | tissue layer[e] |
|---|---|---|---|---|---|
| 48(5) | non-meristematic | J | L10, R10 | R4.5-5 | GGGwG |
| 49(6) | non-meristematic | J | L10, R10 | L8.5-E | wwwww |
| 54(5) | non-meristematic | J | L13, R10[f] | L5-5.5 | GwwGG |
| 57(2) | non-meristematic | J | L7, R7 | R3-3.5 | GwwwG |
| 60(2) | non-meristematic | J | L8, R8 | R4.5-5 | GwGGG |
| 61(4) | non-meristematic | J | L10, R10 | L5,7 | GGGwG |
| 63(5) | non-meristematic | J | L9, R13[f] | R2-2.5 | GwwwG |
| 71(10) | meristematic | M | L13, R19[f] | R13-14.5 | wwwww |
| 78(12) | meristematic | M | L19, R19 | L4-4.5 | wwwww |
| 80(10) | meristematic | M | L19, R19 | L8-8.5 | wwwGw |
| 80(11) | meristematic | M | L21, R21 | R7-7.5 | wwwGw |
| 81(11) | meristematic | M | L21, R21 | R3-4.5 | GwwwG |
| 86(12) | meristematic | M | L23, R23 | R11-12.5 | wwwww |
| 86(13) | meristematic | M | L23, R23 | L3-4 | wwwww |
| 87(11) | meristematic | M | L22, R22 | L 10-12 | GwwwG |
| 87(13) | meristematic | M | L21, R21 | R 9.5-11.5 | GwGwG |
| 88(11) | meristematic | M | L22, R22 | R9.5-10.5 | GwwwG |
| 88(12) | meristematic | M | L22, R22 | ND | ND |
| 90(11) | meristematic | M | L22, R22 | L3-4 | GwwwG |
| 90(12) | meristematic | M | L22, R22 | R7.5-8.5 | GwwwG |

[a] For plants harvested at maturity, six basal leaves were assumed to be lost.
[b] Sectors span more than one phytomer were categorized as meristematic while those restricted in a single phytomer were recognized as non-meristematic.
[c] Leaf stages categorized as: Juvenile leaf (J, leaf#1-#8), Middle stage leaf (M, leaf#9-#13) and Adult stage leaf (A, leaf#14 and beyond).
[d] The sector position relative to the midvein is denoted as: L = left side of midvein; R = right side of midvein; E = leaf edge; ND = not determined.
[e] transverse dimension of leaf is divided into five layers: adaxial L1-adaxial L2-middle L2-abaxial L2-abaxial L1. w = white emp2 null tissue; G = green non-mutant tissue; ND = not determined.
[f] sectors on the normal side of a narrow leaf are designated as not associated with mutant phenotype.

plants grown in the greenhouse subjected to heat stress treatment (2 hours per day at 36°C or 42°C as described in Materials and Methods). Therefore, the emp2 sector phenotypes appear to be unrelated to heat shock or the heat shock response, and reflect additional functions of EMP2 during post-embryonic shoot development.

The mutant phenotypes were summarized into three major classes in Table 1: displaced ligule/auricle structure (Table 3.2, Figure 3.6A), abnormal leaf phyllotaxy (Table 3.3, Figure 3.6) 3.6D), and narrow leaves (Table 3.4, Figure 3.6E-K). As detailed below, the expression of particular mutant phenotypes was correlated with distinct spatial and temporal patterns of emp2/- null sector induction.

**Ligule/auricle displacement sectors**

Grass leaves contain a distal blade and a proximal sheath, which are separated by the ligule/auricle structures (SHARMAN, 1941). The ligule is an epidermis-derived elaboration of fringe-like tissue on the adaxial leaf surface of the sheath/blade boundary. The auricle is a V-shaped structure that initiates from two points on either side of the midrib, and expands outward toward each margin (SYLVESTER et al., 1990). Development of the ligule and auricle are temporally correlated and genetically inseparable (HARPER and FREELING, 1996).

There were eleven emp2 null sectors traversing the ligule and auricle that disrupted the continuity of these structures (Figure 3.6A). Specifically, the ligule/auricle was interrupted at the boundary between the midrib side of non-mutant tissue and the mutant sectored tissue, but it was continuous across the marginal side boundary of the sector. A second ligule/auricle initiated *de novo* on the midrib side boundary of the mutant sector. The newly initiated ligule/auricle was always displaced proximal to the original auricle, and extended laterally to the leaf margin. Although sectors of *liguless1* (*lg1*) mutation also caused proximal displacement of the ligule/auricle structure, the displacement occurred on the non-mutant tissue lying marginal to the sectored mutant tissue (BECRAFT and FREELING, 1991). Within the lg1 mutant sectored tissue the ligule/auricle structure was completely removed (BECRAFT et al., 1990).

As shown in Table 3.1, ligule/auricle displacement phenotypes are associated with both meristematic and non-meristematic *emp2-R/-* hemizygous sectors. Although the majority of ligule/auricle sectors (nine out of eleven) extended through all L2-derived tissue layers (Figure 3.6B) of the leaf, two of the ligule sectors occupied only the adaxial L2-derived leaf tissues (Figure 3.6C). These data suggest that the correct proximodistal positioning of the adaxial ligule/auricle requires EMP2 function in L2-derived adaxial leaf tissues.

**Abnormal phyllotaxy sectors**

Maize leaves initiate in an alternate phyllotaxy; successive leaves arise approximately 180° apart and offset in two ranks. However, eight cases of abnormal phyllotaxy were observed in emp2 mutant sectored plants, in which successive nodes were not located on opposite sides of the stem. The degree of deviation from the 180º degree divergence angle varied among different sectored plants. These included cases wherein two successive leaves arose on the same side of the plant; in extreme cases two leaves arose from a single node. In the example shown in Figure 3.6D (Table 3.3, sectors #66 and #67) only one of these leaves (L14) contained a midrib, and both leaves are arranged in an abnormal phyllotaxy with respect to the previous leaf. In all cases in which a leaf arose in an abnormal phyllotactic pattern, either the affected leaf *or* the previous leaf contained two, separate *emp2-R/* - sectors located on opposite sides of the midvein (Table 3.5, Figure 3.6D). These data indicate that the sectors that generated phyllotaxy phenotypes were present at, or prior to, the founder cell stage of leaf development. Finally, although the majority of these phenotypes arose from sectors marking all L2-derived tissue layers, two partial L2-derived sectors also conferred this phenotype (Table 3.1). These partial L2-derived sectors reveal that EMP2 function is required in *all* cells throughout the meristematic L2 tissue layer in order to establish normal leaf phyllotaxy.

**Narrow leaf sector phenotypes**

Plant leaves are comprised of at least two medio-lateral zones: a central domain, which includes the midrib and leaf tip, and a lateral domain that includes the lower leaf margins. In this clonal analysis, we observed twenty eight cases of lateral leaf domain deletion phenotypes (Table 3.1). The *emp2-R* mutation may correlate with either complete deletion of the lateral leaf domain (i.e. comprising the blade and sheath; seventeen cases) or partial deletion of the lateral leaf domain (i.e. comprising the blade alone or blade plus distal sheath; eleven cases).

Representatives of the complete lateral domain deletion phenotypes are depicted in Figure 3.6E-F. As shown in Figure 3.6E, the sheath and proximal blade of the emp2/- null sectored half leaf are much narrower, and contain fewer lateral veins than the unsectored counterparts. Non-mutant leaf blade margins develop distinctive saw-tooth hairs and a non-chlorophyllic, tapered edge (Figure 3.6H), whereas transverse sections of the emp2/- sectored narrow leaf margins revealed blunted, chlorophyllic leaf edges and the absence of saw-tooth margin hairs (Figure 3.6G). Margin structures were normal, however, in sectored regions of the upper leaf blade. These observations are consistent with previous reports (SCANLON et al., 1996) demonstrating that margins of the upper leaf are derived from a different leaf compartment (i.e. the central domain) than margins of the lower leaf.

The emp2-null albino sectors also gave rise to less severe narrow leaf phenotypes in which the sectored side of the leaf contained fewer lateral veins, yet developed normal margin structures. The sectored sheath was either unaffected or contained a partial deletion that was constrained to the distal sheath region. Furthermore, four sectored narrow leaves were each attached to an accessory leaf (Figure 3.6J); fusion of the narrow leaf to the accessory leaf occurred in the sheath epidermis (data not shown). The accessory leaves were either comprised of sheath plus blade or sheath alone, and were positioned immediately adjacent to the corresponding narrow leaf on the node. The accessory leaf phenotype was only associated with meristematic emp2/- null sectors marking the L2-, but not the L1-derived layers layer (Tables 3.1 and 3.4). In addition, two sectored narrow leaves were associated with abnormal outgrowths of

sheath tissue that contained highly branched, reticulated and discontinuous vasculature near the blade sheath boundary of the leaf (Figure 3.6K). The sheath outgrowth phenotypes correlated with complete L1-L2 layered sectors.

The twenty eight cases of narrow leaf phenotypes were associated with a total of 23 emp2-null sectors. Only meristematic sectors and non-meristematic sectors that extended into both sheath and blade conferred narrow leaf phenotypes (Table 3.1 and 3.4). This suggests that EMP2 function is required prior to the completion of early leaf primordial development, after which time these proximal-distal leaf compartments become clonally distinct (POETHIG and SZYMKOWIACK, 1995). In addition, all narrow leaf sectors displayed fully albino internal (L2-derived) tissue layers, suggesting that the EMP2 function in a subset of L2-derived tissues is enough for the elaboration of the lateral leaf domain. Lastly, although the majority of narrow leaf sectors were astride the abnormal leaf edge (Figure 3.6E), some sectors were internal to the margin (Figure 3.6F-G).

**The expression of narrow leaf phenotypes correlates with the lateral position of emp2-null albino sectors**

Although immunohistolocalization analyses of developing maize shoots reveal equivalent accumulation of EMP2 protein throughout all maize tissues examined (Figure 2.8), a correlation between sector position and the narrow leaf phenotype suggested a compartmentalized function(s) of EMP2. In order to identify the location of this putative EMP2 functional domain, the lateral positions of narrow leaf phenotypic and non-phenotypic *emp2/-* null sectors are compared. However, the non-uniform, post-primordial expansion of different regions of the maize leaf precludes direct comparison of sector positions within mature leaves (STEFFENSON, 1968; Poethig, 1986). Therefore, the sector locations were compared using lateral veins as a reference for sector positioning (Figure 3.7; SCANLON and FREELING, 1997; see Materials and Methods). Lateral veins are established and evenly spaced during early stages of maize leaf development (SHARMAN, 1942; BOSABALIDIS et al., 1994), and thus are good indicators of sector position

within young leaf primordia. As shown in Figure 3.7A, the vast majority (24/28) of narrow leaf mutant sectors were contained on the marginal half of the mutant leaf; this region is termed the emp2 phenotypic domain. The clustering of phenotypes within the emp2 phenotypic domain reveals a localized EMP2 function, instead of uneven distribution of emp2-null sectors (Figure 3.7B).

The fact that not all sectors located within the emp2 phenotypic domain conditioned mutant phenotypes suggests that additional factors, such as the timing of sector induction (Table 3.1), are important for the expression of narrow leaf phenotypes. For example, whereas all meristematic emp2-null sectors within this domain yielded narrow leaf phenotypes, many post-meristematic sectors did not. In addition, the exact location of EMP2 function is not fixed from meristem to meristem, as discussed below. The mapped location of the emp2 phenotypic domain prompted us to investigate whether EMP2 functions within the lateral meristem domain, a region whose boundaries are marked by foci of NARROW SHEATH function and expression (SCANLON, 2000; Nardmann et al., 2004). Correspondingly, the emp2 null phenotypic domain was also mapped onto the shoot meristem by determining the meristematic positions of phenotypic and non-phenotypic multiple leaf sectors (see Materials and Methods). As shown in Figure 3.8, all multiple-leaf sectors associated with narrow leaf phenotypes were localized to the emp2 phenotypic domain, whereas non-phenotypic sectors were all restricted from this region. Interestingly, the emp2 null phenotypic domain overlaps with and extends beyond the NS foci. As the meristem proceeds from middle to adult stages of vegetative development the position of the emp2 null phenotypic domain recedes laterally toward the midrib; a similar phenomenon was observed for the NS foci (SCANLON 2000). It was also noted that the severity of the narrow leaf phenotype correlates with the lateral position of the emp2-null albino sector. That is, emp2 null sectors within the NS foci were mainly associated with a complete lateral domain deletion phenotype (Figure 3.6E-F, Figure 3.8). In contrast, sectors within the emp2 phenotypic domain, but outside the NS focus, caused only partial domain deletion phenotypes (Figure 3.6I, Figure 3.8).

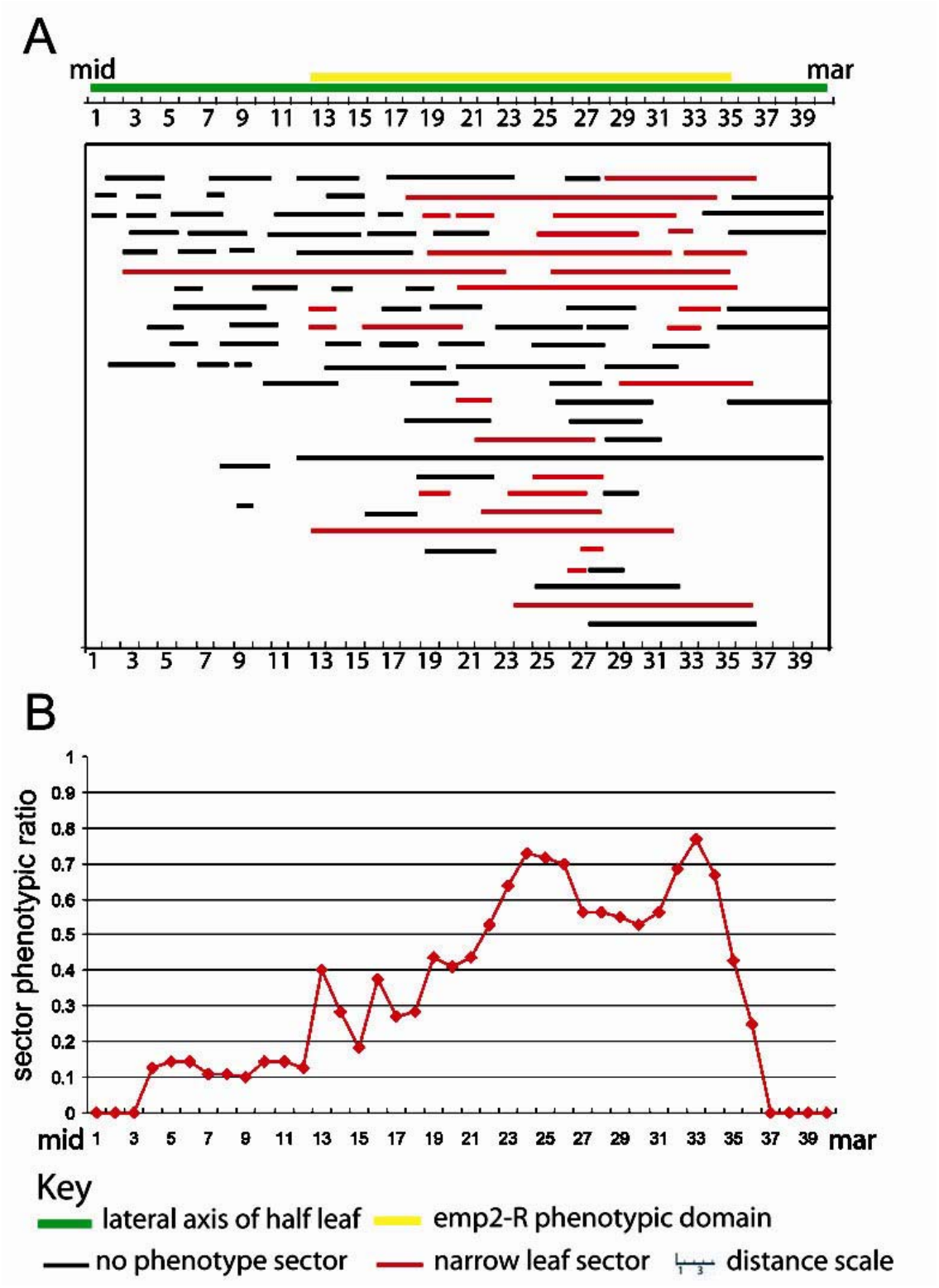
A
mid
mar
1 3 5 7 9 11 13 15 17 19 21 23 25 27 29 31 33 35 37 39
B
sector phenotypic ratio
1
0.9
0.8
0.7
0.6
0.5
0.4
0.3
0.2
0.1
0
mid 1 3 5 7 9 11 13 15 17 19 21 23 25 27 29 31 33 35 37 39 mar
Key
lateral axis of half leaf
emp2-R phenotypic domain
no phenotype sector
narrow leaf sector
distance scale

**FIGURE 3.7** The narrow leaf phenotypic emp2 mutant sectors are clustered in the marginal half of the maize leaf. (A) The positions of 91 emp2 mutant leaf sectors occupying all L2-derived leaf (**FIGURE 3.7** legend continued) tissues were extrapolated to the lateral axis of the half-leaf primordium using the lateral veins as described in FIGURE 3.1 and in the Materials and Methods. The emp2 null phenotypic domain (yellow bar) is defined as the region of a leaf primordium, as measured by percentage of total lateral veins, within which narrow leaf phenotypic sectors are observed. (B) The sector phenotypic ratio represents the percentage of total emp2 mutant sectors in a given mediolateral domain that conditioned narrow leaf sector phenotypes.

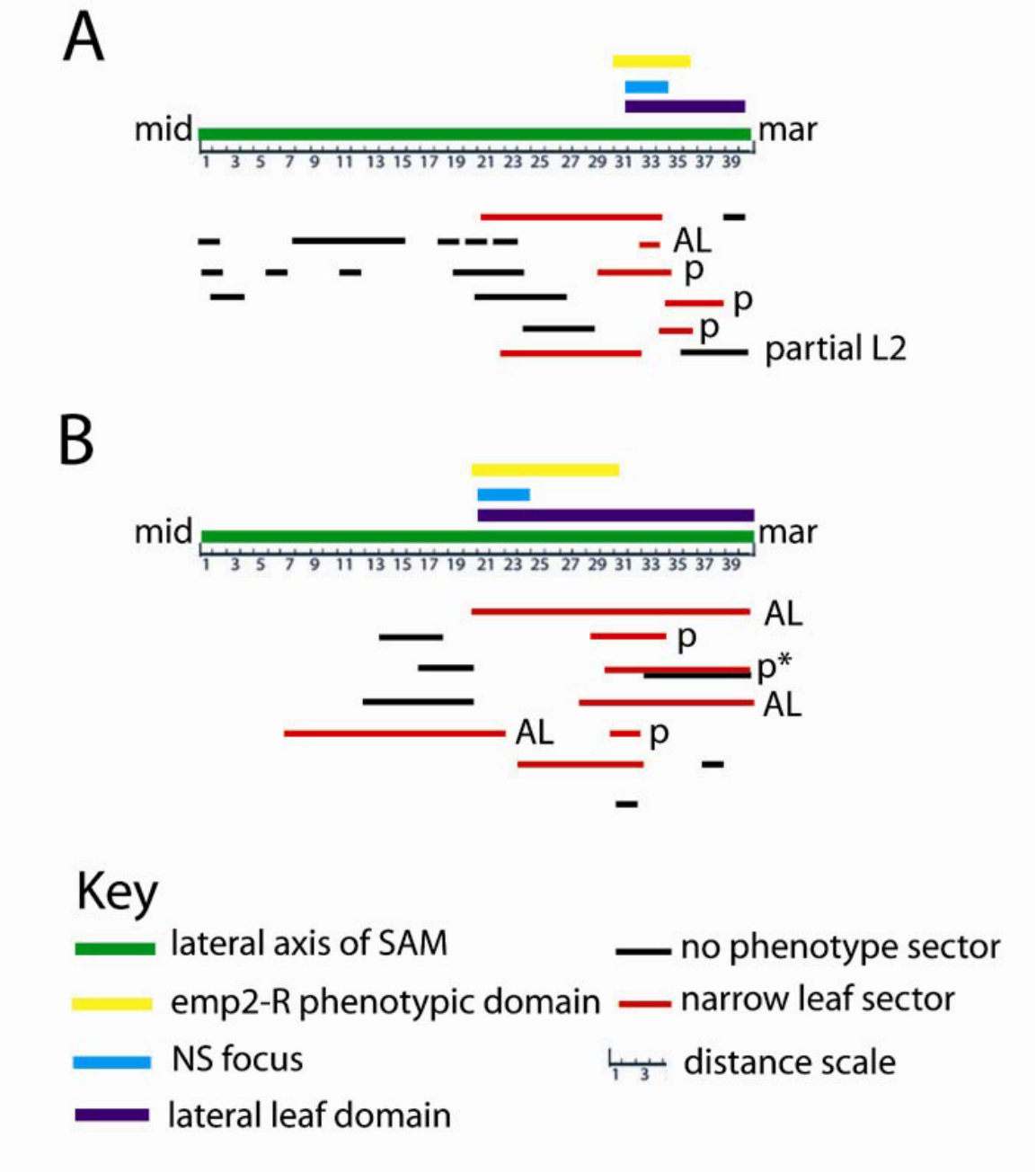


**FIGURE 3.8** Meristematic sectors reveal that the emp2 null phenotypic domain is localized to lateral leaf domains. Sector locations on the SAM were estimated by extrapolation of the lateral position of sectors on the internode, as described in FIGURE 1 and in the Materials and Methods. The emp2 null phenotypic domain (yellow bar) is defined as described above. (A) Phenotypic sectors (red lines) marking middle staged leaves (leaf #9- leaf #13) are localized to the emp2 null phenotypic domain (yellow bar). (B) This emp2 null phenotypic domain maps to a focus located

(**FIGURE 3.8** legend continued) relatively closer to the midrib in adult staged leaves (leaf #14 and above). Sectors in which an accessory leaf was attached are indicated. The NS focus (blue bar) demarcates midrib side boundary of the lateral leaf domain (purple bar, Scanlon, 2000). "*" denotes a broad sector that covers both leaf margins in which only one margin is abnormal. p = partial lateral leaf domain deletion; AL= accessory leaf.

## Discussion

### The maize HSBP proteins have evolved divergent functions

Previously we reported that *hsbp* orthologues were duplicated prior to the speciation of monocot grasses (FU et al, 2002). Herein we demonstrate that the products of the duplicated maize *hsbp* genes, *emp2* and *hsbp2*, accumulate differently during development and stress response. The differential protein accumulation patterns suggest divergent functions for the maize paralogous proteins. Previous emp2 mutant analyses suggested a role for EMP2 in regulating the HSTR in maize embryos, whereas the heat-induced accumulation of the maize HSBP2 protein suggests that HSBP2 carries out this function in maize leaves. In this model, the heat-induced accumulation of HSBP2 protein may bind to and inactivate maize HSFs and consequently attenuates the HSTR. Mutant analysis of *hsbp2* will enable tests of this hypothesis.

Although EMP2 seems not to have an essential role in regulating the HSTR in maize leaves, it does have important, non-redundant functions during maize shoot development. As reported above, a diverse array of developmental defects associates with the sectored loss of EMP2 function in maize shoots, whereas all non-mutant *Emp2/-* sectors included in our analysis were non-phenotypic. Previous mosaic analyses with the *w3* allele also demonstrated that albinism, as well as hemizygosity for most of chromosome arm 2L, does not condition these observed developmental defects in maize shoots (FOSTER et al, 1999; SCANLON, 2000). Thus, these phenotypes were specifically linked to the *emp2-R* mutation.

Heat stress treatment at specific developmental stages is known to induce diverse developmental defects in *Drosophila* (MITCHELL and LIPPS, 1978; PETERSEN and MITCHELL, 1987). Likewise, the aberrant expression of *hsp90* caused dwarfism, radial symmetrical leaves and missing leaves in *Arabidopsis* (QUEITSCH et al, 2002). The requirement of EMP2 during regulation of *hsp* gene expression in maize embryos initially led to the hypothesis that the range of emp2/- null sector phenotypes observed in this study resulted from aberrant *hsp* expression: corn plants in the field are often heat stressed and the emp2-null sectors may not be able to attenuate the HSTR. However, EMP2 is not required to regulate the heat shock response in

young leaves (Figure 3.5), nor did we detect aberrant expression of non-heat inducible *hsp*s in emp2 null sectors (data not shown). More importantly, we found that the growth temperature and stress treatment of the sectored plants did not affect the range of phenotypes conferred by the emp2 null sectors (data not shown). Therefore, the developmental defects in *emp2/-* null sectored plants are not caused by a defective heat shock response, suggesting additional functions of EMP2 are involved in the observed mutant phenotypes. Taken together, genetic and molecular analyses presented herein successfully demonstrated the functional divergence of the maize paralogous proteins EMP2 and HSBP2. EMP2 has evolved additional functions, which are distinct from its conserved function in regulating the HSTR.

**Distinct functions of EMP2 during maize shoot development**

Sectored loss of EMP2 function in the post-embryonic shoot can lead to the deletion of a leaf domain, displacement of the ligule and auricle, or altered phyllotaxy (Figure 3.6). One possible explanation of these results is that the tissue loss and tissue/organ displacement phenotypes are caused by a generalized emp2 mutant defect that causes cell death or lack of cell proliferation in sectored tissues. However, several features of the emp2 mutant sectors fail to support this hypothesis. For example, there is no evidence of cell death associated with emp2-null sectored shoot tissue. In contrast, the emp2 null sectored tissues are expansive and morphologically healthy (Figure 3.6). In addition, the number of cell files between sectored lateral veins is equivalent to that observed in adjoining, non-sectored tissues (Figure 3.6B, G, H and data not shown). These data are especially informative because lateral veins in maize are established during early primordial stages (SHARMAN, 1942), such that a defect in cell proliferation would be manifested as a reduction in inter-vein spacing. Thus, the sector data strongly suggest that EMP2 is not required for general cell proliferation or viability in the post-embryonic maize shoot, although it may be important for proliferation of some specific cell types. It is also possible that

the emp2/- null sectors retard the competency of cells to respond to developmental cues at the appropriate time.

The particular phenotype of any emp2/- null sector is correlated with the developmental timing, lateral positioning, and tissue layer specificity of the mutant sector (Table 3.1). For example, the altered phyllotaxy phenotype was only observed in cases wherein two separate, L2–derived, meristematic emp2 null sectors straddled the midrib-forming region. Current models of phyllotaxy determination inspired by surgical excision of leaf primordia (reviewed in STEEVES and SUSSEX, 1989; SNOW and SNOW, 1933; WARDLAW, 1949), auxin manipulation of the SAM (REINHARDT et al., 1998, 2000, 2003; VERNOUX, 2000), and the phyllotaxy mutation *terminal ear1* (VEIT et al., 1998) suggest that existing leaf primordial generate an inhibitory signal(s) to prevent premature leaf initiation. The sector data presented herein suggest that EMP2 is somehow required in the shoot meristem to initiate, propagate, or otherwise respond to this leaf inhibitory signal. Furthermore, the presence of EMP2 protein within any portion of L2-derived tissue on just one flank of the meristem is sufficient to maintain this inhibitory signal and normal phyllotaxy. In another example, previous analyses revealed that the leaf lateral domain is patterned in the shoot meristem by a non-cell autonomous recruitment function initiating at the NS lateral foci (SCANLON, 2000). Likewise, sectored loss of EMP2 function within the emp2 phenotypic domain also correlates with the complete or partial deletion of a lateral leaf region. These data suggest that EMP2 function in the meristem and early leaf primordium is also required for the elaboration of the lateral leaf domain.

We suggest that these emp2-null sector phenotypes are due to the loss of expanded (i.e. non–HSTR-related) functions of the EMP2 coiled-coil domain in the maize shoot. The coiled-coil is a common protein motif in nature, and specific coiled-coil domain proteins have been shown to

interact with multiple, unrelated protein pairing partners that function in disparate molecular pathways (NEWMAN and KEATING, 2003; reviewed in BURKHARD et al., 2000). Currently, we are utilizing yeast two-hybrid and proteomic approaches to investigate the distinct protein::protein interactions of EMP2 and HSBP2 in maize embryos and shoots. Preliminary results suggest that these maize HSBP paralogues do indeed interact differently with maize HSF isoforms and other maize proteins. (S. Fu, unpublished results). Perhaps the identification of EMP2 interacting proteins will help dissect the molecular pathways governing maize developmental processes such as ligule/auricle positioning, lateral leaf development, and phyllotaxy.

## Acknowledgements

We thank K. DAWE, L. PRATT, R. MEAGHER, and Z.-H. YE for helpful discussions throughout this work, and A. TULL and M. BOYD of the Plant Biology Greenhouses for expert care of maize plants. We thank D. GALLIE and T. YOUNG from UC Riverside for the maize hsp101 cDNA plasmids. We are grateful for M. CRENSHAW and J. PARKER (Athens Regional Medical Center) and JE NOAKES (Center for Applied Isotope Studies) for assistance in irradiation of maize seedlings. We thank K. DAWE, J. JI and reviewers from *Genetics* for critical evaluation of the manuscript. The work was funded by the USDA-CREES-NRICGP grant # 01-01600 to MS.

## Literature Cited

BECRAFT, P. W., BONGARD-PIERCE, D. K., SYLVESTER, A. W., POETHIG, R. S. and FREELING, M. (1990). The *liguleless-1* gene acts tissue specifically in maize leaf development. Dev Biol **141**:220-32.

BECRAFT, P. W. and FREELING, M. (1991). Sectors of liguleless-1 tissue interrupt an inductive signal during maize leaf development. Plant Cell **3**:801-7.

BOSABALIDIS, A.M., EVERT, R.F., and RUSSIN, W.A.(1994). Ontogeny of the vascular bundles and contiguous tissues in the maize leaf blade. Am. J. Bot. **81**:745-752.

BURKHARD, P., STETEFELD, J. and STRELKOV, S. V. (2001). Coiled coils: a highly versatile protein folding motif. Trends Cell Bio*l* **11**:82-8.

FOSTER, T., VEIT, B. and HAKE, S. (1999). Mosaic analysis of the dominant mutant, Gnarley1-R, reveals distinct lateral and transverse signaling pathways during maize leaf development. Development **126**:305-13.

FU, S., MEELEY, R. and SCANLON, M. J. (2002). *Empty pericarp2* encodes a negative regulator of the heat shock response and is required for maize embryogenesis. Plant Cell **14**:3119-32.

GURLEY, W. B. and KEY, J. L. (1991). Transcriptional regulation of the heat-shock response: a plant perspective. Biochemistry **30**:1-12.

HARPER, L. and FREELING, M. (1996). Interactions of *liguleless1* and *liguleless2* function during ligule induction in maize. Genetics **144**:1871-82.

LINDQUIST, S. (1986). The heat-shock response. Annu. Rev. Biochem. **55**:1151-91.

LUND, A. A., BLUM, P. H., BHATTRAMAKKI, D. and ELTHON, T. E. (1998). Heat-stress response of maize mitochondria. Plant Physiol. **116**:1097-110.

MARRS, K. A., CASEY, E. S., CAPITANT, S. A., BOUCHARD, R. A., DIETRICH, P. S., METTLER, I. J. and SINIBALDI, R. M. (1993). Characterization of two maize HSP90 heat shock protein genes: expression during heat shock, embryogenesis, and pollen development. Dev. Genet. **14**:27-41.

MITCHELL, H. K. and LIPPS, L. S. (1978). Heat shock and phenocopy induction in Drosophila. Cell **15**, 907-18.

MORIMOTO, R. I. (1998). Regulation of the heat shock transcriptional response: cross talk between a family of heat shock factors, molecular chaperones, and negative regulators. Genes Dev. **12**:3788-96.

NARDMANN, J, JI, JIABING, WERR, W. and SCANLON, M. J. 2004. The maize duplicate genes *narrow sheath1* and *narrow sheath2* encode a conserved homeobox gene function in a lateral domain of shoot apical meristems. in press *Development*

NEWMAN, J. R. and KEATING, A. E. (2003). Comprehensive identification of human bZIP interactions with coiled-coil arrays. Science **300**:2097-101.

NIETO-SOTELO, J., MARTINEZ, L. M., PONCE, G., CASSAB, G. I., ALAGON, A., MEELEY, R. B., RIBAUT, J. M. and YANG, R. (2002). Maize HSP101 plays important roles in both induced and basal thermotolerance and primary root growth. Plant Cell **14**:1621-33.

PETERSEN, N. S. and MITCHELL, H. K. (1987). The induction of a multiple wing hair phenocopy by heat shock in mutant heterozygotes. Dev. Biol. **121**, 335-41.

PIRKKALA, L., NYKANEN, P. and SISTONEN, L. (2001). Roles of the heat shock transcription factors in regulation of the heat shock response and beyond. Faseb J. **15**:1118-31.

POETHIG, R. S. and SZYMKOWIACK, E. J. (1995). Clonal analysis of leaf development in maize. Maydica **40**:67-76.

QUEITSCH, C., SANGSTER, T.A. and LINDQUIST S. (2002) Hsp90 as a capacitor of phenotypic variation. Nature **417**, 618 - 624

REINHARDT, D., MANDEL, T. and KUHLEMEIER, C. (2000). Auxin regulates the initiation and radial position of plant lateral organs. Plant Cell 12:507-18.

REINHARDT, D., PESCE, E. R., STIEGER, P., MANDEL, T., BALTENSPERGER, K., BENNETT, M., TRAAS, J., FRIML, J. and KUHLEMEIER, C. (2003). Regulation of phyllotaxis by polar auxin transport. Nature **426**:255-60.

REINHARDT, D., WITTWER, F., MANDEL, T. and KUHLEMEIER, C. (1998). Localized upregulation of a new expansin gene predicts the site of leaf formation in the tomato meristem. Plant Cell **10**:1427-37.

SAMBROOK J and D. W. RUSSEL (2001). *Molecular Cloning: a laboratory manual*. 3rd ed. Cold Spring Harbor Laboratory Press, New York.

SATYAL, S. H., CHEN, D., FOX, S. G., KRAMER, J. M. and MORIMOTO, R. I. (1998). Negative regulation of the heat shock transcriptional response by HSBP1. Genes Dev. **12**:1962-74.

SCANLON, M. J. (2000). NARROW SHEATH1 functions from two meristematic foci during founder-cell recruitment in maize leaf development. Development **127**:4573-85.

SCANLON, M. J. and FREELING, M. (1997). Clonal sectors reveal that a specific meristematic domain is not utilized in the maize mutant narrow sheath. Dev Biol. **182**:52-66.

SCANLON, M. J., SCHNEEBERGER, R. G. and FREELING, M. (1996). The maize mutant narrow sheath fails to establish leaf margin identity in a meristematic domain. Development **122**:1683-91.

SHARMAN, B. C. (1941) Development of the ligule in *Zea mays* L. Nature **147**:641

SHARMAN, B. C. (1942) Developmental anatomy of the shoot of *Zea mays* L Ann. Bot. (Lond) **6**:245-284.

SNOW, M. and SNOW, R. (1933). Experiments on phyllotaxis II. The effect of displacing a primordium. Philos. Trans. R. Soc. Lond. **222:** 353-400.

STEEVES, T. A. and SUSSEX, I. M. (1989). Patterns in Plant Development. Cambridge: Cambridge University Press.

STEFFENSON, D. M. (1968). A reconstruction of cell development in the shoot apex of maize. Am. J. Bot. **55**, 354-369.

SYLVESTER, A. W. and RUZIN, S.E**.** (1994). Light Microscopy I: Dissection and Microtechnique. In: *The Maize Handbook* (Freeling, M. and Walbot,V. eds.), pp83-94. New York: Srpinger-Verlag.

SYLVESTER, A. W., CANDE, W. Z. and FREELING, M. (1990). Division and differentiation during normal and liguleless-1 maize leaf development. Development **110**:985-1000.

SYLVESTER, A. W., SMITH, L. and FREELING, M. (1996). Acquisition of identity in the developing leaf. Annu. Rev. Cell. Dev. Biol. **12**:257-304.

TAI, L. J., MCFALL, S. M., HUANG, K., DEMELER, B., FOX, S. G., BRUBAKER, K., RADHAKRISHNAN, I. and MORIMOTO, R. I. (2002). Structure-function analysis of the heat shock factor-binding protein reveals a protein composed solely of a highly conserved and dynamic coiled-coil trimerization domain. J. Biol. Chem. **277**:735-45.

VEIT, B, BRIGGS, S. P., SCHMIDT, R. J., YANOFSKY, M. F. and HAKE, S. (1998). Regulation of leaf initiation by the *terminal ear1* gene of maize. Nature **393**:166-168.

VERNOUX, T., KRONENBERGER, J., GRANDJEAN, O., LAUFS, P. and TRAAS, J. (2000) PIN-FORMED 1 regulates cell fate at the periphery of the shoot apical meristem. Development. **127**:5157-65.

VIERLING, E., HARRIS, L. M. and CHEN, Q. (1989). The major low-molecular-weight heat shock protein in chloroplasts shows antigenic conservation among diverse higher plant species. Mol. Cell. Biol. **9**:461-8.

WARDLAW, C. W. (1949). Experiments on organogenesis in ferns. Growth Suppl. **13**: 93-131.

WIEDERRECHT, G., SETO, D. and PARKER, C. S. (1988). Isolation of the gene encoding the S. cerevisiae heat shock transcription factor. Cell **54**:841-53.

YOUNG, T. E., LING, J., GEISLER-LEE, C. J., TANGUAY, R. L., CALDWELL, C. and GALLIE, D. R. (2001). Developmental and thermal regulation of the maize heat shock protein, HSP101. Plant Physiol. **127**:777-91.

YU, Y. B. (2002). Coiled-coils: stability, specificity, and drug delivery potential. Adv. Drug Deliv. Rev. **54**:1113-29.

# CHAPTER 4

# MAIZE COILED-COIL PROTEIN PARALOGUES, EMP2 AND HSBP2, HAVE DISTINCT PROTEIN-PROTEIN INTERACTION SPECIFICITIES[1]

[1] Fu, S. and Scanlon, MJ. Maize Coiled-coil Protein Paralogues, EMP2 and HSBP2, Have Distinct Protein-Protein Interaction Specificities. To be submitted to Plant Cell.

## Abstract

Rapid and transient expression of heat shock protein (*hsp*) genes during the heat shock response (HSR) requires precise regulation of the HEAT SHOCK TRANSCRIPTION FACTOR (HSF). However, molecular mechanisms by which HSFs are regulated are still not fully understood. Two maize genes, *empty pericarp2* (*emp2*) and *heat shock factor binding protein*2 (*hsbp2*), are putative paralogues that are predicted to encode HEAT SHOCK FACTOR BINDING PROTEINs (HSBPs). Previous genetic and molecular analyses suggested that these genes function non-redundantly in planta. Further characterization of maize HSBPs thus may enable us to understand the regulation of the HSF during HSR, as well as to dissect mechanisms of maize development. Here we report that the maize HSBPs exhibit differential expression patterns and distinct protein-protein interaction specificities. Database searches indicated that the relative abundance of *emp2* and *hsbp2* transcripts is developmentally regulated. Differential regulation of *hsbp* paralogues was corroborated by immunoblot analyses using EMP2 and HSBP2 specific antibodies. In addition to the differential expression pattern, maize HSBPs also exhibit distinct protein-protein interaction specificities as revealed by yeast two-hybrid analyses. HSBP2 can specifically interact with a class A member of maize HSF (HSFA4b) in yeast, whereas EMP2 interacts with an unknown protein from maize embryos. Site-directed mutagenesis revealed that the coiled-coil domain of HSBP2 and HSFA4b is important for their interaction in yeast; substitution of specific residues within this domain abrogates the interaction. In addition, yeast two-hybrid studies revealed that peptide sequences outside the coiled-coil domain of maize HSBPs are also improtant for protein-protein interaction. N- and C-terminal deletion mutants of HSBP2 failed to bind to HSFA4b. In contrast, the coiled-coil domain of EMP2 can interact with HSFA4b when the former is flanked by non-coiled-coil peptide

sequences from HSBP2. Based on these observations, we proposed that mutations in flanking sequences provide the peptide diversity that led to divergence in protein-protein interaction - and thus function of paralogues. In order to experimentally test our predictions that maize HSBP proteins have evolved differential biochemical and developmental functions, recombinant proteins of HSBP2 and EMP2 have been constructed in *E. coli* and purified.

## Introduction

Protein oligomerization is an important and widespread biological phenomenon with several evolutionary advantages (Engel and Kammerer, 2000). First, oligomerization enables the assembly of multi-function complexes from relatively small peptides that may have diminished or no function single-handedly. Secondly, protein oligomerization provides for fast and energy efficient regulation of specific biochemical activities without *de novo* protein synthesis and degradation. Lastly, oligomerization mediates branching of biochemical pathways, because different components of a single complex can interact with multiple downstream modules.

Protein oligomerization is often mediated by evolutionary conserved structural modules like the PDZ domain, PTB domain and SH2 domain (Pawson et al., 2002). The coiled-coil, which is comprised of two to five α-helix strands winding around one another, is also an important protein-protein interaction domain (Crick, 1953). Protein sequences that form coiled-coil structures exhibit a characteristic heptad repeat pattern (**abcdefg**), '**a**' and '**g**' residues of which define the interface between interacting α-helixes (McLachlan and Stewart, 1975). Coiled coils are present in many well studied proteins, including transcription factors (e.g. HSF, GCN4, c-Jun/Fos, c-Myc/Max), protein kinases (e.g. Rho), and membrane fusion complexes (e.g. SNARE), motor proteins (e.g. myosin, kinesin, dynein) as well as cytoskeletal proteins (e.g. intermediate filament) (Burkhard et al., 2001). It was predicted that 3-5% of eukaryotic proteins contain coiled coils (Wolf et al., 1997). Among them, the basic helix-loop-helix (bHLH) transcription factor superfamily alone accounts for 0.2-0.6 % of all genes in higher eukaryotes (Bailey et al., 2003; Ledent and Vervoort, 2001; Waterston et al., 2002).

Previous mutagenic, biophysical and structural analyses of model proteins like GCN4, c-Jun/Fos and c-Myc/Max have ascertained many structural properties of coiled coils in regard to

their oligomerization states, stability and pairing specificities (Harbury et al., 1993; Lavigne et al., 1995; O'Shea et al., 1992). Stability of coiled coils is mainly determined by hydrophobic interactions as well as ionic interactions between charged residues ((Kohn et al., 1997; Sodek et al., 1972). Hydrophobic residues at the '**a**' and '**d**' position of the heptad repeat (**abcdefg**) can also modulate the oligomerization status (Harbury et al., 1993; Tripet et al., 2000). For example, Asn at the '**a**' position of the second heptad repeat in the GCN4 leucine zipper is critical for its exclusive dimer formation (Harbury et al., 1993), whereas Ile and Val at the '**d**' position induced X19a to form trimers (Tripet et al., 2000). The specificity of α-helix pairing during coiled-coil formation is largely dependent upon interhelical electrostatic interactions, because attractive ionic interactions require '**e**' and '**g**' residues from different a-helix strands to be oppositely charged and properly orientated (Krylov et al., 1994; Vinson et al., 1993).

Elucidating the mechanism of coiled-coil interaction and regulation has not only enhanced our understanding of many basic cellular and developmental processes, but also facilitated broad applications in areas such as ionsensor, affinity purification and targeted drug delivery (Chao et al., 1998; Wang et al., 1999). Automated protein design for peptides with expected coiled-coil properties has also been achieved (Havranek and Harbury, 2003). However, current studies of coiled coils are mostly focused on a limited number of model natural proteins and synthesized simple peptides, and accurate prediction of coiled coils formation is only feasible for a small subset of proteins (Fong et al., 2004). Thus, structural and biochemical studies of coiled-coil proteins with more diverse biophysical properties and biological functions are essential for elucidating all the factors that affect coiled-coil interactions and for more accurate computer-based predictions.

Here we report analyses of two paralogous maize coiled-coil proteins: EMPTY PERICARP2 (EMP2) and HEAT SHOCK FACTOR BINDING PROTEIN 2 (HSBP2). EMP2 and HSBP2 are small proteins solely comprised of a coiled-coil domain (Fu et al., 2002). The orthologue of EMP2 in human interacts with HEAT SHOCK FACTOR 1 (HSF1), the main HSF involved in heat shock response (HSR) regulation, and negatively regulates the transcriptional activity of HSF1 (Satyal et al., 1998). Genetic analyses suggested that *emp2* and *hsbp2* have non-redundant functions during heat shock response and normal development (Fu et al. 2002; Fu and Scanlon, 2004). Studies reported herein revealed that the functional divergence of *emp2* and *hsbp2* is associated with their differential expression regulations as well as distinct biochemical properties. BLAST searches indicated that these paralogous genes are differentially expressed in different tissues during maize development, whereas yeast two-hybrid analyses detected different proteins interacting with the maize HSBPs. Site-directed mutagenesis identified multiple protein segments and residues responsible for the divergent protein-protein interaction specificities of EMP2 and HSBP2. Taken together, EMP2 and HSBP2 provide a novel opportunity to understand mechanisms of HSR regulation and maize development. Comparative analyses of the different coiled-coil specificities of these paralogous HSBPs will also elucidate general molecular determinants governing coiled-coil interactions.

## Materials and Methods

### Database Analyses

The cDNA sequence of *emp2* (GenBank #AF494284) and *hsbp2* (GenBank #BG840671) were used to BLAST search the Plant Genomic Database (www.plantgdb.org). The name and

tissue source of cDNA libraries were recorded for each homologous EST hits. The relative abundance of *emp2*/*hsbp* in each tissue was calculated as the ratio of ESTs hits from corresponding cDNA libraries.

**Cloning of the genomic sequence of *hsbp2* and identification of *Mutator* transposon insertion alleles**

Genomic sequences homologous to *hsbp2* EST were identified from PlantGDB and Pioneer Hibryd database. Full length *hsbp2* genomic sequence was cloned by Genome Walker PCR (BD Bioscience, CA) using two gene- specific primers: GW-F1 and GW-F2 (Table 4.1) in combination with universal primers. *Mutator* (*Mu*) transposon insertion alleles were identified by Dr. Meeley through the Trait Utilization System for Maize (TUSC) as described (Bensen, 1995). Gene specific primers (TUSC-F1 and TUSC-R1) used in TUSC analyses were listed in Table 4.1.

**Antibody production, Recombinant Protein Expression and Immunoblot Analysis**

Rabbit anti-EMP2 (Fu et al., 2002) and anti-HSBP2 (Fu and Scanlon, 2004) specific polyclonal antibodies were produced and affinity purified by BioSource Intl. (Camarillo, CA). The specificities of the purified antibodies were assayed by ELISA and Western gel-blot analyses against the multiple antigenic peptides (MAP), which are used for the original immunization of rabbits. The specificities of antibodies were further tested by EMP2 and HSBP2 recombinant proteins expressed in pTriplEx vector (BD Bioscience, CA) and pBAD TOPO TA vector (Invitrogen) respectively. Soluble protein preparation, gel electrophoresis and Coomassie Blue staining (Brilliant Blue R250, BioRad) were carried out as described (Sambrook and Russel, 2001). EMP2 and HSBP2 specific antigen were detected using the ECL system (Amersham Biosciences, NJ).

**Table 4.1** Oligo sequences utilized in this study

| oligo name | usage | sequence |
|---|---|---|
| TUSC-F1 | 225-253 of *hsbp2* genomic sequence | CCAACGAACTCAGATGGTGACTAAGGAAG |
| TUSC-R1 | 1387-1359 of *hsbp2* genomic sequence | CATGCACAAGAGACAAGACTGTCGCCAAA |
| MuTIR | complementary to terminal sequence of *Mutator* transposon | AGAGAAGCCAACGCCAWCGCCTCYATTTCGTC |
| GW-F1 | 2261-2287 of *hsbp2* genomic sequence | CCTCAATGACCTCAAGGCTGAGATAGG |
| GW-F2 | 2517-2542 of *hsbp2* genomic sequence | CGTTCTGTGTAGACCTACCCGTGGTT |
| *emp2*-F1 | 5'-end of *emp2* ORF | CCTCGAATCCCTGGATTCAGATCCATCATCAG |
| *emp2*-R1 | 3'-end of *emp2* ORF | TGACGGATCCCAAGTTAGGCAGAGTCAG |
| *hsbp2*-F1 | 5'-end of *hsbp2* ORF | TCACGAATTCCTGGCGAGTTCCAAGTCCGGCAT |
| *hsbp2*-R1 | 3'-end of *hsbp2* ORF | TAGCGGATCCTCATGCGGAGCTGTCTGAAGGT |
| *hsfA4*-F1 | 5'-end of the HR-A/B domain of *hsfA4b* | CAACGAATTCCCATTACCAGATACCGAAAG |
| *hsfA4*-R1 | 3'-end of the HR-A/B domain of *hsfA4b* | TAGCGGATCCTTAAGAGAAAGATCCTGGTGC |
| *hsfA4*-R2 | 3'-end of *hsfA4b*ORF | CAAGGGATCCGTCTTAAATCGCGGGAAGAGA |
| *hsfA2e*-F1 | 5'-end of the HR-A/B domain of *hsfA2e* | CTCAGAATTCAGGCCGATGGATGTGCTCCA |
| *hsfA2e*-R1 | 3'-end of the HR-A/B domain of *hsfA2e* | ACACTCTAGAGGCTAATGTCTGGGACCATG |
| *hsfA9*-F1 | 5'-end of the HR-A/B domain of *hsfA9* | CACAGAATTCCCGTTCCTGACCAAGGTCTA |
| *hsfA9*-R1 | 3'-end of the HR-A/B domain of *hsfA9* | CTGTTCTAGACGCTCATGCTTCAGTTATGAC |
| *hsfA5*-F1 | 5'-end of the HR-A/B domain of *hsfA5* | CACTGAATTCGCACCAGTCATGGAGGTC |
| *hsfA5*-R1 | 3'-end of the HR-A/B domain of *hsfA5* | AATGTCTAGATCAAGGTCAGAGTTTCAGCTG |
| *hsfA5*-F1 | 5'-end of the HR-A/B domain of *hsfA5* | TCTTCCCGGGCCATTGCCTGATGCTGTTTGCT |
| *hsfA5*-R1 | 3'-end of the HR-A/B domain of *hsfA5* | AGTCTCTAGATGAGATTTGCCTTTGTGTTCTGC |
| *hsfA4d*-F1 | 4d'-end of the HR-A/B domain of *hsfA4d* | TCCTCCCGGGCACTCGCTGCGCACCCAAGC |
| *hsfA4d-R1* | 3'-end of the HR-A/B domain of *hsfA4d* | AGTCTCTAGAAGGCCGGAACACGAACGACC |
| *hsfA3*-F1 | 5'-end of the HR-A/B domain of *hsfA3* | TCTTCCCGGGCCTGGCTCTTCTTCTGGAGAG |
| *hsfA3*-R1 | 3'-end of the HR-A/B domain of *hsfA3* | AGTCTCTAGATCCTCACGAAACTCGGGTTCTG |
| *hsfA4a*-F1 | 5'-end of the HR-A/B domain of *hsfA4a* | TCTTCCCGGGCCACTGGCGGAGTCGGAGAGG |
| *hsfA4a*-R1 | 3'-end of the HR-A/B domain of *hsfA4a* | AGTCTCTAGATCTTCTTCTTGCTGAAGTGGTC |
| *hsfC2a*-F1 | 5'-end of the HR-A/B domain of *hsfC2a* | TCTTCCCGGGAAGCGCAAGGACGACGGCAAC |
| *hsfC2a*-R1 | 3'-end of the HR-A/B domain of *hsfC2a* | AGTCTCTAGACGCGACCTTGACGAGGAACGC |

**Table 4.1** Oligo sequences utilized in this study (continued)

| oligo name | usage | sequence |
|---|---|---|
| *hsbp2*-5255F | mutagenesis primer for substitution of residue 52and 55 of HSBP2 | 5'-ATTTCAAAGAAAGATGAAAAGGGTGCGAGA-3' |
| *hsbp2*-5962F | mutagenesis primer for substitution of residue 59 and 62 of HSBP2 | 5'-GGTGCGAGAAAAGATGAAAAGGAACAGAGC-3' |
| *hsbp2*-7595R | mutagenesis primer that fused the C-terminal 75-95 residues of HSBP2 to EMP2 on the C-terminal | 5'-TCATGCGGAGCTGTCTGAAGGTCTTGACTCTTCCTTCATCTTAGATGGCGTCGACATGCCTTCACCGCCCATCTCAGCTTTGAGATC-3' |
| *hsbp2*-0114F | mutagenesis primer that fused the C-terminal 01-14 residues of HSBP2 to EMP2 on the N-terminal | 5'-ATGGCGAGTTCCAAGTCCGGCATCCCTATCAAGGCAGAACAAGATTCAGATCCATCATCACAG-3' |
| GBK-1323R | first round flanking primer for mutagenesis PCR using pGBK vector | 5'-GTTATGCTAGTTATGC-3' |
| GBK1155F | second round flanking primer for mutagenesis PCR using pGBK vector | 5'-TCATCGGAAGAGAGTAGTAACAAAGGTC-3' |
| GAD1905F | first round flanking primer for mutagenesis PCR using pGADT7 Rec vector | 5'-TAATACGACTCACTAT-3' |
| GAD2152R | second round flanking primer for mutagenesis PCR using pGADT7 Rec vector | 5'-AACTTGCGGGGTTTTTCAGTATCTACG-3' |

For large scale protein expression and purification, the open reading frames (ORF) of *emp2* and *hsbp2* were cloned downstream of the GST tag in pGEX-5X-1 expression vector (Amersham Biosciences, NJ). Optimization of protein expression was carried out according to manufacture's recommendation. Recombinant proteins were purified using the GST•Bind Resin (Novagen, Madison, WI), and visualized on 10% polyacrylamide gels by silver staining (Silver stain plus kit, BioRad, CA).

**Yeast two-hybrid analyses of protein-protein interactions**

In order to identify EMP2 interacting proteins from maize embryos, the *emp2* ORF was cloned into pGBKT7 bait vector, and cDNA libraries made from 14 days after pollination (dap) maize kernels were cloned into the pGADT7 Rec prey vector by in vivo recombination (BD Biosciences, CA). Positive interactions were identified as colonies that were able to grow on SD/-Leu/-Trp/-His/-Ade plates. Subsequent yeast plasmid preparation and characterization were carried out according to manufacture's recommendation.

Genomic sequences of rice HSFs were obtained from Dr. Lutz Nover (Biocenter of the Goethe University, Germany). EST and/or genomic sequences of five maize HSFs were identified from the Plant Genomic Database (www.plantgdb.org) by their homology to rice HSF sequences. All nine maize HSFs (including four indentified by Gagliardi et al., 1995) were renamed according to their closest homologues in rice based on ClustalW alignment (http://searchlauncher.bcm.tmc.edu/multi-align/multi-align.html) (Thompson et al., 1994). Secondary structure prediction of maize HSBPs and HSFs were based on COILS (http://www.ch.embnet.org/software/COILS_form.html) (Lupas et al., 1991). Previous work by Satyl et al (1998) showed that peptide sequences outside of the oligomerization domain (HR-A/B) interfere with the interaction between HSBP and HSF. Therefore only the HR-A/B domains of

maize HSFs were cloned into the pGADT7 Rec prey vector. The bait constructs with either the *emp2* or the *hsbp2* ORF were co-transformed with the prey constructs into AH109 yeast competent cells. Positive bait and prey interaction were defined as growth and blue color development of yeast transformants on SD/-Leu/-Trp/-His/-Ade/X-Gal plates. After HSFA4b was identified as potential interacting protein of HSBP2, both HSBP2 and HSFA4b were systematicly mutagenized to identify residues and domains important for their interaction. Site directed mutagenesis of *hsbp2* and *hsfA4b* was carried out using the mega-primer method (Sambrook and Russell, 2002). Quantitative assessment of the strength of interactions in yeast two-hybrid was carried out as described using 2-Nitrophenyl-b-D-galactopyranoside (ONPG) as a substrate (Sambrook and Russell, 2002). The sequences of oligos used for the above cloning procedures are listed in Table 4.1.

## Results

### The genomic structure of *hsbp2* and *Mutator* (*Mu*) transposon insertion alleles

In order to identify the full genomic sequence of the maize *hsbp2* gene, the EST sequence of *hsbp2* (ZMtuc03-08-11.16292) was used as a query to search GenBank. A single genomic clone (GenBank # BZ681457) apparently corresponding to part of the *hsbp2* EST was retrieved . Full length *hsbp2* genomic sequence was cloned by Genome Walker PCR (GenBank #AY450672) based on the sequence of the genomic fragment. Alignment of the EST sequence against the genomic clone revealed the presence of four introns and five exons. All the intron and exon positions are conserved between *emp2* and *hsbp2* (Fu et al., 2002; Figure 4.1). However, the predicted open reading frame (ORF) of *hsbp2* begins in the first exon, whereas the first exon of *emp2* is completely untranslated.

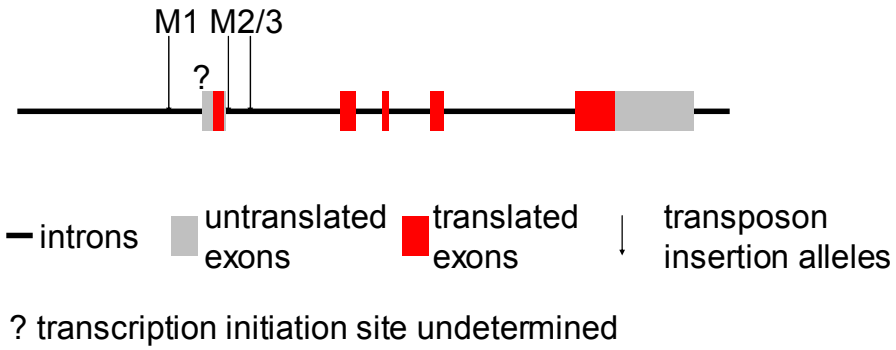


**Figure 4.1** Genomic structures of *hsbp2* and transposon insertion alleles. The *hsbp2* locus is comprised of four introns and five exons. The transcription initiation site has not been determined. Three independent *Mutator* transposon insertion alleles have been identified: one (M1) is upstream of the first exon and two are located in the first intron.

By reverse genetic analyses using the TUSC system (Bensen et al., 1995) in collaboration with Dr. Meeley at Pioneer Hi-Bred, multiple transposon insertion alleles of *hsbp2* were also identified. As shown in Figure 4.1, all three *Mu* transposons were inserted into the 5'-end of *hsbp2* gene. Similar transposon insertion preference has been observed for the paralogous *emp2* locus (Fu et al., 2002).

**Expression of e*mp2* and *hsbp2* are differentially regulated during maize development and stress response**

The *emp2* and *hsbp2* genes were identified as paralogues based on their sequence similarity and intron-exon structure conservation (Fu et al., 2002). Previous immunoblot analyses showed that EMP2 and HSBP2 were accumulated differently in maize embryos and leaves, before and after heat stress (Fu and Scanlon, 2004). In order to study the expression of *hsbp*s in a broader variety of tissues, BLAST search was performed using *emp2* and *hsbp2* cDNA sequences against ESTs from cDNA libraries made from maize tissues at different developmental stages (Table 4.2). By comparing the number of EST hits for *emp2* and *hsbp2* from different tissues, it was found that in most developmental stages, *emp2* is expressed at a higher level than its paralogue *hsbp2*. The relative abundance of *emp2*/*hsbp2* EST deposited in the public Plant Genomic Database (www.plantgdb.org) is increased in cDNA libraries made from more developed tissues (Figure 4.2); the most drastic change is observed for maize ears (Figure 4.2, Table 4.2). No *emp2* homologous EST was identified from the cDNA library made from female inflorescence tissue, at which stage the maize ear is smaller than 2mm in size. In contrast, four *hsbp2* homologous ESTs were present in the same cDNA library. However, the *emp2* homologous ESTs instead were more abundant (10 *emp2* ESTs vs. 1 *hsbp2* EST) in cDNA libraries were made from larger ears (2-20mm in size). The change of *emp2*/*hsbp2* EST ratio suggests that the

**Table 4.2** Number of *emp2* and *hsbp2* hits from EST database

| gene (total EST hits) | kernel | root | apex | seedling | sheath | female inflruores-cence | immature ear | tassel primordi-um | anther and pollen | mature pollen |
|---|---|---|---|---|---|---|---|---|---|---|
| *emp2* (53) | 5 | 4 | 9 | 4 | 8 | 0 | 10 | 2 | 2 | 9 |
| *hsbp2* (17) | 1 | 2 | 4 | 1 | 1 | 4 | 1 | 2 | 1 | 0 |

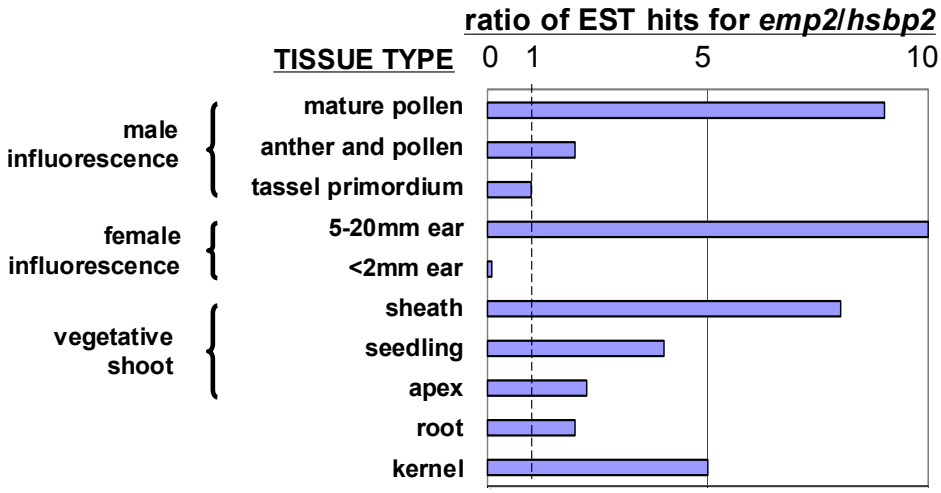


**Figure 4.2** The relative abundance of *emp2* and *hsbp2* ESTs changes during development. The numbers of *emp2* and *hsbp2* homologous ESTs in cDNA libraries made from ten different tissue types were compared. There is no *emp2* EST detected in the female inflorescence (<2mm ear) library, but the ratio of *emp2/hsbp2* (0/4) is assigned as ¼ instead of "0". Similarly, there is no EST of *hsbp2* from mature pollen and the *emp2/hsbp2* ratio (9/0) is assigned as "9" instead of "∞".

paralogous *emp2* and *hsbp2* gene are subjected to different developmental regulation, whereas their differential expression patterns suggest functional divergence of maize *hsbp*s.

**EMP2 and HSBP2 interact with different proteins in yeast two-hybrid**

Previous mutant analyses revealed an essential role of EMP2 in regulating *heat shock protein* gene (*hsp*) expression (Figure 2.6). The heat inducible accumulation of HSBP2 proteins also suggests a role for HSBP2 during HSR in maize leaves (Figure 3.3), perhaps by regulating the function(s) of a maize HSF as suggested by previous studies of HSBP1 in animals (Satyal et al., 1998). To study the possible interaction between EMP2/HSBP2 and HSFs, partial genomic sequence of five maize HSFs were identified from the public database PlantGDB (www.plantgdb.org) in addition to the four partial HSF cDNA sequences reported previously (Gagliardi et al., 1995). Based on the homologies between maize and rice HSFs (personal communication with Dr. Lutz Nover), eight of the maize proteins were categorized as A class HSF, and only one of them belongs to the C class HSF (Figure 4.3). The HR-A/B oligomerization domains of all nine identified maize HSFs were cloned (see Materials and Methods, Figure 4.4), and their capacities to interact with maize HSBPs were tested in the yeast two-hybrid systems (Table 4.3). Surprisingly, none of the maize HSFs tested showed any specific interaction with EMP2, whereas HSBP2 interacted specifically with the HR-A/B domain of maize HSFA4b (Table 4.3). Therefore, interactions between maize HSBP2 and HSFA4b are highly selective in yeast.

Although yeast two-hybrid identified no interactions between EMP2 and any of the nine maize HSFs, potential EMP2 interacting proteins were identified from cDNA libraries prepared from maize embryos. One such example, designated as EMP2 INTERACTING PROTEIN 6 (EMI6), is shown in Figure 4.5. Yeast co-transformed with EMP2 and EMI6 can grow on

**Figure 4.3**

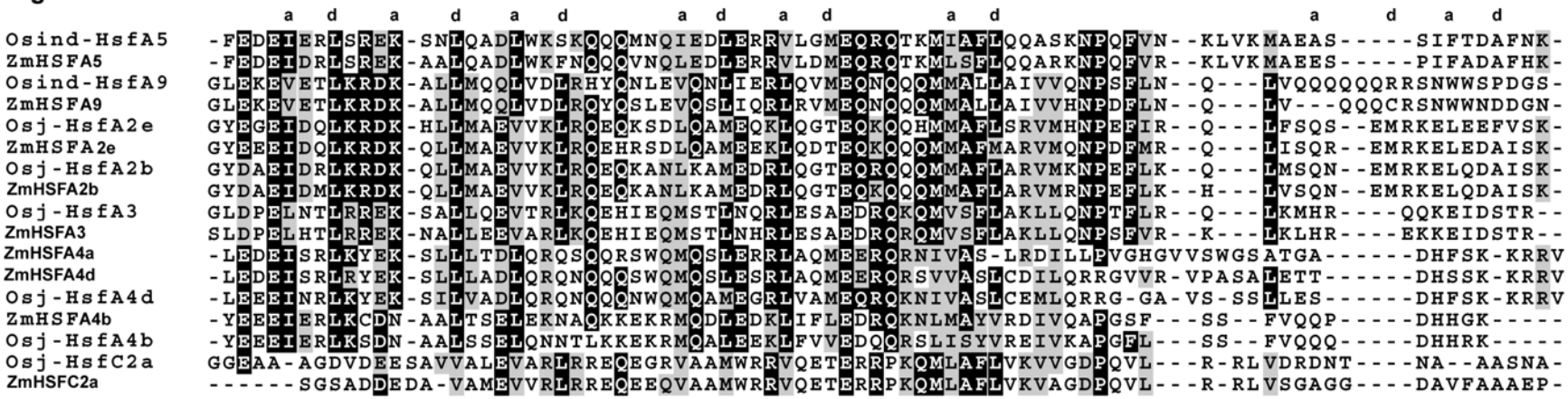
a d a d a d a d a d a d a d
Osind-HsfA5 -FEDEIERLSREK-SNLQADLWKSKQQQMNQIEDLERRVLGMEQRQTKMIAFLQQASKNPQFVN--KLVKMAEAS-----SIFTDAFNK-
ZmHSFA5 -FEDEIDRLSREK-AALQADLWKFNQQQVNQLEDLERRVLDMEQRQTKMLSFLQQARKNPQFVR--KLVKMAEES-----PIFADAFHK-
Osind-HsfA9 GLEKEVETLKRDK-ALLMQQLVDLRHYQNLEVQNLIERLQVMEQNQQQMMALLAIVVQNPSFLN--Q---LVQQQQQQRRSNWWSPDGS-
ZmHSFA9 GLEKEVETLKRDK-ALLMQQLVDLRQYQSLEVQSLIQRLRVMEQNQQQMMALLAIVVHNPDFLN--Q---LV---QQQCRSNWWNDDGN-
Osj-HsfA2e GYEGEIDQLKRDK-HLLMAEVVKLRQEQKSDLQAMEQKLQGTEQKQQHMMAFLSRVMHNPEFIR--Q---LFSQS--EMRKELEEFVSK-
ZmHSFA2e GYEEEIDQLKRDK-QLLMAEVVKLRQEHRSDLQAMEEKLQDTEQKQQQMMAFMARVMQNPDFMR--Q---LISQR--EMRKELEDAISK-
Osj-HsfA2b GYDAEIDRLKRDK-QLLMAEVVKLRQEQKANLKAMEDRLQGTEQRQQQMMAFLARVMKNPEFLK--Q---LMSQN--EMRKELQDAISK-
ZmHSFA2b GYDAEIDMLKRDK-QLLMAEVVKLRQEQKANLKAMEDRLQGTEQKQQQMMAFLARVMRNPEFLK--H---LVSQN--EMRKELQDAISK-
Osj-HsfA3 GLDPELNTLRREK-SALLQEVTRLKQEHIEQMSTLNQRLESAEDRQKQMVSFLAKLLQNPTFLR--Q---LKMHR----QQKEIDSTR--
ZmHSFA3 SLDPELHTLRREK-NALLEEVARLKQEHIEQMSTLNHRLESAEDRQRQMVSFLAKLLQNPSFVR--K---LKLHR----EKKEIDSTR--
ZmHSFA4a -LEDEISRLKYEK-SLLLTDLQRQSQQRSWQMQSLERRLAQMEERQRNIVAS-LRDILLPVGHGVVSWGSATGA------DHFSK-KRRV
ZmHSFA4d -LEDEISRLRYEK-SLLLADLQRQNQQQSWQMQSLESRLAQMEERQRSVVASLCDILQRRGVVR-VPASALETT------DHSSK-KRRV
Osj-HsfA4d -LEEEINRLKYEK-SILVADLQRQNQQQNWQMQAMEGRLVAMEQRQKNIVASLCEMLQRRG-GA-VS-SSLLES------DHFSK-KRRV
ZmHSFA4b -YEEEIERLKCDN-AALTSELEKNAQKKEKRMQDLEDKLIFLEDRQKNLMAYVRDIVQAPGSF---SS--FVQQP-----DHHGK-----
Osj-HsfA4b -YEEEIERLKSDN-AALSSELQNNTLKKEKRMQALEEKLFVVEDQQRSLISYVREIVKAPGFL---SS--FVQQQ-----DHHRK-----
Osj-HsfC2a GGEAA-AGDVDEESAVVALEVARLRREQEGRVAAMWRRVQETERRPKQMLAFLVKVVGDPQVL---R-RLVDRDNT----NA--AASNA-
ZmHSFC2a ------SGSADDEDA-VAMEVVRLRREQEEQVAAMWRRVQETERRPKQMLAFLVKVAGDPQVL---R-RLVSGAGG----DAVFAAAEP-

**Figure 4.3** ClustalW alignment of the HR-A/B domain of nine maize HSFs and their orthologues from rice. The '**a**' and '**d**' denote hydrophobic residues of heptad repeats (**abcdefg**). Nine maize HSFs were identified: ZmHSFA2e, A2b, A3, A4a, A4d, A4b, A5, A9 and C2a. A total of 26 HSFs have been identified in rice genomic sequence, but only eight of them were shown here. Two of the rice HSFs are from the *indica* cultivar 93-11 (Osind-HsfA5, Osind-HsfA9) and the other six are from the *japonica* cultivar Nipponbare (Osj-HsfA2e, A2b, A3, A4d, A4b, C2a). Conserved residues are shaded by BOXSHADE (http://www.ch.embnet.org/software/BOX_form.html).

**Table 4.3** Potential interactions between maize HSBPs and HSFs

| interactions | ZmHSFA2b | ZmHSFA2e | ZmHSFA3 | ZmHSFA4a | ZmHSFA4b | ZmHSFA4d | ZmHSFA5 | ZmHSFA9 | ZmHSFC2a |
|---|---|---|---|---|---|---|---|---|---|
| EMP2 | No | no | no | no | no | weak | no | no | no |
| HSBP2 | No | no | weak | no | strong | no | weak | no | weak |

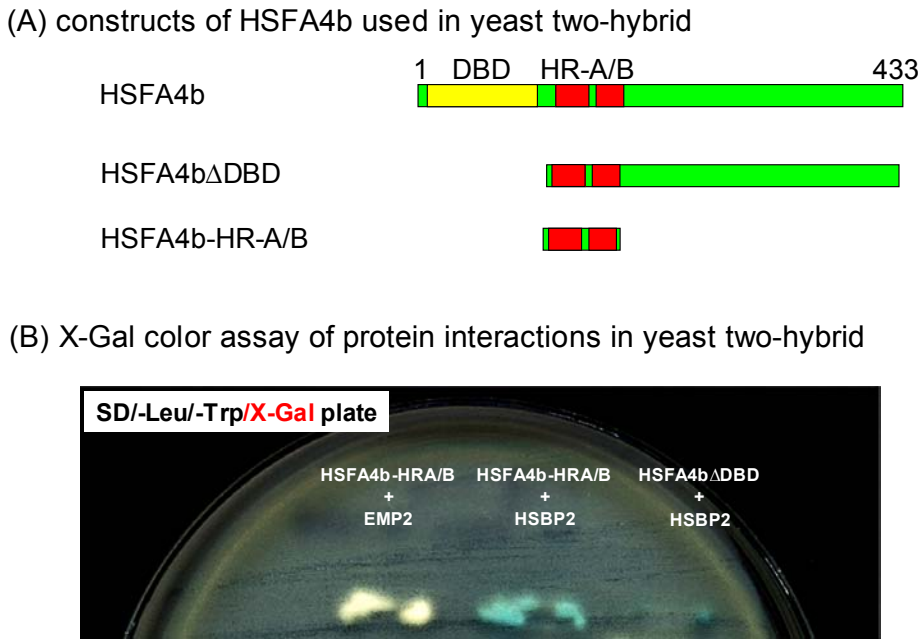


**Figure 4.4** Interactions of HSBP2 with ZmHSFA4b in yeast two-hybrid. (A) The top panel shows structural features of maize HSFA4b and two partial HSFA4b constructs tested in yeast two-hybrid. ZmHSFA4bΔDBD denotes that the DNA binding domain (DBD) is deleted, whereas the ZmHSFA4b-HR-A/B denotes that only the HR-A/B domain is cloned. (B) The lower panel shows the interaction of HSBP2 with ZMHSFA4b using β-galacosidase report assay (development of blue color). Yeast colonies transformed by HSBP2 with both deletion constructs of ZmHSFA4b developed blue color, but not the co-transformants of EMP2 and ZmhsfA4b-HR-A/B

(A)Interaction of EMP2 with EMI6


(B) predicted coiled-coil structure of the unknown protein: EMI6

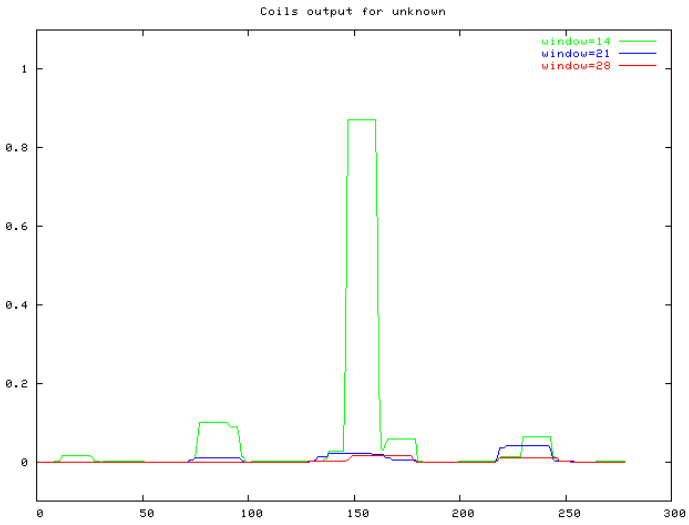


**Figure 4.5** The interaction of EMP2 and EMI6 and the predicted structure of EMI6. (A) Yeast transformats with *emp2* and *emi6* or with *hsbp2* and *emi6* grew on nutrition selection media. (B) The predicted coiled-coil structure of EMI6 by COILS. The horizontal axis represents the number of residues of the EMI6 protein, and the vertical axis denotes the probability of coiled coil formation (maximum is 1).

nutritional selection media and exhibited blue color development. In contrast, the yeast transformed with HSBP2 and EMI6 showed no growth on the same selective media, suggesting that EMI6 can interact with EMP2, but not HSBP2, in yeast. The deduced amino acid sequence of EMI6 was predicted to form a coiled-coil, although no other functional domain can be detected (Figure 4.5).

**Hetero-oligomerization of HSBP2 and HSFA4b is mediated through the coiled-coil domain**

The coiled-coil is the sole recognizable protein domain in maize HSBPs (Fu et al., 2002), whereas the oligomerization domain (HR-A/B) of HSFs is comprised of two coiled coils with a non-coiled-coil linker spaced in-between (Nover et al., 2001). In order to test whether the hetero-oligomerization of HSBP2 and HSFA4b depends on the coiled-coil domain, hydrophobic residues at '**a**' and '**d**' positions of the heptad repeat (**abcdefg**) were replaced by polar Lysine residues (Figure 4.6). As shown in Figure 4.6, mutant constructs of HSBP2 (e.g. I52K/M55K, I59K/M62K) can not interact with the HR-A/B domain of HSFA4b. Conversely, the mutated form of HSFA4b also exhibited no interaction with HSBP2 in yeast two-hybrid (Figure 4.6). The class A plant HSFs contain a characteristic long linker sequence between the HR-A and HR-B domain; the linker sequence is not predicted to form a coiled-coil (Nover et al., 2001). Not surprisingly, the HR-A/B domain of HSFA4b can still interact with HSBP2 when the residues at '**a**' and '**d**' positions within the linker region are mutated (Figure 4.6). Therefore, the hetero-oligomerization of HSBP2 and HSFA4b depends upon their coiled-coil domains. In addition, when the HR-A/B domain of HSFA4b is linked to its C-terminal sequence found on the native HSFA4b protein, the strength of interaction between HSBP2 and HSFA4b is decreased (Figure 4.4). Such an observation suggests that sequences outside of the coiled-coil domain of HSFs may negatively regulate their protein-protein interactions (Satyl et al., 1998).

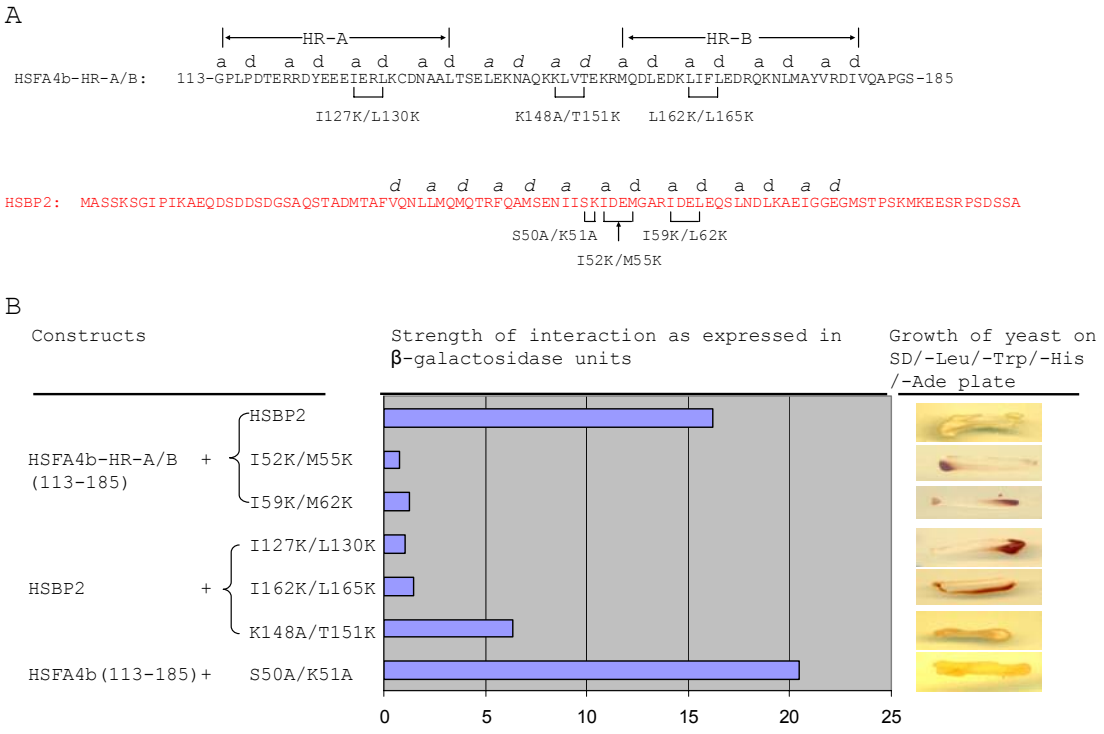


**Figure 4.6** Mutant constructs of HSBP2 and HSFA4b and their interactions in yeast two-hybrid (A) Protein sequences of the HR-A/B domain of HSFA4b (113-185) (in black) and the HSBP2 (in red). The '**a**' and '**d**' denote the heptad repeats (**abcdefg**) as predicted by COILS in a 14 residue window. The italic '***a***' and '***d***' indicate the coiled-coil probability is lower than 50%. (B) Quantitative and qualitative assessment of protein-protein interactions in yeast two-hybrid. The left panel shows each combination of constructs transformed into yeast. The middle panel shows the strength of interaction calculated by units of β-Galactosidase from each OD600 yeast cells. Each transformants have three duplicates and the average value is shown above. The right panel shows the growth of each transformants on SD/-Leu/-Trp/-His/-Ade. Healthy yeast growth is white or yellow.

Attractive electrostatic interactions between '**e**' and '**g**' positions of the heptad repeat (**abcdefg**) from different helix strands are also proposed to be important for the stability of coiled coils (Burkhard et al., 2001). However, the interaction between HSBP2 and HSFA4b was not interfered by substitution of the Lysine residue at one of the 'g' positions (K51) on HSBP2 with a non-charged Alanine residue (Figure 4.6).

**The specificity of HSBP2-HSFA4b interaction is mainly conferred by non-coiled-coil sequences flanking the coiled-coil domain of HSBP2.**

Protein sequences of paralogous maize HSBPs are highly homologous within the coiled-coil domain. However, the N-terminal of HSBP2 is 13 residues longer than that of EMP2, and EMP2 has a three-residue C-terminal deletion compared to HSBP2 (Figure 4.7). In order to determine whether these variations between EMP2 and HSBP2 are important for differential interactions with HSFA4b in yeast, several deletion and domain swap constructs were tested in yeast two-hybrid. As shown in Figure 4.7, when the N-terminal 12 residues of HSBP2 were deleted, the strength of HSBP2 and HSFA4b interaction was greatly reduced. An even stronger negative affect was observed for HSBP2 mutants with the 77-79 residues deleted (H77-79d, Figure 4.7). Therefore, the N-terminal extension and C-terminal insertion of HSBP2 compared to EMP2 are important for the former to interact with HSFA4b. Indeed, the coiled-coil domain of EMP2, if flanked by N- and C-terminal sequences from HSBP2, can also interact with HSFA4b (Figure 4.7). Thus, the specificity of HSBP2 and HSFA4b interaction is conferred by peptide sequences outside of the coiled-coil domain.

Although the coiled-coil domains of EMP2 and HSBP2 seem to be equivalent in their capabilities to interact with HSFA4b, amino acid substitutions of HSBP2 by corresponding residues from EMP2 affect the interaction between HSBP2 and HSFA4b. As shown in

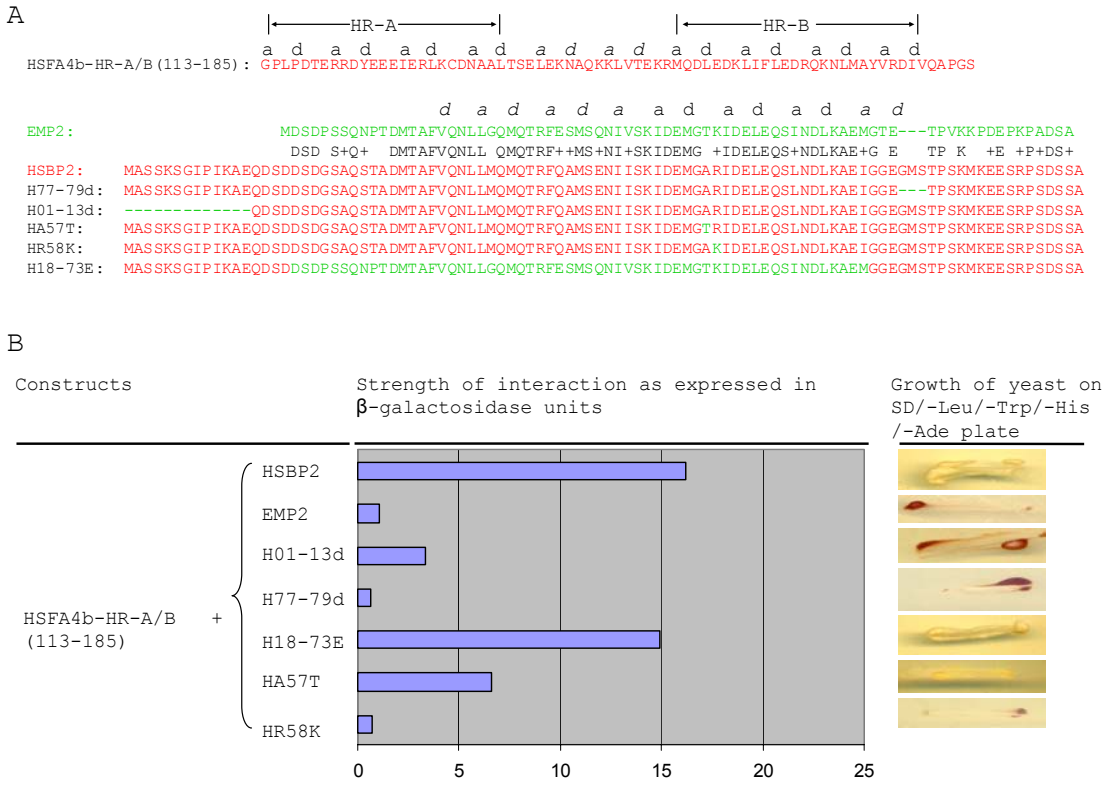


**Figure 4.7** Mutant constructs of HSBP2 and their interactions with the HR-A/B domain of HSFA4b (113-185). (A) Protein sequences of the HR-A/B domain of HSFA4b (113-185) (in black), the EMP2 (in green) and the HSBP2 (in red), as well as the mutant constructs of HSBP2. The green coded residues in the HSBP2 mutant proteins represent residues replaced by corresponding residues found on EMP2. The green dashed lines represent truncations and deletions that mimic EMP2 protein. The '**a**' and '**d**' denote the heptad repeats (**abcdefg**) as predicted by COILS in a 14 residue window (see Materials and Methods). Italics designate residues for which the coiled-coil probability is lower than 50%. (B) Quantitative and qualitative assessment of protein-protein interactions in yeast two-hybrid. The left panel shows each combination of constructs transformed into yeast. The middle panel shows the strength of interaction calculated by units of β-Galactosidase from each OD600 yeast cells. Each transformants have three duplicates and the average value is shown above. The right panel shows the growth of each transformants on SD/-Leu/-Trp/-His/-Ade. Healthy yeast growth is white or yellow.

Figure 4.7, when the Arginine at position 58 (R58) of HSBP2 is replaced by Lysine (K) found on EMP2, the mutated form of HSBP2 (HR58K) can no longer interact with HSFA4b. It has been proposed that interhelical attractive electrostatic interactions between '**e**' and '**g**' positions of heptad repeats (**abcdefg**) are important for the stability of coiled-coil formation (Lavigne et al., 1995). The R58 of the mutated HSBP2 (HR58K) is predicted to be in the '**g**' position, and thus may not be in the correct position for interhelical electrostatic interaction. In contrast, when the Alanine (A57) residue adjacent to K58 is replaced by the corresponding residue from EMP2, the mutated form of HSBP2 (HA57T) can still interact with HSFA4b. Such an observation is consistent with previous reports that residues at the '**f**' position are not directly involved in coiled-coil interactions (Yu, 2002).

**Purification of EMP2 and HSBP2 proteins**

The different protein interaction specificities of EMP2 and HSBP2 suggest that these paralogous maize proteins are structurally and biochemically divergent. Structural studies of EMP2 and HSBP2 require highly purified recombinant proteins. To this end, the open reading frame (ORF) of both *emp2* and *hsbp2* were cloned into pGEX-5X-1 vector in frame with GST fusion tag (Novagen, Madison, WI). As shown in Figure 4.8, *E.coli* transformed with the pGEX-5X-1-*hsbp2* construct showed background level of recombinant protein expression even under non-induced conditions. The expression level of recombinant proteins peaked after 2 hour (h) of 1mM IPTG induction. However, recombinant proteins prepared after 2h of induction exhibited more degradation than those prepared after 1h of IPTG induction (Figure 4.8). Accordingly, large scale purification of EMP2 and HSBP2 recombinant proteins were prepared after 1h IPTG induction, and more than 30mg of each recombinant protein was purified (data not shown).

Figure 4.8

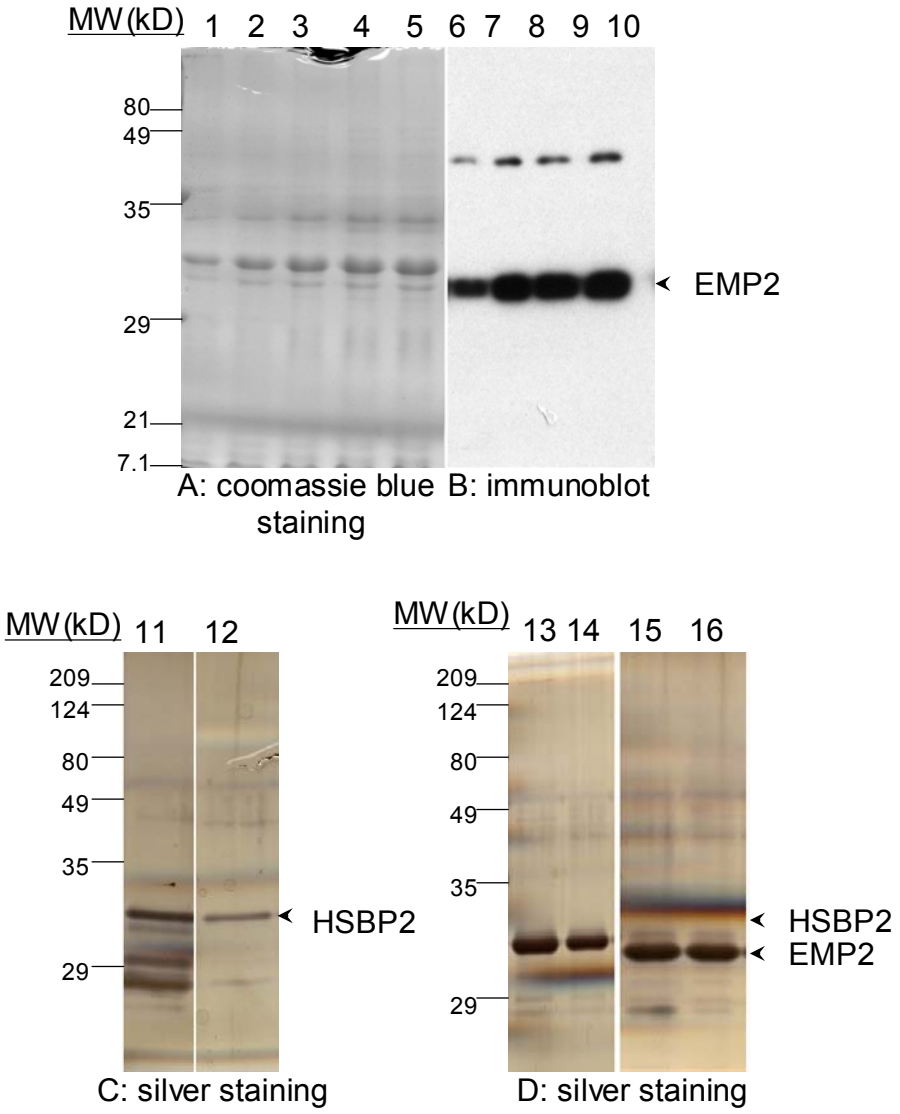


**Figure 4.8** Expression and purification of GST-tagged recombinant proteins of EMP2 and HSBP2. (A) Coomasie blue staining of 5µg of soluble proteins prepared from *E.coli* transformed by pGEX-5X-1-*emp2* construct. Lanes 1-5 represent proteins extracted after 1mM IPTG induction for 1h, 2h, 3h, 4h and 0h. (B) Immunoblot analyses of protein expression using rabbit anti-EMP2 antibodies. Lanes 6-10 are duplicates of lanes 1-5. Rabbit anti-EMP2 antibodies detect a strong band close to the estimated size of GST-EMP2 fusion protein, as well as a higher molecular weight antigen. (C) Silver staining of GST-tag resin purified HSBP2 recombinant

(**Figure 4.8** legend continued) proteins prepared from *E.coli* after 2h (lane 11) and 1h (lane 12) of 1mM IPTG induction. The size of the uppermost band is close to the estimated molecular weight of intact GST-HSBP2 fusion protein. (D) Silver stained purified GST-HSBP2 (lane 13 and 14) and GST-EMP2 (lane 15 and 16) from *E.coli* after 1h, 1mM IPTG induction.

## Discussion

### Differential expression patterns and protein-protein interaction specificities may have contributed to the functional divergence of maize HSBPs.

HSBPs are evolutionary conserved proteins that were identified by their interaction with HSFs in animal systems (Satyl et al., 1998). The *hsbp* gene is duplicated in all grass species, the maize paralogues were named *emp2* and *hsbp2* (Fu et al., 2002). Previous genetic and molecular analyses of the *emp2* mutation revealed multiple defects during both HSR and paltn development, indicating that the maize *hsbp* paralogues function non-redundantly throughout maize development (Fu et al., 2002; Fu and Scanlon, 2004). Functional divergence of paralogues is indicative of non-overlapping expression profiles and/or divergent biochemical properties. The molecular and biochemical analyses presented in this study suggest that both of these factors contributed to the non-redundant functionality of maize HSBP paralogues. Using the number of EST hits as an indicator of transcript abundance, BLAST search analyses revealed that the expression of maize *hsbp* genes is differentially regulated (Figure 4.2; Table 4.2). The functional divergence of maize *hsbp*s is further augmented by their different biochemical properties. As shown in yeast two-hybrid analyses reported herein, HSBP2 specifically interacts with HSFA4b, whereas EMP2 binds to a previously unidentified protein, EMI6 (Figure 4.4; Figure 4.6). Transposon insertion alleles of *hsbp2* have already been identified by reverse genetics (Figure 4.1). We are also preparing to screen for mutations in both the *hsfA4b* and the *emi6* loci. These genetic resources will enable the elucidation of mechanisms by which maize HSBPs regulate HSR and normal development.

We were very surprised that no maize HSFs was identified among the EMP2 interacting proteins in yeast two-hybrid. Based on the observation that *emp2* is required to regulate *hsp*

expression (Fu et al., 2002), the EMP2 protein is predicted to interact with some maize HSF. There are several possible factors that may have enabled maize HSFs to escape identification in our yeast two-hybrid analyses. First, there are probably more than twenty HSFs in maize, the majority of which are as yet unidentified. The upcoming release of maize ESTs from the private sector into the public domain may enable us to identify more maize HSFs and test them one by one in yeast two-hybrid. Secondly, the maize HSF cDNAs cloned in our embryo cDNA library may contain intrinsic features that interfere with their interactions with EMP2 as monomers. As shown by Satyl et al (1998) and also in this study, both the human HSF1 and maize HSFA4b have built-in features that hinder the interaction between HSBP and HSF monomers. Lastly, other factors including the formation of EMP2 homodimers or requirement of additional proteins may also prevent the detection of maize HSFs interaction with EMP2 in yeast system. In an effort to complement yeast two-hybrid analyses, GST pull down or immunoprecipitation analyses will also be performed to retrieve EMP2 interacting proteins from soluble protein preparations from different maize tissues.

**The specificity of HSBP2 and HSFA4b interaction are determined by peptide sequences that flank the coiled-coil domain**

Previous studies carried out with c-Jun/Fos, c-Myc/Max and synthetic peptides revealed many important features of coiled-coil formation (Burkhard et al., 2001 and references therein). It was reported that residues at the '**a**' and '**d**' residues are generally hydrophobic and positioned on the interface of interacting α –helixes (Figure 1.5; Crick 1953). In contrast residues at the '**e**' and '**g**' positions are often polar, placed adjacent to the interhelical interface and involved in electrostatic interactions (Kohn et al., 1995; Spek et al., 1998).

The maize HSBPs, for the first time, enabled us to understand how homologous native proteins can confer distinct coiled-coil specificities. As reported herein, the paralogous EMP2 and HSBP2 interact with different proteins in yeast. Through site-directed mutagenesis, it was found that the hydrophobic residues at the '**a**' and '**d**' positions are essential for coiled-coil interactions (Figure 4.6), which is consistent with previous observations that the coiled-coil is mainly maintained by hydrophobic packing (Crick, 1953). Interestingly, the K148A/T151K mutant of HSFA4b can still interact with HSBP2 in yeast two-hybrid. The K148 and T151 residues are located between the HR-A and HR-B domain, and they are predicted to occupy '**a**' and '**d**' positions respectively if this region also forms a coiled-coil. The observation that mutations at these two sites did not affect protein-protein interaction indicates that residues K148 and T151 are not part of the coiled-coil. Therefore, the above mutation analyses provide the first experimental evidence that HR-A and HR-b domains of maize HSF do not form a long and continuous α-helix. Currently, we are investigating how the linker region between HR-A and HR-B may affect the specificity and regulation of protein-protein interactions.

It was also found that the replacement of polar residue R58 of HSBP2 by K (R58K, Figure 4.7) abrogated the interaction of HSBP2 and HSFA4b, whereas the substitution of K51 by Alanine (K51A) did not (Figure 4.6). The K51 and R58 both are at the '**g**' position, which is predicted to be adjacent to the coiled-coil interaction surface and involved in electrostatic interactions. Such observations have two-fold significance. First, the data support past observations that residues of similar properties (e.g. K and R are both polar and positively charged under neutral pH) can confer different coiled-coil selectivity (Yu, 2002 and references therein). Secondly, the data indicate that the R58 but not K51 is involved in interhelical electrostatic interactions. In turn, such observation allows us to predict that R58 is physically

adjacent to, and interacts with negatively charged residues from the α–helix strand of HSFA4b. Further structural analysis of HSBP2 and HSFA4b dimer will enable us to test this model

Even more interesting results were observed from the deletion and domain swap experiments. As shown in Figure 4.7, the N-terminal truncation and C-terminal internal deletion mutants (H01-13d and H77-79d) of HSBP2 were unable to interact to HSFA4b, whereas the coiled-coil domain of EMP2 flanked by N- and C-terminal sequences from HSBP2 was able to bind to HSFA4b. First, these data enabled us to reveal the evolutionary events that lead to the functional divergence of EMP2 and HSBP2. Secondly and more importantly, the novel EMP2 protein represents the first gain-of-function mutation among coiled-coil proteins. It has been shown previously that mutations in peptide sequences adjacent to coiled-coil domain affect the stability of coiled coils (Brown et al., 1996), but it has never been shown that flanking peptide sequences can confer novel protein-protein interaction specificities. Based on these observations, we propose that mutations in flanking sequences may represent a general evolutionary mechanism that leads to the divergence of protein-protein interaction specificities of paralogues. The maize HSBP paralogues and the HSF family provide a tractable system to thoroughly test this hypothesis.

## Acknowledgements

We thank Dawe, L. Pratt, R. Meagher, and Z.-H. Ye for helpful discussions throughout this work. We are grateful for Dr. R. Meeley from Pioneer Hi-Bred for performing the TUSC analyses. We thank L. Nover from Goethe University, Germany for rice HSF sequences. We are grateful for M. Osterlund for technical assistance. The work was funded by the USDA-CREES-NRICGP grant # 01-01600 to MS.

## References

**Bailey, P. C., Martin, C., Toledo-Ortiz, G., Quail, P. H., Huq, E., Heim, M. A., Jakoby, M., Werber, M. and Weisshaar, B.** (2003). Update on the Basic Helix-Loop-Helix Transcription Factor Gene Family in Arabidopsis thaliana. *Plant Cell* **15**, 2497-502.

**Bensen, R. J., Johal, G.S., Crane, V.C., Tossberg, J.T., Schnable, P.S., Meeley, R.B., and Briggs, S.B.** (1995). Cloning and characterization of the maize An1 gene. *Plant Cell* **7**, 75-84.

**Brown, J. H., Cohen, C. and Parry, D. A.** (1996). Heptad breaks in alpha-helical coiled coils: stutters and stammers. *Proteins* **26**, 134-45.

**Burkhard, P., Stetefeld, J. and Strelkov, S. V.** (2001). Coiled coils: a highly versatile protein folding motif. *Trends Cell Biol* **11**, 82-8.

**Chao, H., Bautista, D. L., Litowski, J., Irvin, R. T. and Hodges, R. S.** (1998). Use of a heterodimeric coiled-coil system for biosensor application and affinity purification. *J Chromatogr B Biomed Sci Appl* **715**, 307-29.

**Crick, F. C. H.** (1953). The packing of a-helices:simple coiled coils. *Acta Crystallographica* **6**, 689-697.

**Engel, J. and Kammerer, R. A.** (2000). What are oligomerization domains good for? *Matrix Biol* **19**, 283-8.

**Fong, J. H., Keating, A. E. and Singh, M.** (2004). Predicting specificity in bZIP coiled-coil protein interactions. *Genome Biol* **5**, R11.

**Harbury, P. B., Zhang, T., Kim, P. S. and Alber, T.** (1993). A switch between two-, three-, and four-stranded coiled coils in GCN4 leucine zipper mutants. *Science* **262**, 1401-7.

**Havranek, J. J. and Harbury, P. B.** (2003). Automated design of specificity in molecular recognition. *Nat Struct Biol* **10**, 45-52.

**Invitrogen.** (2002). pBAD directional TOPO expression kits.

**Kohn, W. D., Kay, C. M. and Hodges, R. S.** (1995). Protein destabilization by electrostatic repulsions in the two-stranded alpha-helical coiled-coil/leucine zipper. *Protein Sci* **4**, 237-50.

**Kohn, W. D., Kay, C. M. and Hodges, R. S.** (1997). Salt effects on protein stability: two-stranded alpha-helical coiled-coils containing inter- or intrahelical ion pairs. *J Mol Biol* **267**, 1039-52.

**Krylov, D., Mikhailenko, I. and Vinson, C.** (1994). A thermodynamic scale for leucine zipper stability and dimerization specificity: e and g interhelical interactions. *Embo J* **13**, 2849-61.

**Lavigne, P., Kondejewski, L. H., Houston, M. E., Jr., Sonnichsen, F. D., Lix, B., Skyes, B. D., Hodges, R. S. and Kay, C. M.** (1995). Preferential heterodimeric parallel coiled-coil formation by synthetic Max and c-Myc leucine zippers: a description of putative electrostatic interactions responsible for the specificity of heterodimerization. *J Mol Biol* **254**, 505-20.

**Ledent, V. and Vervoort, M.** (2001). The basic helix-loop-helix protein family: comparative genomics and phylogenetic analysis. *Genome Res* **11**, 754-70.

**Lupas, A., Van Dyke, M. and Stock, J.** (1991). Predicting coiled coils from protein sequences. *Science* **252**, 1162-4.

**McLachlan, A. D. and Stewart, M.** (1975). Tropomyosin coiled-coil interactions: evidence for an unstaggered structure. *J Mol Biol* **98**, 293-304.

**Nover, L., Bharti, K., Doring, P., Mishra, S. K., Ganguli, A. and Scharf, K. D.** (2001). Arabidopsis and the heat stress transcription factor world: how many heat stress transcription factors do we need? *Cell Stress Chaperones* **6**, 177-89.

**O'Shea, E. K., Rutkowski, R. and Kim, P. S.** (1992). Mechanism of specificity in the Fos-Jun oncoprotein heterodimer. *Cell* **68**, 699-708.

**Pawson, T., Raina, M. and Nash, P.** (2002). Interaction domains: from simple binding events to complex cellular behavior. *FEBS Lett* **513**, 2-10.

**Satyal, S. H., Chen, D., Fox, S. G., Kramer, J. M. and Morimoto, R. I.** (1998). Negative regulation of the heat shock transcriptional response by HSBP1. *Genes Dev* **12**, 1962-74.

**Sodek, J., Hodges, R. S., Smillie, L. B. and Jurasek, L.** (1972). Amino-acid sequence of rabbit skeletal tropomyosin and its coiled-coil structure. *Proc Natl Acad Sci U S A* **69**, 3800-4.

**Spek, E. J., Bui, A. H., Lu, M. and Kallenbach, N. R.** (1998). Surface salt bridges stabilize the GCN4 leucine zipper. *Protein Sci* **7**, 2431-7.

**Thompson, J. D., Higgins, D.G., and Gibson, T.J.** (1994). CLUSTAL W: improving the sensitivity of progressive multiple sequence alignment through sequence weighting, positions-specific gap penalties and weight matrix choice. *Nucleic Acids Research* **22**, 4673-4680.

**Tripet, B., Wagschal, K., Lavigne, P., Mant, C. T. and Hodges, R. S.** (2000). Effects of side-chain characteristics on stability and oligomerization state of a de novo-designed model coiled-coil: 20 amino acid substitutions in position "d". *J Mol Biol* **300**, 377-402.

**Vinson, C. R., Hai, T. and Boyd, S. M.** (1993). Dimerization specificity of the leucine zipper-containing bZIP motif on DNA binding: prediction and rational design. *Genes Dev* **7**, 1047-58.

**Wang, C., Stewart, R. J. and Kopecek, J.** (1999). Hybrid hydrogels assembled from synthetic polymers and coiled-coil protein domains. *Nature* **397**, 417-20.

**Waterston, R. H. Lindblad-Toh, K. Birney, E. Rogers, J. Abril, J. F. Agarwal, P. Agarwala, R. Ainscough, R. Alexandersson, M. An, P. et al.** (2002). Initial sequencing and comparative analysis of the mouse genome. *Nature* **420**, 520-62.

**Wolf, E., Kim, P. S. and Berger, B.** (1997). MultiCoil: a program for predicting two- and three-stranded coiled coils. *Protein Sci* **6**, 1179-89.

**Yu, Y. B.** (2002). Coiled-coils: stability, specificity, and drug delivery potential. *Adv Drug Deliv Rev* **54**, 1113-29.

# CHAPTER 5

# CONCLUSIONS AND PERSPECTIVES

## The HEAT SHOCK FACTOR BINDING PROTEIN 1 (HSBP1) Promises New Answers for an Old Question

Induction of HEAT SHOCK PROTEINS (HSPs) is one of the core events of the heat shock response (HSR) in all organisms studied up to date. HEAT SHOCK FACTORS (HSFs) are the key players in regulating *hsp* gene expression. As a result, one of the most fundamental questions about the HSR is how HSFs themselves are regulated. Simply, are HSFs the first receptors in the high temperature signaling pathway? It has been well known in animals that activation of HSF1 is associated with multiple modifications, including phosphorylation, disulfide bridge formation, homo-trimerization, as well as hetero-oligomerization with proteins like HSP70, HSP90, RalBP1, α-TUBULIN and HSBP1 (Guo et al., 2001; Hu and Mivechi, 2003; Satyal et al., 1998; Shi et al., 1998). However, it is not clear whether these modifications are the consequences of HSF1 activation or the initial steps that activate HSF1. Compared to the studies in animals, little is known about HSF regulation in plants.

The *hsbp* gene was first cloned in human due to its ability to interact with the human HSF1 in yeast two-hybrid screens (Satyal et al., 1998). Here we reported that one of the maize HSBP paralogues, HSBP2, can also specifically interact with the maize HEAT SHOCK FACTOR A4b (HSFA4b, Figure 4.5). The evolutionarily conserved interactions between HSBP and HSF crossing different kingdoms strongly suggest that this type of interaction is extremely important, although currently there is no direct evidence supporting the notion that maize HSBP2 and HSFA4b are functional homologues of human HSBP1 and HSF1. It was observed that null mutations of the other maize *hsbp* gene, *emp2*, lead to over expression of many *hsp* genes (Figure 2.4). It is not clear whether the observed *hsp* over expression resulted from de-repressed HSF activity under non-stressed temperature or unattenuated HSR after being exposed to heat

stress. Nonetheless, it strongly suggests an essential role of maize HSBPs in repressing HSF activity.

The coiled-coil is sensitive to temperature modulations (Thompson, 1993). Therefore, it is possible that the hetero-oligomerization of HSF-HSBP can also respond to temperature shifts. In such a model, disassociation of HSBP from HSF upon heat stress or re-association of HSF and HSBP during attenuation of heat stress enables dynamic regulation of HSF activity. The affects of temperature, pH, redox status and phosphorylation on the formation of coiled coils between HSF and HSBP can be experimentally tested both *in vitro* and *in vivo*. Such studies will shed important insights regarding whether there is a "built-in thermometer" in HSFs.

It is also worth mentioning that plant HSFs are different from their animal counterparts in several aspects. First, plant HSFs do not have the HR-C domain, which represses transactivation of animal HSFs under non-stressed conditions (Pirkkala et al., 2001). Thus, plants may have evolved additional HSF regulatory mechanisms. Secondly, plants often have more than twenty HSFs, compared to three HSFs in animals (Nover et al., 2001). Finally, transcription of some plant HSFs is heat inducible, possibly due to alterations in regulatory regions such as promoters (Nover et al., 2001). emp2 is the first mutant in plants that leads to derepressed or unattenuated HSR expression, indicating an essential role of *hsbp* in regulating the activity of plant HSFs (Figure 2.4). Molecular and biochemical characterization of *emp2* and *hsbp2* provides a unique opportunity to understand how HSFs are regulated in plants. Furthermore, there may be important differences between monocots and eudicots with regard to HSF regulation. As reported herein, grasses have two distinct forms of HSBP, whereas dicots only have one (Figure 2.5). In addition, our genetic and molecular studies suggest that both of the maize HSBPs are involved in HSR regulation (Figure 2.4; Figure 4.2; Figure 4.5). It will be interesting to study

how eudicot HSBPs interact with HSFs, and what is the impact of the functional divergence of HSBPs in grasses.

**The Functions of HSBP in Normal Development**

In addition to the role in heat responses, the *emp2* gene may also play a role for normal development, based on the observation of the developmental defects associated with the *emp2-R* mutation in embryonic and postembyonic tissues (Figure 2.1; Figure 3.4). Homozygous emp2-R mutant embryos and the hemizygous *emp2-R/-* null sectors in shoot tissue exhibited developmental defects. HSFs and HSPs are well known to be involved in normal development. However, the developmental defects of *emp2* mutant sectors were not associated with heat stress and abnormal expression of *hsp* genes. The retardation phenotype of *emp2* mutant embryos also precedes the over expression of maize *hsp*s. Preliminary yeast two-hybrid results suggested that EMP2 can interact with non-HSF proteins (Figure 3.3). Therefore, EMP2 is likely to have other functions during normal development distinct from its role in HSR (Figure 4.6). The question is what and how the developmental functions of EMP2 evolved.

Protein oligomerization provides one of the most convenient and energy efficient ways of regulating protein activities. In this process, no protein synthesis is required, no protein is degraded and the regulation is easily reversible. Proteins with coiled-coil domains often have multiple pairing partners. The multiple pairing specificities may have allowed the small coiled-coil protein HSBP to be recognized by other proteins during evolution to regulate their own activities. If this proves to be true, it will be another elegant demonstration of Mother Nature's propensity to reuse existing regulatory modules instead of creating new ones.

**The Pairing Specificities of Coiled-coil Interactions**

It has been a long held concept that structural specificities of the coiled-coil are determined at the sequence level (Yu, 2002). Single amino acid mutations can drastically affect the oligomerization states (two stranded or three stranded), orientation (parallel or antiparallel) and pairing selectivity (homotypic or heterotypic). Based on this concept, we would predict that the interacting HSF and HSBP should maintain sequence conservation during evolution. Primary and secondary structural level conservations were detected among HSBP orthologues across animals and plants (Figure 2.4). However, there is no sequence similarity between the HR-A/B domain of human HSF1 and maize HSFA4b. This suggests that protein sequence is not the sole determinant of coiled-coil interactions. The question is then what ultimately determines the interaction specificities in coiled coils. On going projects analyzing EMP2 and HSBP2 may address the above question. We are preparing to use the purified EMP2 and HSBP2 recombinant proteins to retrieve all proteins that can bind to these maize HSBPs. Biochemical and biophysical analyses of EMP2 and HSBP2 interacting proteins may reveal the structural properties required for specific interactions. It will also be interesting to see how amino acid substitutions affect the structures and ultimate protein-protein interaction specificities of EMP2 and HSBP2.

In conclusion, we cloned two maize paralogues, *emp2* and *hsbp2*. Transposon insertion alleles have been identified for both loci. The consequences of *emp2* null mutation have been thoroughly studied in maize embryos as well as in developing shoots, and distinct roles of EMP2 in HSR and normal development were implicated. Yeast two-hybrid assays revealed potential interacting partners for both EMP2 and HSBP2. Recombinant proteins of EMP2 and HSBP2 have also been purified. More significantly, our studies established a great model system to

study many important questions, including HSR in general and HSF regulation in plants, the specificity and co-evolution of protein-protein interactions, as well as multiple developmental aspects of maize.

## References

Guo, Y., Guettouche, T., Fenna, M., Boellmann, F., Pratt, W. B., Toft, D. O., Smith, D. F. and Voellmy, R. (2001). Evidence for a mechanism of repression of heat shock factor 1 transcriptional activity by a multichaperone complex. *J Biol Chem* 276, 45791-9.

Hu, Y. and Mivechi, N. F. (2003). HSF-1 interacts with Ral-binding protein 1 in a stress-responsive, multiprotein complex with HSP90 in vivo. *J Biol Chem* 278, 17299-306.

Nover, L., Bharti, K., Doring, P., Mishra, S. K., Ganguli, A. and Scharf, K. D. (2001). Arabidopsis and the heat stress transcription factor world: how many heat stress transcription factors do we need? *Cell Stress Chaperones* 6, 177-89.

Pirkkala, L., Nykanen, P. and Sistonen, L. (2001). Roles of the heat shock transcription factors in regulation of the heat shock response and beyond. *Faseb J* 15, 1118-31.

Satyal, S. H., Chen, D., Fox, S. G., Kramer, J. M. and Morimoto, R. I. (1998). Negative regulation of the heat shock transcriptional response by HSBP1. *Genes Dev* 12, 1962-74.

Shi, Y., Mosser, D. D. and Morimoto, R. I. (1998). Molecular chaperones as HSF1-specific transcriptional repressors. *Genes Dev* 12, 654-66.

Thompson, K. S., Vinson, C. R. and Freire, E. (1993). Thermodynamic characterization of the structural stability of the coiled-coil region of the bZIP transcription factor GCN4. *Biochemistry* **32**, 5491-6.

Yu, Y. B. (2002). Coiled-coils: stability, specificity, and drug delivery potential. *Adv Drug Deliv Rev* 54, 1113-29.

# APPENDICES

A COPYRIGHT RELEASE LETTER FROM THE PUBLISHER OF PLANT CELL

Subject: RE: ask for copy right permission for dissertation

Date: Thu, 10 Jun 2004 15:19:18 -0400

From: Diane McCauley <diane@aspb.org>

To: Suneng Fu <fsneng@plantbio.uga.edu>

Dear Suneng Fu

We are happy to grant your request regarding copyright release of paper titled "empty pericarp2 Encodes a Negative Regulator of the Heat Shock Response and Is Required for Maize Embryogenesis" . Citations may be written in any appropriate standard format, with a credit line noting that the material is copyrighted by the American Society of Plant Biologists and is used with permission.

Good luck completing your thesis.

Diane McCauley

Publications Assistant

American Society of Plant Biologists

15501 Monona Drive

Rockville, MD 20855

phone: 301-251-0560 ext. 133

fax: 301-279-2996

diane@aspb.org

http://www.aspb.org

## B COPYRIGHT RELEASE LETTER FROM THE PUBLISHER OF GENETICS

Subject: Re: (urgent)ask for copy right permission

Date: Tue, 29 Jun 2004 10:31:27 -0400

From: Tracey DePellegrin Connelly <td2p@andrew.cmu.edu>

To: Suneng Fu <fsneng@plantbio.uga.edu>

Dr. Fu -

Yes, you have our permission to reprint the paper titled "Clonal mosaic analysis of EMPTY PERICARP2 reveals nonredundant functions of the duplicated HEAT SHOCK FACTOR BINDING PROTEINs during maize shoot development" in your thesis. Use the copyright line Genetics Society of America.

By the way, we do not require formal permission to use published papers

(your own) in a dissertation.

Best,

Tracey DePellegrin Connelly

Managing Editor

GENETICS

Mellon Institute

4400 Fifth Avenue

Box I

Pittsburgh PA 15217 USA

412.268.1812 phone

412.268.1813 fax

email: td2p@andrew.cmu.edu

http://submit.genetics.org

http://www.genetics.org